



THE HONG KONG
POLYTECHNIC UNIVERSITY

香港理工大學

Pao Yue-kong Library

包玉剛圖書館

Copyright Undertaking

This thesis is protected by copyright, with all rights reserved.

By reading and using the thesis, the reader understands and agrees to the following terms:

1. The reader will abide by the rules and legal ordinances governing copyright regarding the use of the thesis.
2. The reader will use the thesis for the purpose of research or private study only and not for distribution or further reproduction or any other purpose.
3. The reader agrees to indemnify and hold the University harmless from and against any loss, damage, cost, liability or expenses arising from copyright infringement or unauthorized usage.

If you have reasons to believe that any materials in this thesis are deemed not suitable to be distributed in this form, or a copyright owner having difficulty with the material being included in our database, please contact lbsys@polyu.edu.hk providing details. The Library will look into your claim and consider taking remedial action upon receipt of the written requests.

The Hong Kong Polytechnic University

Department of Applied Biology and Chemical Technology

Development and Optimization of Fluorescent Biosensors from

Various

Class A beta-Lactamases

Chung Wai Hong

A Thesis Submitted

in

Partial Fulfillment of the Requirements

for

Degree of Doctor of Philosophy

August, 2008

Certificate of Originality

I hereby declare that this thesis is my own work and that to the best of my knowledge and belief, it reproduces no material previously published or written nor material which has been accepted for the award of any other degree or diploma, except where due acknowledgement has been made in the text.

Chung Wai Hong

September, 2008

Abstract

Abuse of antibiotics results in the emergence of antibiotic-resistance pathogenic bacteria which cause undesirable effect on human health. Because of the effectiveness of β -lactam antibiotics, they are commonly used in food producing animals and can thus cause contamination in food. Monitoring and avoiding contamination of β -lactams in food is thus extremely important. Although several tests and protocols for detecting β -lactam residues in food are available, they are either time consuming or semi-quantitative. To solve this problem, several promising fluorescent biosensors based on fluorophore-modified β -lactamase from *B. cereus* (PenPC), *B. licheniformis* (PenP) and *E. cloacae* (AmpC P99) have been developed.

To further improve the sensitivity and detection limit of modified β -lactamase biosensors, different modifications were applied to three class A β -lactamases, namely PenP, PenPC and TEM-1. Different amino acid residues in these enzymes were chosen to be mutated to cysteine, and these mutants were separately labeled with 3 different fluorophores (6-bromoacetyl-2-dimethylaminonaphthalene (badan), tetramethylrhodamine-5-maleimide (TMRM), and fluorescein-5-maleimide (FM)). The badan-labeled PenP N170C mutant (PenP N170Cb) has the best performance

among all prepared PenP-based biosensors and gives the largest improvement in sensitivity with a 3 folds increase in fluorescence intensity upon penicillin V binding. The FM-labeled TEM-1 V216C (TEM-1 V216Cf), with 2 folds fluorescence increase upon penicillin G binding, has a better sensitivity than the other prepared TEM-1 based FM-labeled biosensor, TEM-1 E166Cf. The sensitivity of TEM-1 V216Cf was further improved by 3 additional mutations (E104K, M182T and G238S) which resulted in 3.6 folds increase in fluorescence intensity upon penicillin G binding, and the improved biosensor was denoted as TEM-52 V216Cf. E166 is the best residue for cysteine mutation and fluorophore labeling in the PenPC biosensor. The FM-labeled PenPC E166Cf has 2 folds increase in fluorescence intensity upon addition of penicillin G and the fluorescence increase is raised to 3 folds by introducing the Y105W mutation. Labeling TMRM to PenPC Y105W/E166C (PenPC Y105W/E166Cr) produced an even better biosensor, with 4 folds increase in fluorescence intensity upon penicillin G addition.

Molecular model of TEM-52 V216Cf showed that the binding of penicillin G caused the departure of the FM label from the active site and increased the distance between the FM label and tyrosine 105 (Tyr-105), which is a well known fluorescence quencher. The Increase in fluorescence lifetime of TEM-52 V216Cf

upon penicillin G binding supported that the FM-label was quenched by Tyr-105 in the active site. In PenPC Y105W/E166Cr, replacing Tyr-105 by tryptophan (trp), which is a stronger fluorescence quencher than tyrosine, caused reduction in quantum yield of the free enzyme PenPC Y105W/E166Cr but not the substrate bound PenPC Y105W/E166Cr. The background fluorescence intensity of PenPC Y105W/E166Cr was therefore suppressed and the sensitivity of the biosensor was improved. The information obtained thus provides direction for the future design of more efficient biosensors.

Acknowledgments

I am deeply indebted to my chief supervisor, Prof K.Y. Wong for his support, encouragement, supervision, and invaluable suggestion on this project. In addition, I would like to express my sincere gratitude to my co-supervisor, Dr Thomas Y.C. Leung for his valuable comments.

Moreover, I would like to thank Dr. H.K. Yap for teaching me molecular biology technique, Dr. D.L Ma for teaching me molecular modeling and Dr. K.C. Chan for teaching me spectroscopic technique. I would also like to thank Dr. P.H. Chan for his comments on the selection of fluorophore labeling positions, Ms. Kareena M.S. Tsang for cloning and developing the expression system of TEM-1 β -lactamase, and Mr. P.K. So for his generous assistance in mass spectrometry.

In addition, I am also greatly indebted to Dr. H.L. Leung, Dr. T.S. Lai, Dr. K.C. Cheung, Dr. N.Y. Kwok, Dr. K.P. Ho, Mr K.M. Lam, Mr. C.L Chan, Mr. S.C. Choi, Ms. F.Y. Chan, Ms. K.H. Lee and Ms L. Zou for their suggestions and encouragement.

Furthermore, I would like to acknowledge the Research Committee of the Hong Kong Polytechnic University for the awards of a research studentship and for the traveling grant supporting my attachment in Lakehead University in 2008.

Last, but not least, I would like to give my special thank to my family for their persistent love and support.

Table of Contents

| | |
|---|------------|
| Declaration | i |
| Abstract | ii |
| Acknowledgement | v |
| Table of contents | vii |
| Abbreviations | xv |
| | |
| Chapter 1 Introduction | 1 |
| 1.1 β-Lactam antibiotics | 2 |
| 1.2 Penicillin binding proteins | 7 |
| 1.3 β-Lactamases | 13 |
| 1.4 Food contamination and detection of βlactam residues | 19 |
| 1.5 Fluorescent biosensors based of modified β-lactamases | 25 |
| 1.6 Aims and objectives of this project | 27 |
| | |
| Chapter 2 Materials and Methodology | 29 |
| 2.1 Materials | 30 |

| | | |
|------------------|---|-----------|
| 2.1.1 | Bacterial strains | 30 |
| 2.1.2 | Plasmids | 30 |
| 2.1.3 | DNA manipulation reagents | 31 |
| 2.1.4 | Media | 31 |
| 2.1.5 | Chemicals | 32 |
| 2.2 | Cloning and DNA manipulation | 36 |
| 2.2.1 | Preparation of <i>E. coli</i> competent cells | 36 |
| 2.2.2 | Transformation of competent cells | 36 |
| 2.2.3 | Subcloning of β -lactamase gene into expression vector | 37 |
| 2.2.4 | Site-directed mutagenesis and plasmid modification | 37 |
| 2.3 | Preparation of β-lactamase mutants | 39 |
| 2.4 | Labeling of β-lactamase mutants with different fluorophores | 42 |
| 2.5 | Steady state and time dependent fluorometric studies of labeled β-lactamase mutants | 46 |
| 2.6 | Fluorescence lifetime measurement of labeled β-lactamase mutants | 47 |
| | | |
| Chapter 3 | Fluorescent biosensors based on modified PenP | |
| | β-lactamase | 49 |
| 3.1 | Introduction | 50 |

| | | |
|------------------|--|-----------|
| 3.2 | Methods | 54 |
| 3.2.1 | Site-directed mutagenesis and cloning of MBP-PenP cysteine mutants | 54 |
| 3.2.2 | Preparation and labeling of MBP-PenP cysteine mutants | 54 |
| 3.2.3 | Steady state fluorescence measurement of labeled MBP-PenP cysteine mutants | 55 |
| 3.2.4 | Time dependent fluorescence measurement of MBP-PenP N170Cb | 55 |
| 3.3 | Results | 57 |
| 3.3.1 | Preparation and labeling of MBP-PenP cysteine mutants | 57 |
| 3.3.2 | Fluorescence signals of labeled MBP-PenP cysteine mutants | 57 |
| 3.4 | Discussion | 72 |
| 3.4.1 | Fluorescence signals of labeled MBP-PenP cysteine mutants | 72 |
| 3.4.2 | Time dependent fluorescence signals of MBP-PenP N170Cb | 76 |
| 3.5 | Concluding remarks | 80 |
| | | |
| Chapter 4 | Fluorescent biosensors based on some modified TEM β-lactamases | 81 |
| 4.1 | Introduction | 82 |
| 4.2 | Methods | 87 |
| 4.2.1 | Site-directed mutagenesis and cloning of TEM cysteine mutants | 87 |

| | | |
|------------------|--|------------|
| 4.2.2 | Preparation and labeling of TEM cysteine mutants | 88 |
| 4.2.3 | Fluorometric measurement of labeled TEM cysteine mutants | 88 |
| 4.2.4 | Molecular modeling of TEM-52 V216Cf | 88 |
| 4.3 | Results | 90 |
| 4.3.1 | Preparation and labeling of TEM cysteine mutants | 90 |
| 4.3.2 | Fluorescence signals of labeled TEM cysteine mutants | 90 |
| 4.3.3 | Fluorescence lifetimes of TEM-52 V216Cf | 91 |
| 4.3.4 | Molecular models of TEM-52 V216Cf | 92 |
| 4.3.5 | Time dependent fluorescence signals of TEM-52 V216Cf | 92 |
| 4.4 | Discussion | 110 |
| 4.4.1 | Fluorescence signals of labeled TEM cysteine mutants | 110 |
| 4.4.2 | Signal generation mechanism and fluorescence lifetimes of TEM-52 V216Cf | 114 |
| 4.4.3 | Time dependent fluorescence signals of TEM-52 V216Cf | 120 |
| 4.5 | Concluding remarks | 122 |
| | | |
| Chapter 5 | Fluorescent biosensors based on modified PenPC | |
| | β-lactamase | 125 |
| 5.1 | Introduction | 126 |

| | | |
|------------|--|------------|
| 5.2 | Methods | 134 |
| 5.2.1 | Construction of pHMal-c2xK | 134 |
| 5.2.2 | Subcloning of PenPC beta-lactamase genes with and without his-tag into pRsetK and pHMal-c2xK | 136 |
| 5.2.3 | Site-directed mutagenesis and cloning of H-MBP-PenPC cysteine mutants | 137 |
| 5.2.4 | Introduction of Y105W mutation by site-directed mutagenesis | 138 |
| 5.2.5 | Preparation and labeling of different PenPC cysteine mutants | 139 |
| 5.2.6 | Fluorometric measurement of labeled PenPC cysteine mutants | 140 |
| 5.3 | Results | 142 |
| 5.3.1 | Preparation and labeling of TEM cysteine mutants | 142 |
| 5.3.2 | Fluorescence signals of different tagged PenPC E166Cf | 142 |
| 5.3.3 | Fluorescence signals of labeled H-MBP-PenPC mutants | 143 |
| 5.3.4 | Fluorescence signals of labeled H-MBP-PenPC Y105W/E166C | 144 |
| 5.3.5 | Fluorescent lifetimes and quantum yields of H-MBP-PenPC Y105W/E166Cr | 145 |
| 5.3.6 | Time dependent fluorescence signals of H-MBP-PenPC Y105W/E166Cr | 146 |
| 5.4 | Discussion | 180 |
| 5.4.1 | Effect of affinity tags on PenPC biosensors | 180 |

| | | |
|------------------|--|------------|
| 5.4.2 | Fluorescence signals of PenPC biosensors with different fluorophore labeling locations | 181 |
| 5.4.3 | Fluorescence signals of fluorophore labeled H-MBP-PenPC Y105W/E166C | 184 |
| 5.4.4 | Properties of TMRM labeled H-MBP-PenPC Y105W/E166C | 187 |
| 5.5 | Concluding remarks | 192 |
| Chapter 6 | Conclusions | 195 |
| Reference | | 200 |
| Appendix | | 223 |

Abbreviations

| | |
|-------------------------|--|
| AmpR | Ampicillin resistance |
| Amp | Ampicillin |
| Badan | 6-bromoacetyl-2-dimethylaminonaphthalene |
| <i>B. cereus</i> | <i>Bacillus cereus</i> |
| <i>B. subtilis</i> | <i>Bacillus subtilis</i> |
| <i>B. licheniformis</i> | <i>Bacillus licheniformis</i> |
| Cef | Cefuroxime |
| DMF | Dimethyl formamide |
| DNA | Deoxyribonucleic acid |
| dNTP | Deoxyribonucleoside triphosphate |
| <i>E. coli</i> | <i>Escherichia coli</i> |
| Elution buffer | Buffer with 20 mM sodium phosphate, 0.5 M NaCl and 0.5 M imidazole at pH 7.4 |
| FM | Fluorescein-5-maleimide |
| H-MBP | Maltose binding protein with his tag at N-terminal |
| kDa | Kilodaltons |
| KanR | Kanamycin resistance |

| | |
|--------------------|---|
| LB medium | Luria-Bertani medium |
| MBP | Maltose binding protein |
| min | Minute(s) |
| MW | Molecular weight |
| MCS | Multi-cloning site |
| PBP | Penicillin binding protein |
| PCR | Polymerase chain reaction |
| PenP | Beta-lactamase from <i>Bacillus licheniformis</i> 749/C |
| PenPC | Beta-lactamase I from <i>Bacillus cereus</i> 569/H |
| PenG | Penicillin G |
| QY _{dyn} | Dynamic quantum yield |
| QY _{ss} | Steady state quantum yield |
| QY _{stat} | Static quantum yield |
| rpm | revolutions per minute |
| Running buffer | Buffer with 20 mM sodium phosphate and 0.5 M NaCl at pH 7.4 |
| SDS PAGE | Sodium dodecyl sulphate polyacrylamide gel electrophoresis |
| T _m | Melting temperature |

| | |
|--------|--|
| TICT | Twisted intermolecular charge transfer |
| TY | Tryptone with yeast extract |
| TMR | Tetramethylrhodamine |
| TMRM | Tetramethylrhodamine-5-maleimide |
| UV-vis | Ultraviolet light – visible light |
| τ | Fluorescence lifetime |

Chapter 1

Introduction

1. Introduction

1.1 β -lactam antibiotics

Dominating more than 50% antibiotic consumption [1-3] and 65% of the antibiotic market [4] around the world, β -lactams are undoubtedly the most important and commonly prescribed antibiotics. Reasons for that are not just the good pharmacokinetics properties [5, 6] and low toxicity to human, but the ease of modification and the low production cost. Therefore, thousands of β -lactams have been synthesized and assayed from 1940s by pharmaceutical companies, universities and other research institutions. Besides those prodrugs and β -lactamase inhibitors, there are still more than 100 clinically approved β -lactams [5], which can satisfy the treatment of a wide variety of bacterial infections. The number of clinically approved β -lactams is still increasing

Such large number of β -lactams require logical and systematic classifications that can clearly show the structure – activity relationship. Antimicrobial spectrum and pharmacokinetics properties are often used to classify these antibiotics [5-8], but the most widely used and commonly known approach is the structural based classification

[9, 10].

The basic structure shared among all these antibiotics is the β -lactam ring. Molecules with monocyclic β -lactam ring and different substituents at the nitrogen atom (N1) are grouped into monobactams. Skeletons with bicyclic structure in which a five or six member ring is fused, are named as penam, penem and cephem. Most of β -lactam antibiotics and β -lactamase inhibitors are derivatives of these four basic skeletons with variations at the position 1 (designated as "X") and the substituent at C-6 α and C-2 penam / penem, or C-7 α and C-3 in cephem. In penam, X can be carbon, oxygen, sulfur and sulfone, whereas in penem and cephem, it can be carbon, oxygen and sulfur except sulfone. The structure and names of some variations are shown in Figure 1.1. It should be noted that there can be a single substituent, which forms a double bond with C-2 in penam or penem rather than a di-substituted C-2.

Among all these groups, penicillins and cephalosporins are the two largest and most commonly known groups of β -lactams. These antibiotics are also subdivided into several subclasses by different systems [5, 7]. In the case of penicillins, the simplest classification is based on their antibacterial spectrum – (1) natural penicillins with relatively narrow spectrum (e.g. penicillin G and penicillin X), (2) broad

spectrum penicillins with amino-group substituted (e.g. ampicillin and amoxicillin), (3) penicillins with antistaphylococcal activities and resistance to *S. aureus* β -lactamase (e.g. methicillin, oxacillin), and (4) penicillins with antipseudomonal activities (e.g. carbenicillin, ticarcillin). Cephalosporins are divided into four different generations. Different generations were discovered or synthesized for the need at a particular period of time, but the most distinct difference between these generations is their antibacterial spectrum [7, 11]. The first generation cephalosporins are the earliest discovered and are mainly targeted on gram positive bacteria. The “Secondary generation” cephalosporins are quite confusing sometimes, as cephamycins which have an additional C7 α -methoxy group and different activities are often classified into this group. This generation of antibiotics are more active against gram-negative bacteria but with reduced activities towards gram-positive ones. The third generation cephalosporins, which are also called extended spectrum β -lactam antibiotics, were designed with a broader antibacterial activities and β -lactamase resistances [11].

These classifications of penicillins and cephalosporins are over-simplified, because many properties, such as bio-availability and stability are not included. In addition, bacteria within the same group can respond differently to the same antibiotic; therefore, the so-called “antibacterial spectrum” of a β -lactam antibiotic is just a very

rough picture. In some cases, only penicillins can be classified into seven groups. Moreover, the classification of all β -lactams can be even more complicated when more groups, such as oxacephem and carbapenem are included. Therefore, it is difficult to have a simple scheme to list out the precise structure-activities relationship.

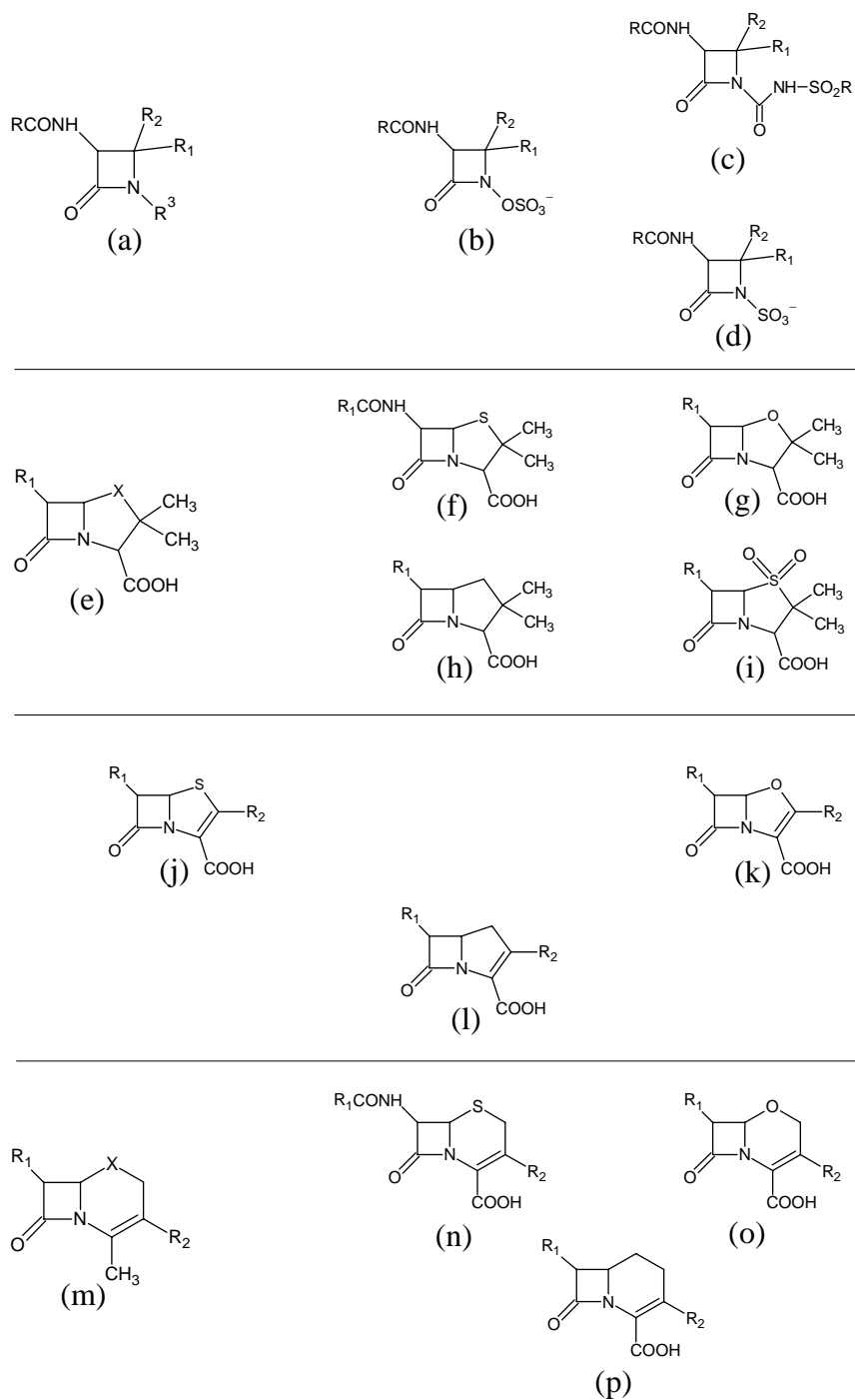


Figure 1.1 Classification of β -lactam; (a) monocyclic β -lactam; (b), monocarbams; (c) monosulfactams; (d) monobactams; (e) penam; (f) penicillins; (g) oxapenam; (h) carbapenam; (i) sulbactam; (j) penem; (j) oxapenam; (l) carbapenam; (m) cephem, (n) cephalosporins; (o) oxacephem; and (p) carbacephem.

1.2 Penicillin binding proteins

Just after the isolation of penicillin, Duguid discovered that low concentration of this antibiotic can induce morphological change in bacteria and he proposed that this was a result of inhibition of bacterial cell wall synthesis [12]. During that time, the detail structure of bacterial cell wall was not well understood and how the cell wall was synthesized remained a mystery. The explanation for this phenomenon was fully supported until the isolation of “Penicillin binding proteins (PBPs)” and the uncover of the antibacterial mechanism of β -lactams in the late 1960s [13, 14]. The isolated proteins are D-alanyl-D-alanyl-transpeptidase (DD-transpeptidase) or D-alanyl-D-alanyl-carboxypeptidase (DD-carboxypeptidase) which are responsible for the cell wall synthesis and control the degree of crosslinkage within the bacterial cell wall, whereas β -lactams can mimic the substrate of these enzymes. The synthesis of bacterial cell wall involves several complex biochemical reactions and pathways, where the target of β -lactams, transpeptidation / carboxpeptidation, appear at the last step of cell wall synthesis (Figure 1.2).

Bacterial cell wall is mainly composed of substituted carbohydrates (N-acetylglucosamine and N-acetylmuramic acid) and pentapeptide subunits.

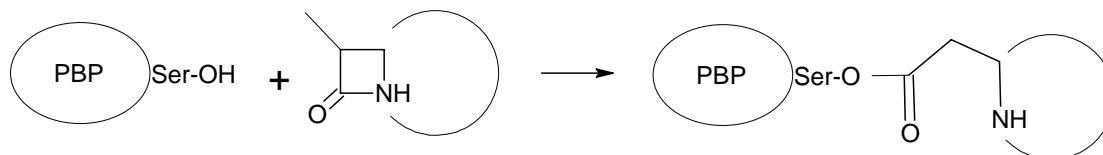
Therefore, “peptidoglycan” is used as the name of this crosslinked biopolymer. The carbohydrate chain of peptidoglycan is uniform over all known bacteria but the peptide linkage in which PBP acts on shows large variation [15]. The first three amino acid residues of the pentapeptide subunit that linked to muramic acid are variable but the third residue shows the greatest heterogeneity. There are at least eleven different amino acids identified to appear at this position. Moreover, different short chain amino acid extensions were linked to the third amino acid, resulting in a large variety of peptide moiety. However, this variation occurs mainly in gram positive bacteria, in gram-negative bacteria, meso-diaminopimelic acid are most likely present in this position. The third position residue or the short peptide extension is also used as a crosslinking bridge between different carbohydrate groups. The free amino group at the end of this position is used to form an amide bond with the carboxylate group of D-alanyl residue at position four. This reaction is catalyzed by DD-transpeptidase whereas DD-carboxypeptidase is used to remove the terminal D-alanine and prevents further transpeptidation [14-16].

Although PBPs are either DD-transpeptidase or DD-carboxypeptidase, these enzymes are highly diverse and each member has very different physiological roles, such as cell division, cell growth, elongation and spore development [16-18]. It is

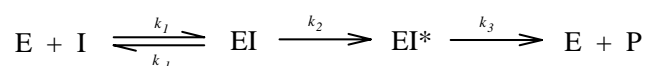
commonly accepted that PBPs can be classified into two categories, high molecular weight (HMW) PBPs and low molecular weight (LMW) PBPs [17, 19]. In general, HMW PBPs are DD-transpeptidase and LMW PBPs are DD-carboxypeptidase. Based on sequence homology, HMW PBPs can be further divided into two classes (class A and B) [17, 19]. Although both of them are proteins with two domains, the N-terminal domain of class A PBPs has a glycosyltransferase activity and that in class B PBPs participates in protein-protein interaction with the unknown target. Many HMW PBPs are susceptible to β -lactams inhibition and thus are lethal targets of bacteria. LMW PBPs, on the contrary, are usually not essential for cell viability. Nevertheless, it still plays an important and non-replaceable role in bacteria growth [17].

The diversity of PBPs function and the degree of inhibition by penicillin show significant variations. However, they still share some fundamental characteristics: they are all serine-active peptidase and have the same mode of action with β -lactams – the active serine residue in PBPs is acylated by β -lactams, which blocks the active site and inhibit the enzyme activities (scheme 1.1).

Scheme 1.1



The reaction in scheme 1.1 follows the Michaelis-Menten mechanism as follow



where E represents PBP, I represents β -lactam, EI and EI* are the non-covalent and covalent complex of PBP and β -lactam respectively, P is the hydrolyzed β -lactam, k_2 is usually referred as the acylation rate constant, and k_3 is the deacylation rate constant.

The kinetics of the reaction between some PBPs and β -lactams have been studied by mass spectrometry [20-22] and fluorescence spectroscopy [23, 24]. The second order acylation rate constant and deacylation rate constant can have 3 orders of magnitude difference depending on the type of PBP and β -lactams. For example, in *E. coli*, k_3 of the penicillin insensitive PBP5 is $2.3 \times 10^{-3} \text{ s}^{-1}$ whereas the penicillin sensitive PBP1b is $3 \times 10^{-5} \text{ s}^{-1}$ [10, 17]. Mutations leading to reduction of acylation

rate or raise of deacylation rate in β -lactam sensitive PBP is believed to be an important mechanism of antibiotics resistance [25]. For example, PBP2a, an extra PBP present in methicillin resistant *S. aureus* (MRSA), is the major β -lactam resistance factor for that bacteria [22]. PBP2x in *Streptococcus pneumoniae* is also a well studied example, in which the deacylation rate constant was found to increase more than 70-folds [20, 25]. Such increase in deacylation rate enables fast regeneration of the enzyme activity and restoration of the cell wall synthesis.

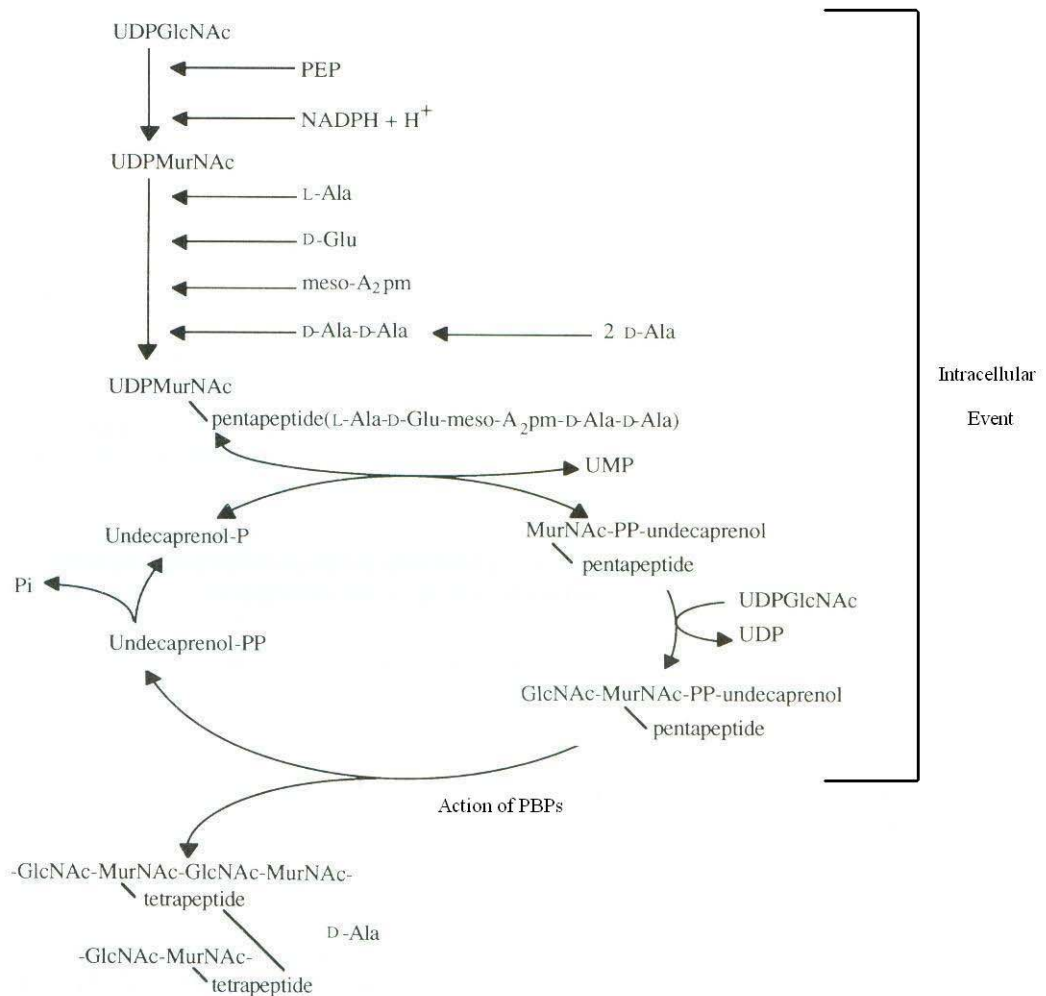


Figure 1.2 Biochemical pathway of peptidoglycan synthesis. Unusually abbreviations: GlcNAc, N-acetylglucosamine; MurNAc, N-acetylmuramic acid; A₂pm, 2,6-diaminopimelic acid; UDP, uridine diphosphate.

1.3 β -Lactamases

Over the evolution time, PBPs with fast β -lactam deacylation were selected under β -lactam selection pressure. These “PBPs” lost their transpeptidase / carboxypeptidase activity and become specialized for inactivating β -lactam antibiotics, which in turn protect other PBPs from β -lactams inactivation. It is now believed that this is the origin of β -lactamases [26, 27]. The exact time when β -lactamases appeared is not clear, but it should be much earlier than the discovery of this enzyme [27-30].

β -Lactamases were firstly identified just after the use of penicillin as antibacterial agent in 1940s [28, 29]. At that time, many different bacteria were shown to be naturally resistant to β -lactams and can produce “penicillin inactivating enzyme” [31]. The resistance in these bacteria came from natural selection rather than selection pressure created by human, because some bacteria met β -lactams in laboratory at the first time [28]. Human abuse of β -lactams, however, creates a new and strong selection pressure towards pathogenic bacteria, which accelerates the transfer of β -lactamase genes among pathogen and evolution of these enzymes. TEM-1, for example, firstly isolated from *E. coli* in 1960s, has given rise to a large number of mutants (the latest reported is about 160 mutants) in different bacteria.

The long and complex evolution history of β -lactamases implies that these enzymes are highly diverse. There are indeed more than 470 different β -lactamases isolated from different bacteria [30]. Again, different classifications of β -lactamases were proposed [32-34], which are mainly based on either functional properties or sequence homology of these enzymes. The first classification was proposed after the identification of “cephalosporinase” which has a higher catalytic efficiency in hydrolyzing cephalosporins than that of penicillins [35]. Later classification schemes were also based on the substrate profile and were expansion of the ones that discriminate “penicillinase” and “cephalosporinase” [36-38]. This type of classification scheme is still commonly used, especially in medical research, because it mainly focuses on the activities on different β -lactams. However, the phylogenetic relationship and evolution pathway of these enzymes cannot be shown. In 1980, Ambler proposed another classification based on alignment study of 4 available β -lactamases sequences [39]. The classification became the most popular one because it not only revealed the phylogenetic relationship of β -lactamases, but also showed in parallel with the standard numbering of amino acid residues of these enzymes, which is important in figuring out structure-activity relationship [40, 41].

In Ambler’s classification, 4 groups (A, B C and D) with limited sequence

homology were firstly recognised [39]. It should be noted that class B β -lactamases are metallo- β -lactamases which are structure, sequence and evolutionary distinct from the other three group of β -lactamases and PBPs . Proteins that are most structurally related with class B β -lactamases are oxidoreductases, eubacterial arylsulfatases and polyketide synthases which are totally unrelated to cell wall synthesis [42, 43]. Class A, C and D β -lactamases have the same α/β fold as PBPs and are all serine-active enzymes. These three group of β -lactamases and all PBPs are grouped into the “penicillin-recognizing proteins” family which contains three conserved motifs important in β -lactam binding [10]. The first and the most important motif is the SXXK tetrad, where S is the active serine residue responsible for the acylation of penicillin and K is the lysine activating the serine hydroxyl group. The other two motifs are the (S/Y)XN triad and the (K/H)(S/T)G triad which are important for the hydrogen bonding network with the C-3 or C-4 carboxylate group in penicillins and cephalosporins.

Some additional features are present in serine-active β -lactamases and PBPs, for example, the oxyanion hole [44, 45]. During the hydrolysis of β -lactams, an activated water molecule is added to the carbonyl group of the β -lactam ring and a tetrahedral oxyanion transition state is formed. This transition state is stabilized by the amide

backbone of the active serine residue and the alanine at position 237 (standard numbering of Ambler class A β -lactamases [45], or equivalent residue in other classes of β -lactamases). Such stabilization is important in the catalysis because it reduces the activating energy and allows the hydrolysis of β -lactam to pass through a lowered energy pathway. Therefore, the area formed by the two amino acid residues is named as oxyanion hole.

The key structure characteristic of β -lactamases is the one that enables the fast hydrolysis of the ester bond between the carbonyl carbon in β -lactam and the hydroxyl group of the active serine residue. Different β -lactamases have different structural motifs for this reaction, but the well known conserved motif which appears only in class A β -lactamases is the E₁₆₆XEXN₁₇₀. [10, 46, 47]. This motif is located in a small loop near the active site and is commonly named as Ω -loop. The first residue in this conserved sequence, glutamic acid at position 166, is very important in class A β -lactamases. Early chemical modification and mutation studies showed that the deacylation rate is reduced more than 2000-folds by replacing the glutamic acid to aspartic acid at the 166 position [48-52]. This distinctive role of Glu-166 attracts more people to study the reaction mechanism and the role of the residue in the catalysis in class A β -lactamases. It was proposed that this residue is a general base that activates

the hydroxyl group of Ser-90 [52, 53]. However, another proposal claimed that its major role of the residue is to activate the water molecule in the active site. Now, more evidences show that Glu-166 has a critical role in deacylation but less importance in acylation, and thus, the latter hypothesis seems to be more rational [49, 51, 52].

Apart from the reaction mechanism, the clinical dominance and the wide variety of class A β -lactamases also attract people's attention. Indeed, most of the clinically isolated β -lactams resistant bacteria contain either plasmid encoded or chromosome encoded class A β -lactamase genes. To fight against these β -lactamases, third generation cephalosporins and also β -lactamase inhibitors have been applied extensively since the 1970s [10, 11]. However, class A β -lactamases mutated so quickly that many different β -lactamases with extra-activities against third generation cephalosporins or resistance to inhibitors appear in the 1980s [30, 54, 55]. These so-called extended spectrum β -lactamases (ESBL) and inhibitor-resistant β -lactamases (IRBL) now widely spread all over the world.

Nowadays, this problem seems getting more serious and urges scientist to study structures and properties of these enzymes in order to develop new β -lactams and

β -lactamase inhibitors. Therefore, class A β -lactamases become one of the most well-documented enzymes. Nevertheless, this contributes not just to drug discovery research, but also to protein engineering. Actually, some β -lactamases, such as PenP and TEM-1, which were used in this study, become popular protein models for protein engineering researches [56-62]. In addition, these information are particularly important and helpful for the work in this project.

1.4 Food contamination and detection of β -lactam residues

The abuse use of β -lactam antibiotics occur not only in hospital but also in agriculture and food production. Indeed, penicillins were used to treat bacterial infection in cattle just after the initial use in human [63]. These antibiotics are even used as food supplements for agricultural animals when the cost of production has been reduced. The use of β -lactams in agriculture greatly raises the production; however, the contamination by these antibiotics in the products result in various problems.

The most obvious problem is the hindrance of the bacterial processing or fermentation of dairy products. The contamination of β -lactams can inhibit the growth of starter microorganism for the fermentation of sour milk, yogurt and cheese, affecting the dairy industry [63, 64]. However, the effect of β -lactam residues on human health attracts most public concern. β -Lactam residues in food may cause allergic reaction in some people, but the low concentration of β -lactams is unlikely to be immunogenic [65]. Another health impact that can be caused by antibiotic contamination is the alteration of the microflora in human intestine. Some studies revealed that long term exposure to low concentration of antibiotics in food can

change the population and antimicrobial resistance patterns in human intestine [66]. It is more worrying that the bacteria population which originally responds for detoxification could be reduced. Many food and safety departments over the world, such as FDA in United States, set up regulation and acceptance limit of antibiotics contamination in food in order to ensure food safety. Under these regulations, food with β -lactam residues exceeding the limit are not allowed to be imported or sold. As a result, monitoring β -lactam residues in food is important in food industry.

Basically, there are two types of testing methods to assay the β -lactam residues in food. The first one is referred as “chemical method” which is more traditional and relies heavily on analytical instruments, such as high performance liquid chromatography (HPLC) [67], capillary electrophoresis (CE) [68], or liquid chromatography – mass spectrometry (LCMS) [69]. These methods are highly quantitative and sensitive, and the usual detection limit is about 1 $\mu\text{g/L}$ (approximately 2 nM) penicillins. However, all these methods involve complicated sample preparation and extraction procedures, thus, the requirement of the technique of operator is demanding. In addition, expensive equipment are needed, and in general, the operation cost is high. Therefore, these methods are limited by their low output and are difficult to be used in routine analysis.

The other type of assays is usually referred as “bioactivity test” which is based on inhibition of bacterial growth, drug-drug target interaction or antigen-antibody interaction. These assays do not require sophisticated instrument and skillful operators; therefore they are commonly used in the farming industry for day-to-day monitoring. The oldest and cheapest test is the microbial growth inhibition test. The principle of this assay is to monitor the inhibition of the β -lactam sensitive bacterial growth by β -lactam residues in samples. The changes in the growth of bacteria can be monitored by measurement of colony forming unit (CFU), optical density or oxygen consumption in automatic systems. This test, however, is highly non-specific and the results can be interfered by many different factors, such as contamination by other antibiotics or the presence of β -lactam resistant bacteria. The other more reliable tests, which are fast, specific and sensitive to β -lactams, have been developed and commercialized as a kit. They are mainly designed for detecting antibiotic residues in milk. Detailed information and reports can be obtained from the Food Safety Authority of Ireland [70] and via the webpage of the Association of Official Analytical Chemists (AOAC) [8]. Some rapid tests with best performance, such as Penzyme III test, SNAP Beta-Lactam Assay, Charm SL6 beta-lactam Assay and BetaStar β -lactam Assay, are approved and recommended by AOAC [8, 70].

The Penzyme III test, which is similar to the previous versions (penzyme I and II), makes use of the activity of PBPs as an indicator of β -lactam in milk [71]. During the measurements, freeze-dried PBPs in this kit are firstly dissolved into a solution sample and incubated for several minutes at elevated temperature. The dissolved PBPs are inhibited depending on the concentration of the antibiotics residues. After incubation, D-amino acid oxidase and PBP substrate with D-alanine at the N-terminal were added. The non-inhibited PBPs hydrolyze the peptide and then release D-alanine into the solution, which is then oxidized by D-amino acid oxidase. The oxidation process generates hydrogen peroxides, which changes the color of the redox indicator provided in the kit. The intensity of the color indicates the concentration of the β -lactam residues.

The SNAP β -Lactam Assay is also based on PBPs but with a competitive binding mode for detection of antibiotic residues [72]. The PBPs used in this kit are conjugated with horseradish peroxidase. These modified PBPs are also incubated with solution samples for several minutes at elevated temperature. The solution with PBPs is then transferred to the tube or filter papers which is immobilized with β -lactams. Non-inhibited PBPs can be trapped onto the solid support. Horseradish peroxidase conjugated with PBPs on the solid support can generate color change after the

addition of peroxidase substrate and redox color indicator. The relative amount of β -lactam residues in samples is shown by the changes in color intensity from the control. Idexx, the manufacturer of SNAP β -Lactam Assay, also provides an automatic color reader for semi-quantitative analysis.

The working principle of BetaStar β -Lactam Assay is almost the same as SNAP β -Lactam Assay [72]. The main difference is that the PBP in this kit is conjugated with gold particles rather than the horseradish peroxidase. The sample solution with gold particles-conjugated PBP is also transferred to a solid support with immobilized β -lactams. Color bands will develop in some regions of the support when the non-inhibited PBP-gold particles conjugates become concentrated in the region. The working procedure and sample compartment of the Charm III test are very similar to BetaStar β -lactam Assay, though the exact details are not released. Therefore, it is possible that the Charm III test has similar detection mechanism as the BetaStar β -lactam Assay.

Most of these tests are well developed, and having high sensitivity and specificity. However, all these detection methods suffer from some problems. Firstly, those methods are usually semi-quantitative and further quantification with tests

described previously are needed. In addition, most of these methods are competitive assays, which give an inverse dose response curve. In other words, the lower the substrate concentration, the stronger the signal. Moreover, false positive results were also reported for some tests under certain conditions. High protein concentration and difference in sampling method could also cause these errors.

1.5 Fluorescent biosensors based on modified β -lactamases

Because of the importance of β -lactam detection, new assays aiming at fast and quantitative analysis are continuously developed. They include chemiluminescence [73] electrochemiluminescence [74] and surface plasmon resonance [75] methods. However, these new methods usually require expensive instruments and reagents. Recently, our research group has developed a reagentless fluorescent biosensor which is a fluorescein-conjugated mutated β -lactamase, designated as PenPC E166Cf [76]. This biosensor is reagentless, simple, fast responding, and more sensitive than most recently reported new assays.

PenPC E166Cf indeed is a chemically modified β -lactamase which originates from *B. cereus*. The wild type β -lactamase, of which the gene was named as *penPC*, was mutated at the 166 position from glutamic acid to cysteine. Fluorescein with maleimide as linker was used for conjugating the fluorophore to the thiol group of the mutated cysteine. As described previously, the amino acid residue at position 166 is close to the active site and located on the flexible Ω -loop, the conjugated fluorescein can thus move into or out from the β -lactam binding pocket. It is now proposed that the binding of β -lactam departs the fluorescein from the β -lactam binding pocket in which fluorescein is located and protected from contact of solvent. The

conformational change results in changing the solvent exposure area of fluorescein, thus enhancing the fluorescence which serves as an indicator on the presence of β -lactams. This biosensor can detect penicillin as low as 10^{-8} M and can be used for quantitative measurement. The success of PenPC E166Cf promoted the development of β -lactam biosensor by using different β -lactamases in order to further improve β -lactamase based biosensors. β -lactamase from *B. licheniformis* (PenP) was modified by the same approach [77]. This β -lactamase has much higher melting temperature (T_m) and is more stable towards thermal denaturation.

1.6 Aims and objectives of this project

In order to make use of fluorophore-labeled β -lactamases as practical biosensors, some problems should be overcome. The improvement in sensitivity and long term stability are the major issues. For example, detection of penicillin V by the PenP based biosensor gave only a 2 folds increase in fluorescence. If this change in fluorescence can be further enhanced, the sensitivity in detecting trace amount of β -lactams can be greatly improved.

It is believed that the sensitivity of these fluorescent biosensors is controlled by the magnitude of change in solvent accessible area of labeled fluorophore upon substrate binding. This change in solvent accessibility can be amplified by several approaches. Firstly, different amino acid residues on β -lactamase may experience different spatial movement upon substrate binding. Thus, changing the position of fluorophore labeling could change the difference in solvent accessible area caused by substrate binding. Therefore, different amino acid residues on PenP, PenPC and TEM β -lactamases were mutated to cysteine for fluorophore labeling. The results are reported separately in chapters 3, 4 and 5. In addition, the solvent accessibility is highly dependent on the environment around the active site accommodating the

fluorophore. Therefore, modifying the active site may also alter the fluorescence signal properties of these biosensors. One of the TEM β -lactamase mutants, TEM-52, with enlarged active site was chosen for labeling with fluorophore, and the fluorescence properties of labeled TEM-52 mutants are reported in chapter 4. It has been previously reported that tryptophan can significantly quench the fluorescence of many organic fluorophore. Therefore, a tryptophan residue was strategically added to the active site to replace the tyrosine at the 105 position. This modification can suppress the background fluorescence and enhance the fluorescence signal. The properties of these mutants are also reported in chapter 5.

Chapter 2

Materials and Methodology

2.1. Materials

2.1.1. Bacterial strains

E. coli XL-1 Blue was used as a recipient of recombinant plasmids and for plasmids amplification. *E. coli* BL21 (DE3) was used as a host for the over-expression of β -lactamase mutants

2.1.2. Plasmids

Plasmid pMal-c2x from New England Biolabs was modified to have kanamycin resistant marker rather than ampicillin resistant marker. This vector was constructed previously [77] and denoted as pMal-c2xK in this thesis. It was used for expression of PenP β -lactamase mutants. pHMal-c2xK was constructed from pMal-c2xK (described in sections 5.2.1) and used for expression of PenPC β -lactamase mutants. pRset-K, a resistant marker modified pRset-A and cloned with TEM-1 gene, was employed for production of TEM-1 β -lactamase mutants. Maps of three plasmids are shown at Figures 2.1 – 2.3.

2.1.3. DNA manipulation reagents

PCR reaction and site-directed mutagenesis were performed by PfuUltra High-Fidelity DNA Polymerase (Stratagene). Primers used in PCR were purchased from Sigma-Proligo. Restriction digestion enzymes (BamHI, DpnI, HindIII) and dNTPs were purchased from Promega. The PCR purification kit was purchased from Roche

2.1.4. Media

Tryptone, yeast extract, nutrition agar and Luria-Bertani (LB) medium were purchased from Oxoid Ltd. LB medium was used for transformation and preparation of *E. coli* competent cells. 2 × TY medium was prepared by addition of 16 g tryptone, 10 g yeast extract and 5 g sodium chloride into 1 L deionized H₂O and sterilized. This medium was used for β-lactamase mutants expression. All nutrient agar plates containing 50 µg/ml kanamycin were prepared by addition of 0.5 ml kanamycin (10 mg/ml) into 100 ml sterilized molten agar at about 50 °C.

2.1.5. Chemicals

Penicillin G, penicillin V, ampicillin, cefuroxime, cefoxitin, moxalactam and kanamycin were purchased from Sigma-Aldrich. Urea, sodium chloride, potassium hydroxide, guanidine hydrochloride (GuHCl) and potassium dihydrogenphosphate were from USB. 6-bromoacetyl-2-dimethylaminonaphthalene (badan), fluorescein-5-maleimide (FM), and tetramethylrhodamine-5-maleimide (TMRM) were purchased from Invitrogen.

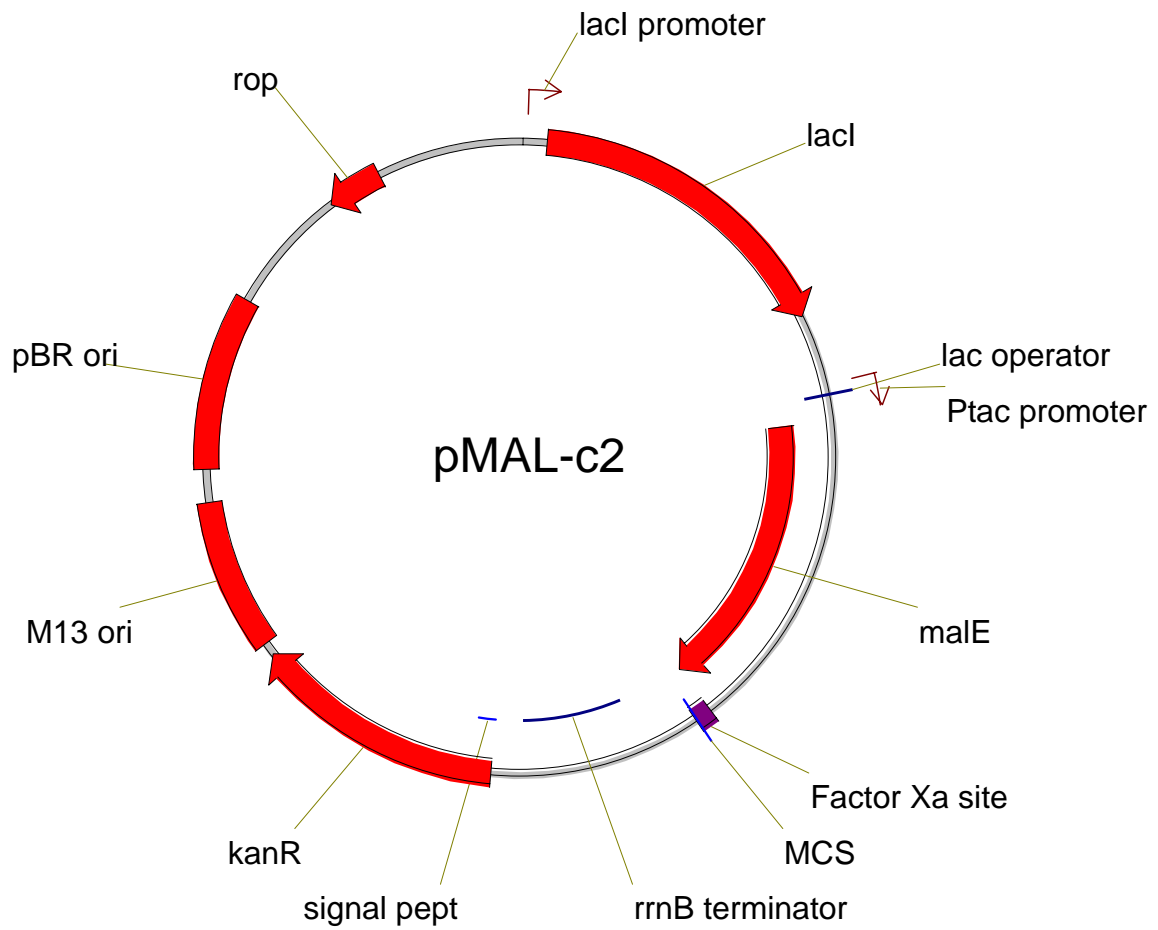


Figure 2.1 Plasmid map of pMal-c2xK. The ampicillin resistant marker was replaced by kanamycin resistant marker (*kanR*). PenP β -lactamase mutants were cloned between BamH I and Hind III located in the multi-cloning site (MCS)

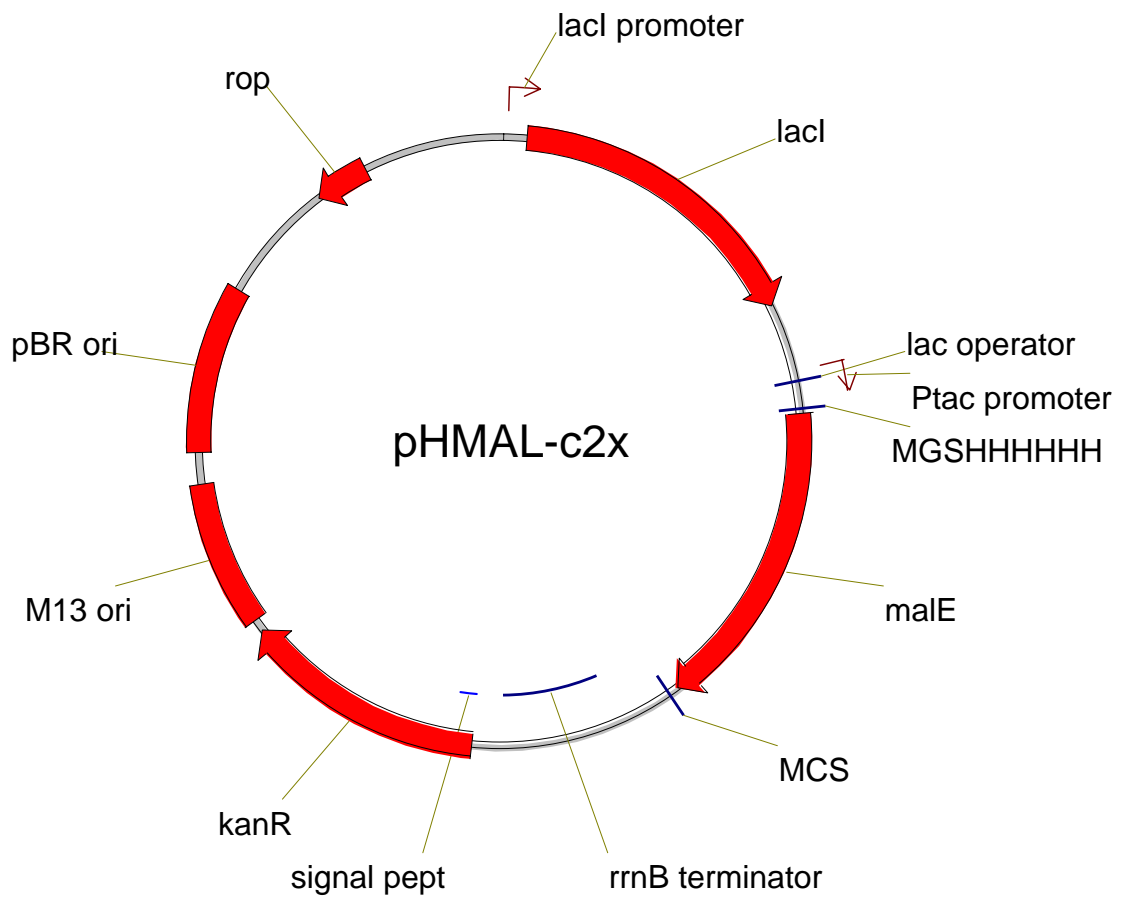


Figure 2.2 Plasmid map of pHMAL-c2x. Nine codons which encoded MGSHHHHHHH were added before the start codon of *malE*.

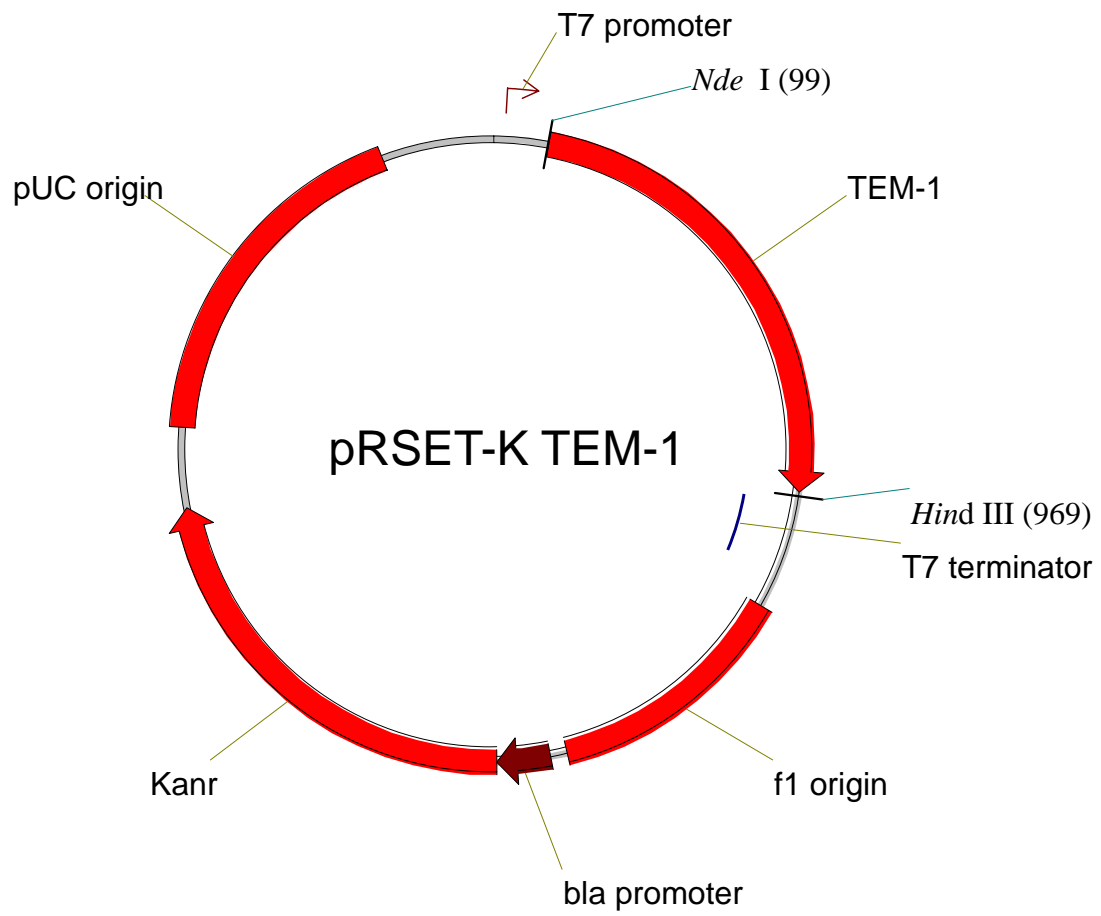


Figure 2.3 Plasmid map of pRset-K-TEM-1. The TEM-1 gene was cloned between Nde I and Hind III site.

2.2. Cloning and DNA manipulation

2.2.1. Preparation of *E. coli* competent cells

E. coli XL-1 Blue and BL21 (DE3) strains were cultured in 5 ml sterilized LB medium overnight at 37 °C with shaking at 280 rpm. A portion of 200 µl overnight culture was inoculated into 100 ml sterilized LB medium. After incubated at 37 °C with shaking at 280 rpm for 2-3 hours ($OD_{600} = 0.3 - 0.4$), cells were harvested by centrifugation at 4000 rpm for 20 min at 4 °C. The cell pellet was resuspended in 10 ml sterilized ice-cold 100 mM $CaCl_2$ and kept in ice for 25 min. The cells were pelleted again by centrifugation and the pellet was resuspended in 700 µl ice-cold $CaCl_2$. 50% sterilized glycerol (300 µl) was added to make up a final glycerol concentration of 15 %, and the mixture was aliquoted into eppendorf. These competent cells were frozen quickly by liquid nitrogen and stored at – 80 °C.

2.2.2. Transformation of competent cells

Ligation product or plasmid DNA was added into and mixed thoroughly with 50 µl competent cells. After incubated on ice for 25 min, the competent cells were heat shocked at 42 °C for 2 min. Then 200 µl LB medium was added to the eppendorf, and

the competent cells were incubated at 37 °C for 1 hour. These competent cells were plated on nutrient agar with 50 µg/ml kanamycin and incubated at 37 °C overnight.

2.2.3. Subcloning of β -lactamase gene into expression vector

Only PenPC β -lactamase gene was required to be cloned into different expression vectors for the optimization of expression of the mutants. Details are described in section 5.2.2

2.2.4. Site-directed mutagenesis and plasmid modification

Genes of different β -lactamase mutants were prepared by QuickChange® II Site-Directed Mutagenesis Kits (Stratagene), using procedures described in the protocol of the kit. Primers used for mutagenesis were listed separately in each chapter. Basically, the PCR cycling conditions were the same except that the annealing temperature (x) and extension time (y) were case dependent (95 °C for 5 min, 16 cycles of 95 °C for 30 s, x °C for 1 min, 68 °C for y min). The protocol and reaction condition for plasmid modification are similar to site-directed mutagenesis, but the reaction cycle number was 18 instead of 16. Only plasmid pMal-c2xK was

modified and the detail is described in section 5.2.1 of chapter 5.

2.3. Preparation of β -lactamase mutants

A single colony of *E. coli* BL21 (DE3) which was transformed with appropriate vector was inoculated into 5 ml 2 \times TY medium with 50 μ g/ml kanamycin in a universal bottle. This pre-culture was grown overnight at 37 $^{\circ}$ C with shaking at 250 rpm. After 14-16 hour, 1 ml pre-culture was added into 100 ml 2 \times TY medium with 50 μ g/ml kanamycin and incubated at 37 $^{\circ}$ C with shaking at 250 rpm. The OD₆₀₀ of the culture was monitored until it reached 0.8. 150 μ l of filtered isopropylthiogalactoside (IPTG, 0.2 M) solution was added to the culture for inducing β -lactamase mutants expression. After incubation for an additional 4 hours, the culture was collected by centrifugation at 10000 g at 4 $^{\circ}$ C for 30 min. The pelleted cells were collected and stored at -80 $^{\circ}$ C.

Before chromatographic purification, the β -lactamase mutant in the cell pellet was extracted by homogenization. The cell pellet from 100 ml culture was resuspended in 10 ml of solubilization buffer (20 mM Tris-HCl, 0.2 M sodium chloride and 1 mM EDTA, pH 7.4). 100 μ l of 75 mg/ml lysozyme was added to the fully resuspended mixture and then incubated at 30 $^{\circ}$ C for 45 min. The suspended cells were then lysed in ice by a Soniprep 150 ultrasonic disintegrator with short

pulses of 30 s for 5 cycles. Bacterial lysate was subjected to centrifugation at 18000 g for 30 min at 4 °C. Depending on the type of β -lactamase mutants, different fractions were collected. In the case of PenP and PenPC β -lactamase mutants, the supernatant was collected. TEM β -lactamase mutants were all expressed as inclusion body, and therefore the insoluble fraction was collected.

As PenP mutants were all cloned into pMal-c2xK, the MBP fusion tag was available for chromatographic purification which has been described previously. The supernatant was filtered through 0.45 μ m filter before loading onto an amylose affinity column, which was pre-equilibrated with binding buffer (20 mM Tris-HCl, 0.2 M sodium chloride and 1 mM EDTA, pH 7.4). After the loading of supernatant, the column was then washed with 2.5-column volume of the binding buffer. The PenP mutant was eluted by two maltose gradient segments from 0 to 4 mM and from 4 to 10 mM. Eluates showing UV absorbance peak was collected and buffer-exchanged with 20 mM ammonium bicarbonate. The mutants was then freeze-dried and stored at -20 °C.

For PenPC mutant, the presence of histidine-tag at the N-terminal of MBP allowed enzymes to be purified by nickel affinity chromatography. A nickel affinity

column connected to peristaltic pump was used for simple and fast purification. A HiTrap chelating column was firstly pre-equilibrated with binding buffer (20 mM sodium phosphate 0.5 M NaCl at pH 7.4) before loading of filtered cell lysate. The column was washed by 6 column volumes of binding buffer and 3 column volume of a mixture of 90% binding buffer and 10% elution buffer (binding buffer with 0.5 M imidazole). The PenPC mutant was eluted by 2 column volume of elution buffer. The purity of eluent was analyzed by SDS-PAGE before buffer-exchanged with 20 mM ammonium bicarbonate and freeze-dried.

The TEM mutant was expressed as inclusion body. An unfolding step was therefore required before purification. 10 ml of 8 M urea was added to the insoluble fraction from 100 ml culture. The mixture was stirred at room temperature until all insoluble fractions dissolved into the urea solution. The unfolded protein solution was dialyzed against binding buffer for nickel affinity chromatography at 4 °C in order to refold the TEM β -lactamase mutant. The solution was clarified by centrifugation at 18000 g at 4 °C for 15 min. The re-dissolved protein solution was subjected to column purification under the same condition as PenPC mutant and the eluent was analyzed by SDS-PAGE. The purified TEM β -lactamase mutant was buffer exchanged with 50 mM potassium phosphate (pH 7) and stored at -20 °C.

2.4. Labeling of β -lactamase mutants with different fluorophores

The three selected fluorophores (badan, FM and TMRM, Figure 2.4) are all environment sensitive and can conjugate to macromolecule to detect the change in solvent polarity accompanied by conformational change. Labeled badan, which behaves similarly to prodan, exhibit blue shift in emission maximum when it experiences reduction in solvent polarity (Figure 2.5). Labeled TMRM also shows increase in fluorescence quantum yield when the solvent polarity is reduced, but the bathochromic shift is much smaller than labeled badan. On the contrary, labeled FM exhibits increase in fluorescence quantum yield when solvent polarity is increased. In the case of β -lactamase based biosensor, binding of β -lactam antibiotic may cause local conformational change, which can be detected by these labeled fluorophores.

All these fluorophores were labeled to β -lactamase mutants in the same way – 3 mg of the freeze-dried β -lactamase mutant was dissolved into 3 portions of 6 M guanidium chloride solutions (each 2 ml) which were buffered by 50 mM potassium phosphate at pH 7. The enzyme was incubated for 30 min at room temperature for effective unfolding. Three different fluorophores, 6-bromoacetyl-2-dimethylaminonaphthalene (badan), fluorescein-5-maleimide (FM),

and tetramethylrhodamine-5-maleimide (TMRM), were dissolved in DMF to make up a 20 mM solution respectively. 10 folds molar excess fluorophores were added into the unfolded-enzyme solutions. After 1 hour incubation, guanidium chloride was removed by dialysis with 50 mM potassium phosphate solution (pH 7).

All PenP and PenPC β -lactamase mutants were labeled under the same procedures. TEM β -lactamase mutants were labeled with fluorescein-5-maleimide (FM) and tertamethylrhodamine-5-maleimide (TMRM) in 50 mM potassium phosphate and were labeled with 6-bromoacetyl-2-dimethylaminonaphthalene (badan) in 3 M guanidium chloride solutions.

The badan, FM and TMRM labeled mutants were abbreviated with b for badan, f for FM and r for TMRM respectively. For example, E166C mutant labeled with badan, FM and TMRM were abbreviated as E166Cb, E166Cf and E166Cr respectively.

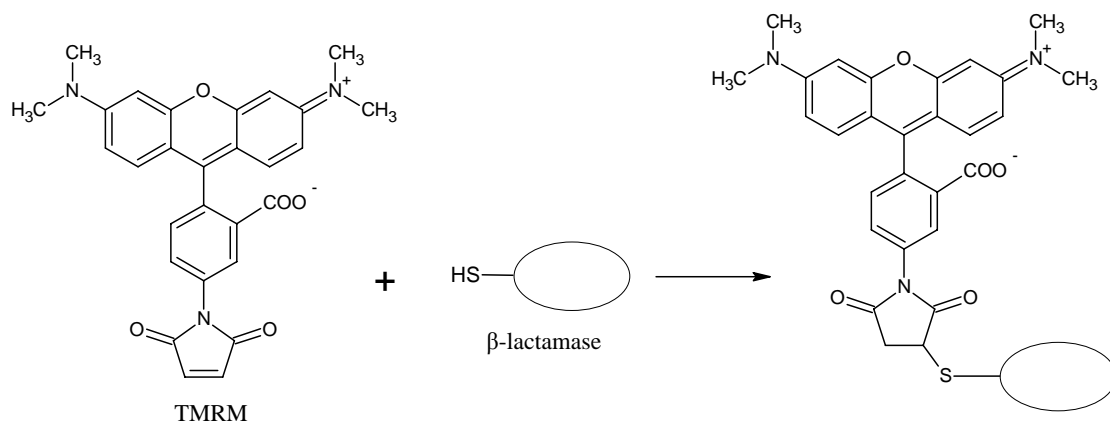
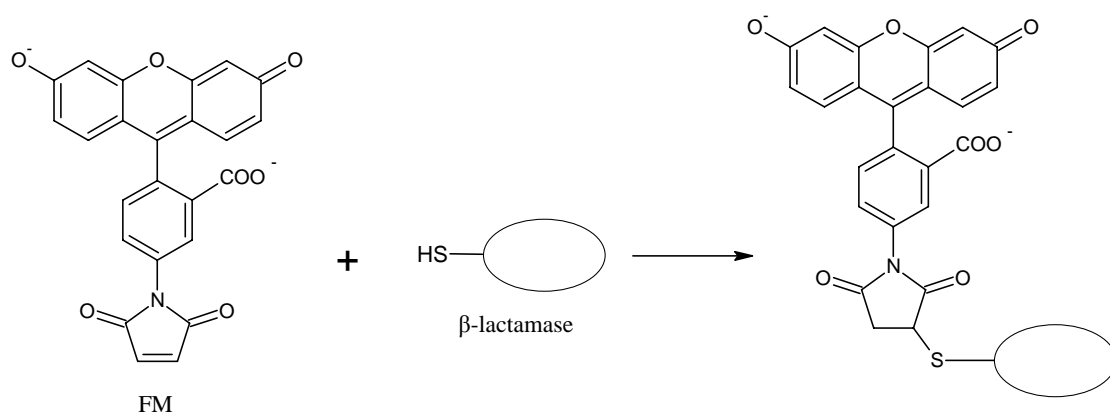
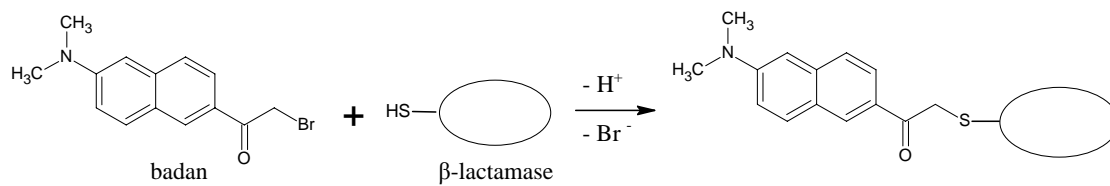


Figure 2.4 Schematic diagram of conjugation of badan, FM and TMRM to thiol group on the cysteine residue of β -lactamase

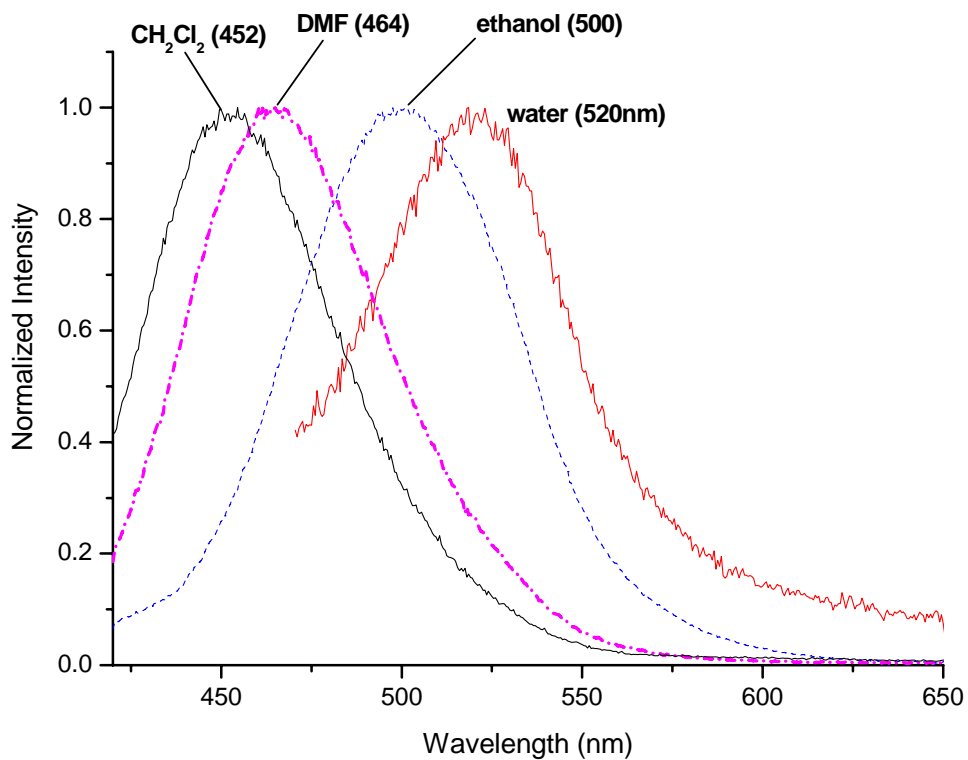


Figure 2.5 Shift in emission maximum of badan when it experiences change in solvent polarity

2.5. Steady state and time dependent fluorometric studies of labeled β -lactamase mutants

All steady state fluorescence measurements were performed on a Pekin Elmer LS-50B spectrofluorometer. In all fluorescence measurement, a solution of the labeled β -lactamase mutants and β -lactam antibiotics were made up to 500 μ L. The concentration of labeled β -lactamase mutants were about 1.6×10^{-7} M. The excitation wavelengths used in spectra measurement of three fluorophore labeled mutants were 385 nm for badan, 494 nm for FM and 555 nm for TMRM respectively. In time dependent fluorescence measurements, excitation wavelengths were the same as spectra measurements, and the emission wavelength were 515 nm for FM and 580 nm TMRM.

2.6. Fluorescence lifetime measurement of labeled β -lactamase mutants

Time resolved fluorometric measurements were determined by time-correlated single photon counting measurement with a FluoroCube spectrofluorometer (Horiba Jobin Yvon IBH). The excitation light source was a NanoLED-495 LED with repetition rate at 500 kHz. Emission was monitored at 515 nm with 5 nm slit width for FM-labeled mutant, and at 575 nm and slit width was set at 12 nm for TMRM-labeled mutant.

Chapter 3

Fluorescent biosensors based on modified PenP β -lactamase

3.1. Introduction

β -Lactamase (PenP) from *B. licheniformis* was identified in the early stage of studies on β -lactam resistance [31, 78], but the bacterium was wrongly identified as *B. subtilis* at that time [79]. Strains which produced PenP β -lactamase were later classified as *B. licheniformis* because of the improvement in biochemical test and also the discovery of the absence of β -lactamase activity in all *B. subtilis*. This enzyme as well as PenPC from *B. cereus* were commonly used during the 1970s for studying β -lactam resistance [80]. As both enzymes are secretory protein, they can be studied directly without any extraction and purification.

Nowadays, PenP β -lactamase is still a very good model enzyme for protein engineers and molecular biologists [61, 62, 81, 82]. This β -lactamase is more easily expressed intracellularly than some commonly used β -lactamases, like TEM-1, which contain disulfide bond. The availability of several crystal structures of PenP β -lactamase provides useful structure-activity information for protein engineering and modification [83, 84]. In addition, the melting temperature (T_m) and stability of this protein is highest among all characterized β -lactamases [85], which allow the enzyme to tolerate different deteriorate mutations and modifications.

In our research group, this enzyme has been mutated for the construction of β -lactam biosensor [77]. The principle of the construction of this biosensor was similar to the firstly reported PenPC β -lactamase-based fluorescent biosensor [76, 86]. Cysteine mutation was introduced into the position 166, and the mutant was then expressed, purified and labeled with FM and badan. The fluorophore is believed to undergo conformational change during the binding of β -lactams to the active site. The change leads to an alteration in solvent exposure area of the fluorophore and fluorescence quantum yield which can be used as an indicator for the presence of antibiotics. This labeled PenP mutant is able to give fluorescence signal in the presence of penicillins and cephalosporins. In addition, N170Q was also introduced to PenP E166C to give a double mutant, which can increase the signal stability by reducing the hydrolytic activities on the substrate when compared with the E166C single mutant [77].

These biosensors, as expected, have a relatively high T_m at about 50 °C. However, it did not show improved sensitivity over the PenPC based biosensors. The fluorescence signal of the PenP E166C biosensor increase by almost 80 % increase upon the addition of penicillins, and about 50 % upon the addition of cephalosporins. These changes in fluorescence are 60% smaller than that of PenPC β -lactamase based

biosensor. Therefore, it is desirable that the fluorescence signal of PenP fluorescent biosensor can be improved. One possible modification that can be done is to label β -lactamase with fluorophores at different positions on PenP β -lactamase. As proposed by Banerjee, the Ω -loop, on which E166 is located, is flexible during the catalysis [46], and this is believed to be important to the signal generation of PenPC β -lactamase based fluorescent biosensor. Therefore, fluorophores attached to residues on the Ω -loop other than position 166 should also experience similar change in solvent exposure. In this study, three amino acid residues on the Ω -loop were selected for this purpose. They are N170, V172 and E176, and their side chain orientation and distance from the active site are shown in Figure 3.1.

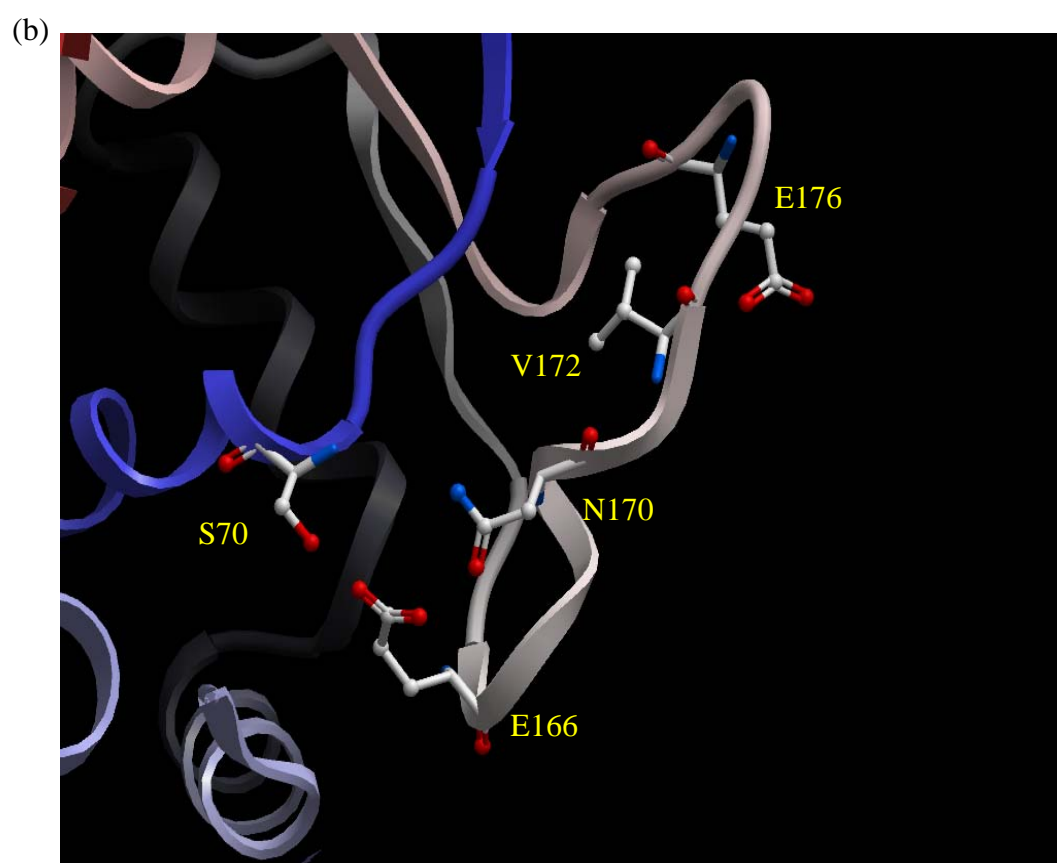


Figure 3.1 (a) The 3D structure of PenP β -lactamase, the Ω -loop is highlighted in yellow, (b) a closer view of the Ω -loop showing Ser70, Glu166, Asn170 and Glu176.

3.2. Methods

3.2.1. Site-directed mutagenesis and cloning of MBP-PenP cysteine mutants

All site-directed mutagenesis were done by using pMal-c2xK-PenP E166C as template and the procedures were described in section 2.2.4. Before introducing cysteine mutation at the three selected amino acid residues (N170, V172 and E176), the glutamic acid at position 166 was mutated to alanine by using two primers, P-E166A-F and P-E166A-R (Table 3.1). The three cysteine mutations were done by using primer pairs P-N170C-F / P-N170C-R, P-V172C-F / P-V172C-R, and P-E176C-F / P-E176C-R (Table 3.1). The PCR cycling conditions were 95 °C for 5 min, 16 cycles of 95 °C for 30 s, x °C for 1 min, 68 °C for 7.5 min, where x is the T_m of the primer pairs minus 5 °C

3.2.2. Preparation and labeling of MBP-PenP cysteine mutants

All mutants were expressed and purified under the same procedures described previously [77]. All these mutants were labeled with 3 different fluorophores, badan, FM and TMRM, and purified by dialysis as described in section 2.4.

3.2.3. Steady state fluorescence measurement of the labeled MBP-PenP cysteine mutants

The maximum fluorescence signals of each fluorescent biosensor was obtained by addition of penicillin G and cefuroxime at a concentration to give the saturated signal (5×10^{-4} M). In the case of FM and TMRM labeled mutants, there is no change in emission maximum upon binding of antibiotics. The change in fluorescence signal was thus measured at the emission maximum of 515 nm (FM) and 575 nm (TMRM) respectively. Badan-labeled mutants show a blue-shift in emission upon substrate binding, and the change in fluorescence signal was measured at the new emission peak at 498 nm.

3.2.4. Time dependent fluorescence measurement of MBP-PenP N170CCb

Time dependent fluorescence measurements were carried out on PenP N170Cb which shows a largest fluorescence change upon binding with β -lactam with antibiotics. Detailed procedures are described in section 2.5

Table 3.1 DNA sequence of primers for cysteine mutations

| Primers | Sequence | T _m (°C) |
|------------------------|---|------------------------|
| P-E166A-F P-E166A-R | CAAATCCCGAACGATTCGCACCAGAGTTAAATG CATTAACTCTGGTGCGAATCGTTCGGGATTG | 70.3 |
| P-N170C-F P-N170C-R | GCACCAGAGTTAT <u>TGT</u> GAAGTGAATCCG CGGATTCACTT <u>CACATA</u> ACTCTGGTGC | 60.9 |
| P-V172C-F P-V172C-R | GAGTTAAATGAAT <u>TGT</u> AATCCGGGTGAA TTCACCCGGATT <u>CAC</u> ATTCATTAACTC | 57.7 |
| P-E176C-F P-E176C-R | GTGAATCCGGGT <u>TGT</u> ACTCAGGATACC GGTATCCTGAGT <u>ACA</u> ACCCGGATTAC | 60.8 |

3.3. Results

3.3.1. Preparation and labeling of the MBP-PenP cysteine mutants

The three mutants, N170C, V172C and E176C were successfully expressed and purified by using amylose column. The chromatograms of the three mutants during purification are shown in Figures 3.2 - 3.4, and the purity was analyzed by SDS-PAGE. All chromatograms show a single peak of MBP-fusion protein with about 95% purity. The purified proteins were successfully labeled with the three fluorophores and were analyzed by SDS-PAGE (Figure 3.5). A total of nine different biosensors (N170Cb, N170Cf, N170Cr, V170Cb, V170Cf, V170Cr, E176Cb, E176Cf and E176Cr) were prepared accordingly.

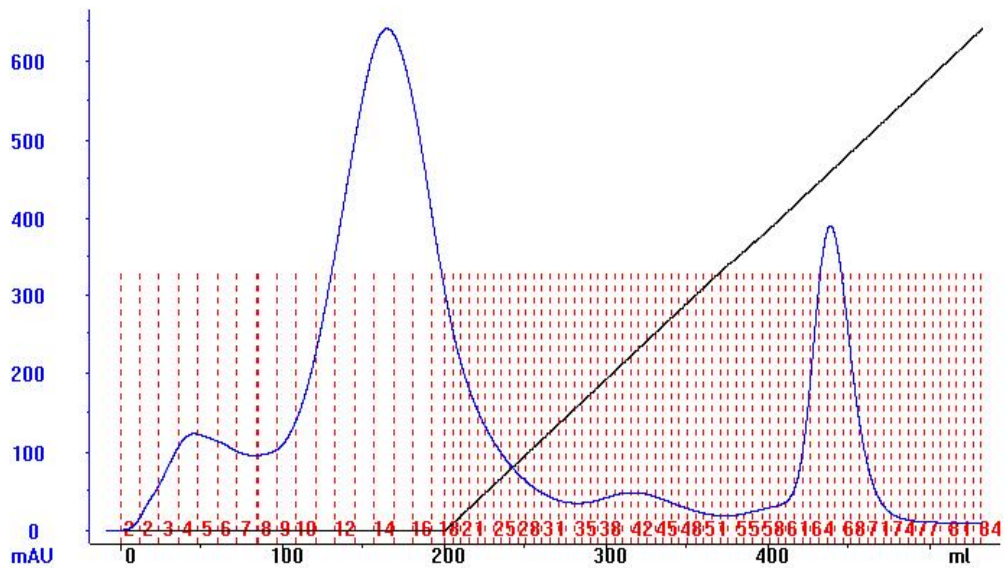
3.3.2. Fluorescence signal of the labeled MBP-PenP cysteine mutants

Although only nine labeled mutants were prepared, it was time consuming to study all of them in details. Therefore, only the most sensitive one was selected for detail study. To screen out the most sensitive labeled mutant, preliminary test was performed by employing two β -lactam substrates, penicillin G and cefuroxime, for fluorometric studies. The fluorescence spectra of all labeled mutants before and after

the addition of β -lactams were measured and shown in Figures 3.6 - 3.8.

All labeled E176C mutants show no fluorescent change upon addition of penicillin G and cefuroxime. The FM or TMRM labeled V172C and N170C mutants give relatively weak or no fluorescence signal but the badan labeled mutants give fluorescence signal in the presence of both penicillin G and cefuroxime. These spectra are blue shifted in different extent, and the degree of blue shift is accompanied by an increase in fluorescence. The largest change in fluorescence among these combinations is the N170Cb mutant upon addition of penicillin G, which has its emission maximum blue shifted from 513 nm to 497 nm. The largest change in fluorescence intensity, with 2 folds increase, at 488 nm. The best performed PenP N170Cb was chosen for time dependent fluorescence study which is reported as follows.

(a)



(b)

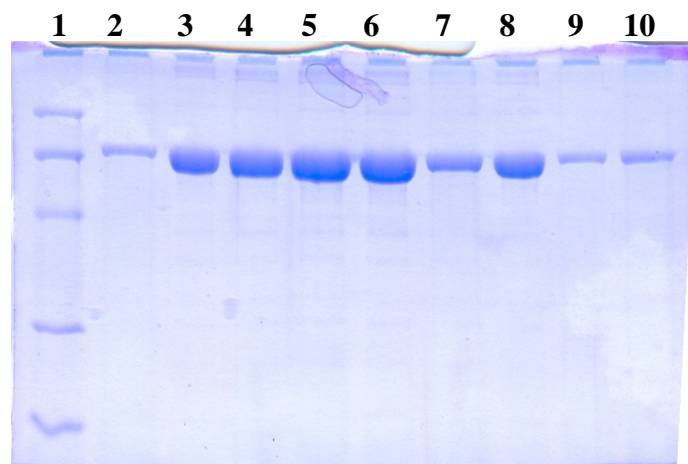
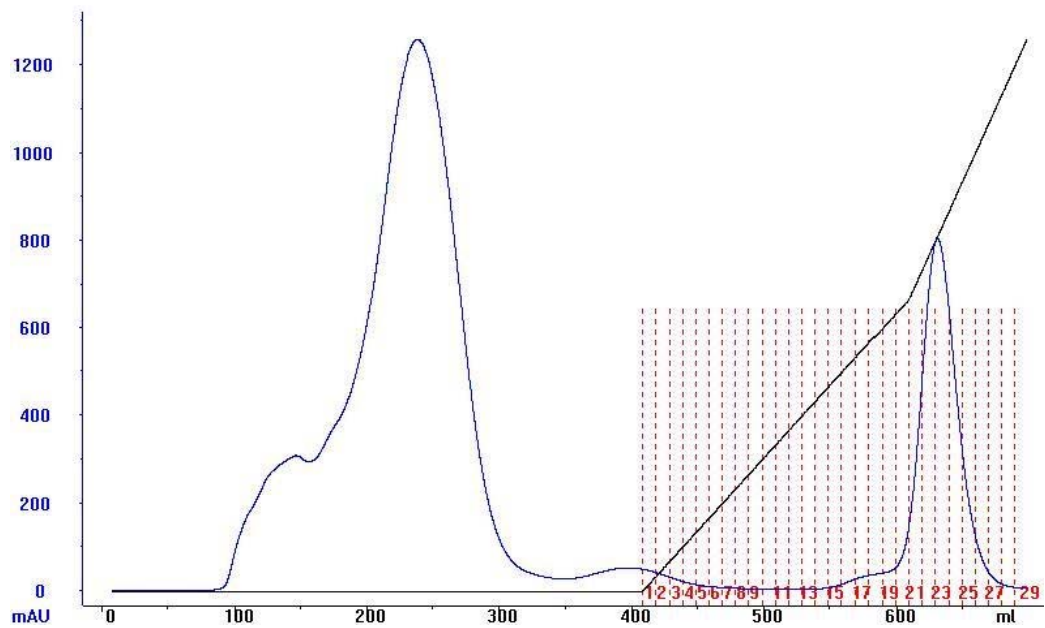


Figure 3.2 Purification of MBP PenP E166A N170C (a) Elution profile of the enzyme from cell lysate obtained from 200 ml culture (b) SDS-PAGE. Lane 1, low range molecular marker: rabbit muscle phosphorylase b (97400 Da), BSA (66200 Da), hen egg white ovalbumin (45000 Da), bovine carbonic anhydrase (31000 Da), soybean trypsin inhibitor (21500 Da), hen egg white lysozyme (14400 Da); lanes 2-6, 10 μ l of fractions 62-66; lane 7, 10 μ l of fraction 68; lane 8, 10 μ l of fraction 67; lanes 9 and 10, 10 μ l of fractions 69 and 70.

(a)



(b)

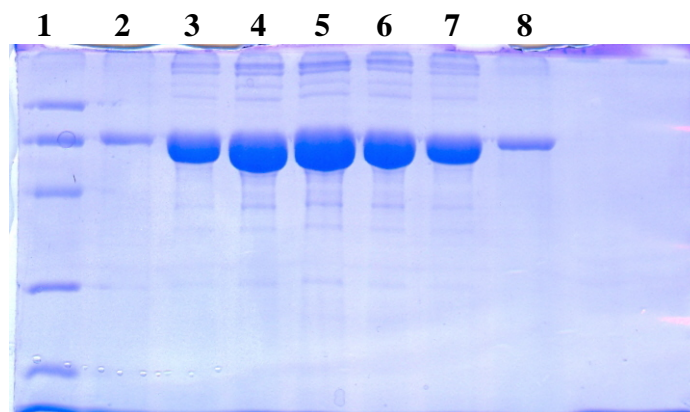
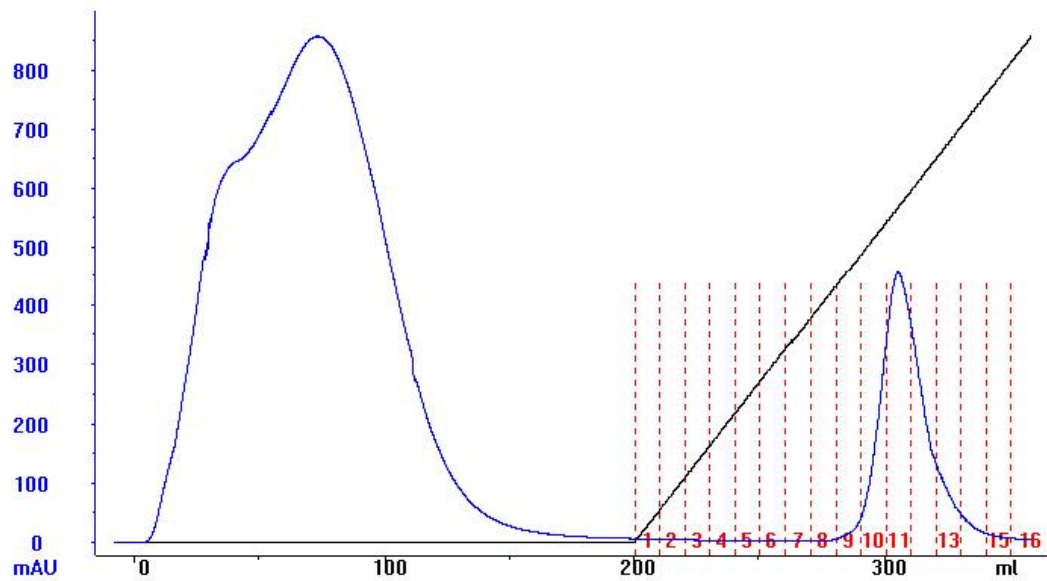


Figure 3.3 Purification of MBP PenP E166A V172C (a) Elution profile of the enzyme from cell lysate obtained from 200 ml culture (b) SDS-PAGE. Lane 1, low range molecular marker: rabbit muscle phosphorylase b (97400 Da), BSA (66200 Da), hen egg white ovalbumin (45000 Da), bovine carbonic anhydrase (31000 Da), soybean trypsin inhibitor (21500 Da), hen egg white lysozyme (14400 Da); lanes 2-8, 10 μ l of fractions 20-26.

(a)



(b)

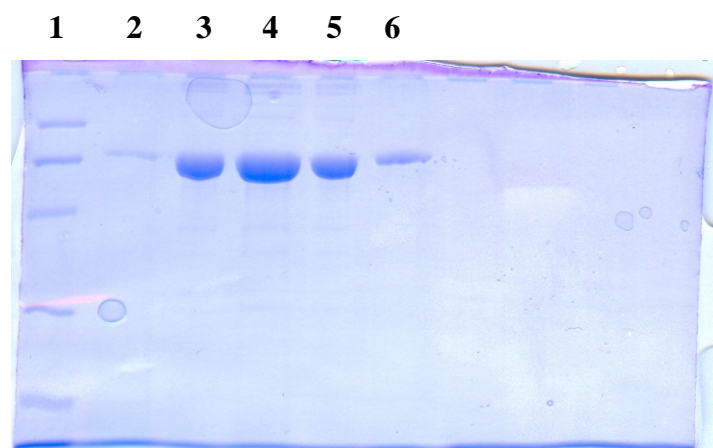


Figure 3.4 Purification of MBP-PenP E176C (a) Elution profile of the enzyme from cell lysate obtained from 200 ml culture (b) SDS-PAGE. Lane 1, low range molecular marker: rabbit muscle phosphorylase b (97400 Da), BSA (66200 Da), hen egg white ovalbumin (45000 Da), bovine carbonic anhydrase (31000 Da), soybean trypsin inhibitor (21500 Da), hen egg white lysozyme (14400 Da); lanes 2-6, 10 μ l of fractions 9-13.

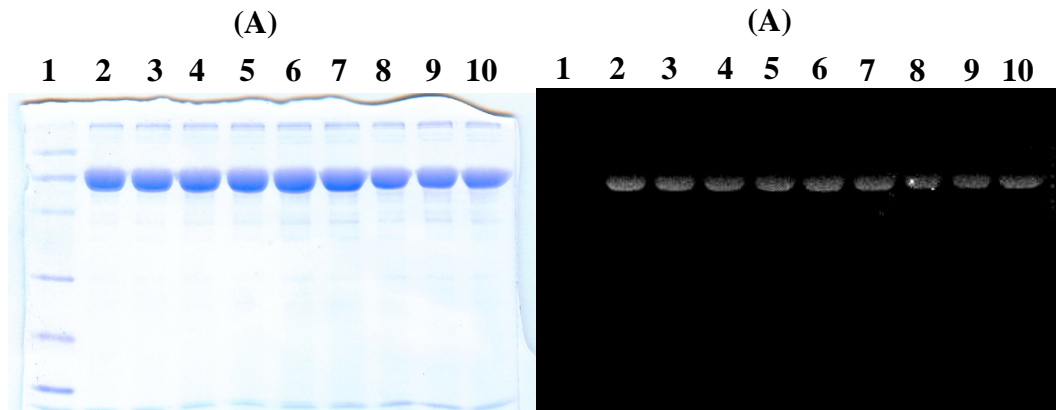


Figure 3.5 SDS-PAGE of fluorophore labeled MBP-PenP N170C, V172C and E176C stained with Coomassie-blue (a) and under UV illumination. (b). Lane 1, low range molecular marker: rabbit muscle phosphorylase b (97400 Da), BSA (66200 Da), hen egg white ovalbumin (45000 Da), bovine carbonic anhydrolase (31000 Da), soybean trypsin inhibitor (21500 Da), hen egg white lysozyme (14400 Da); lane 2, MBP-PenP N170Cb; lane 3, MBP-PenP N170Cf; lane 4, MBP-PenP N170Cr; lane 5, MBP-PenP V172Cb; lane 6, MBP-PenP V172Cf; lane 7, MBP-PenP V172Cr; lane 8, MBP-PenP E176Cb; lane 9, MBP-PenP E176Cf; lane 10, MBP-PenP E176Cr

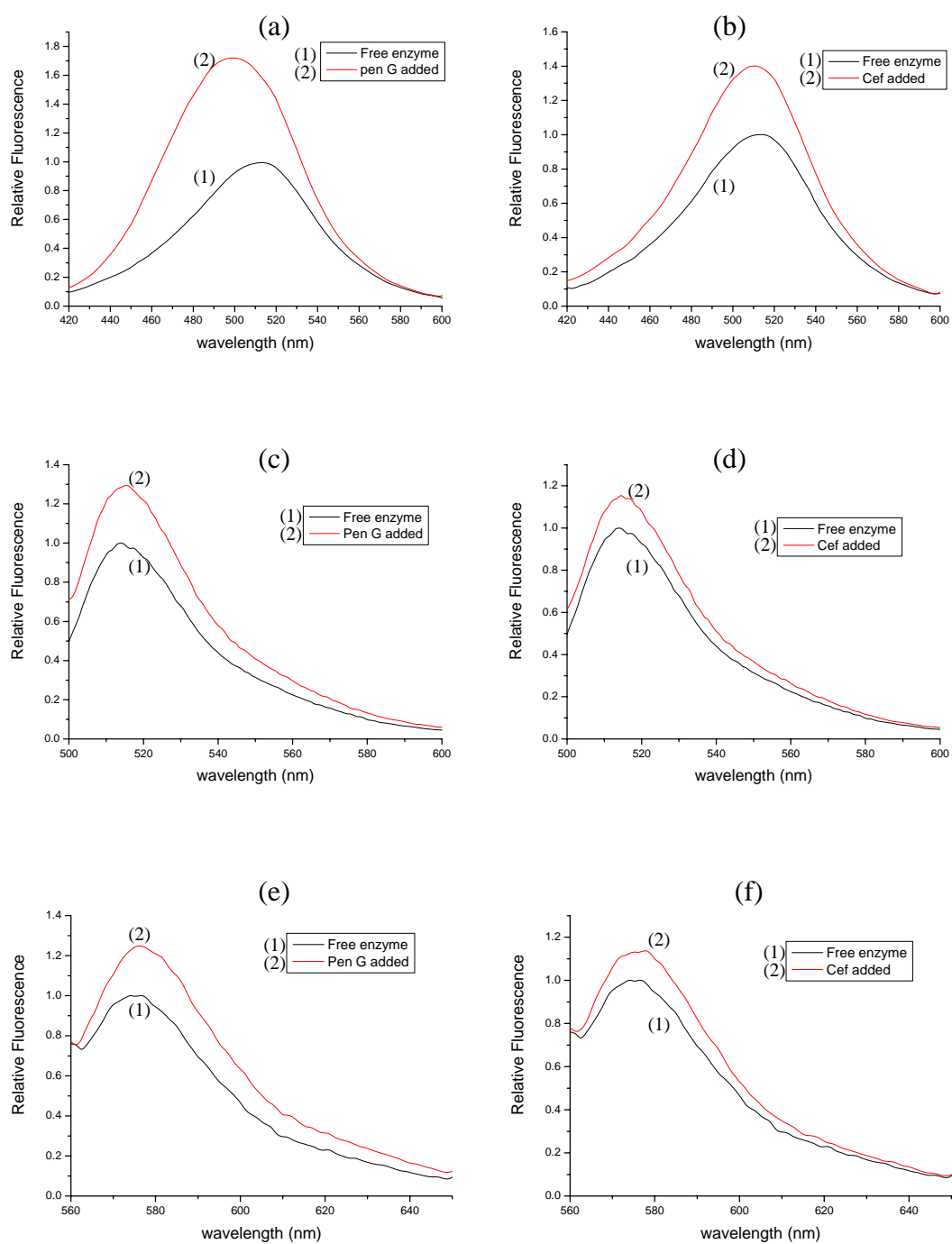


Figure 3.6 Fluorescence spectra of PenP N170C labeled with badan ((a) and (b)), FM ((c) and (d)), and TMRM ((e) and (f)), in the presence of 2 mM penicillin G and cefuroxime.

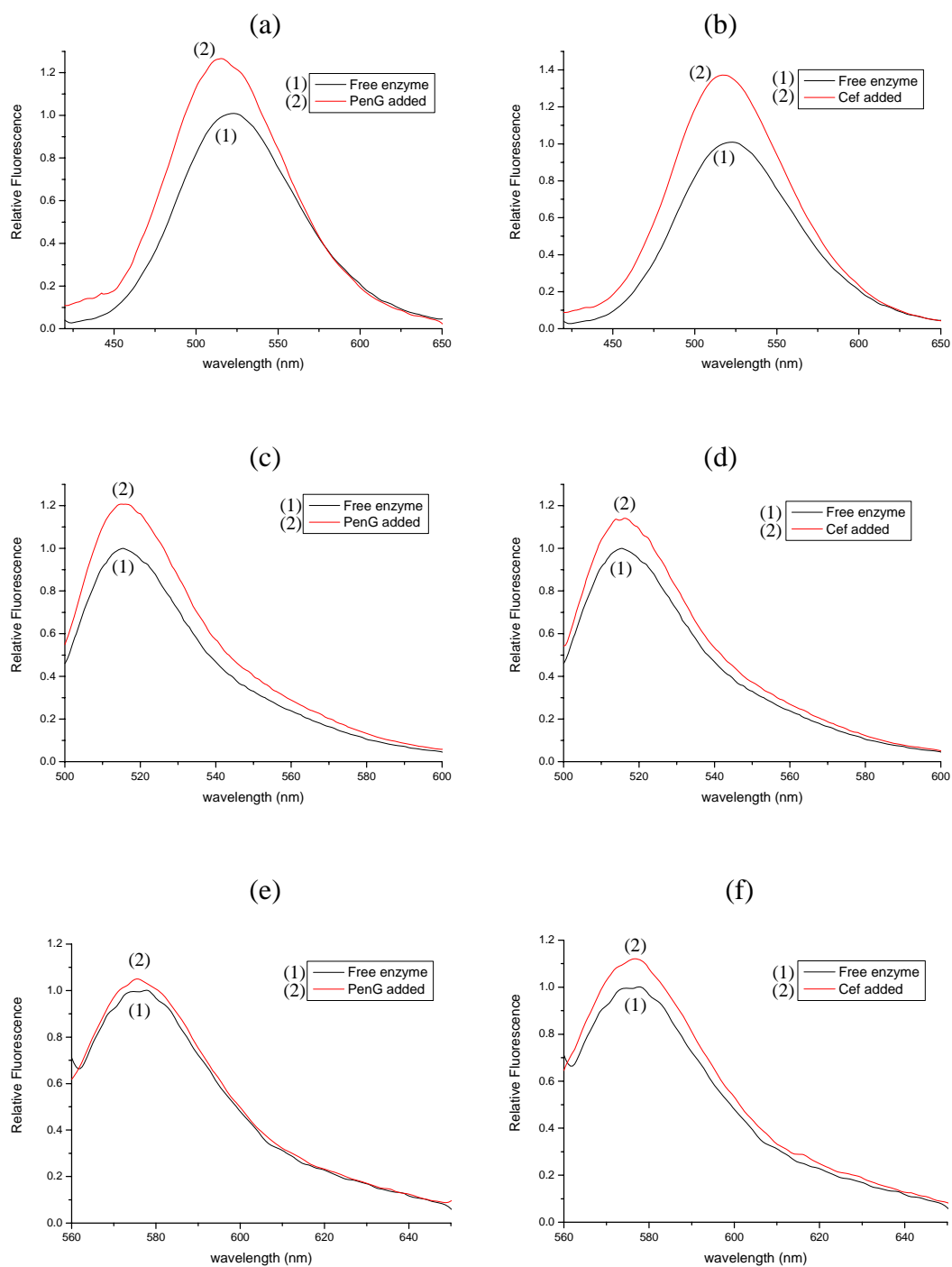


Figure 3.7 Fluorescence spectra of PenP V172C labeled with badan ((a) and (b)), FM ((c) and (d)), and TMRM ((e) and (f)), in the presence of 2 mM penicillin G and cefuroxime.

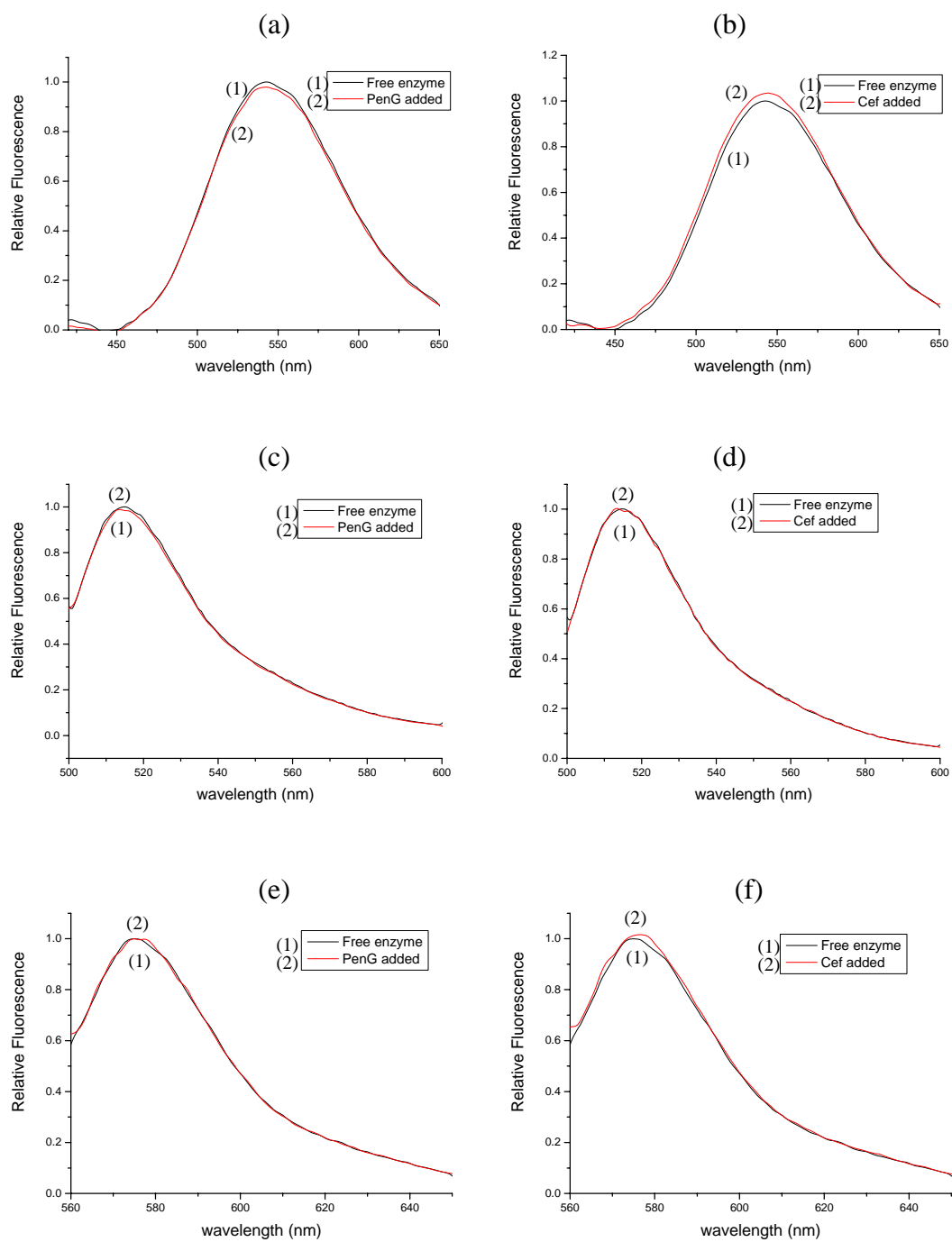


Figure 3.8 Fluorescence spectra of PenP E176C labeled with badan ((a) and (b)), FM ((c) and (d)), and TMRM ((e) and (f)), in the presence of 2 mM penicillin G and cefuroxime.

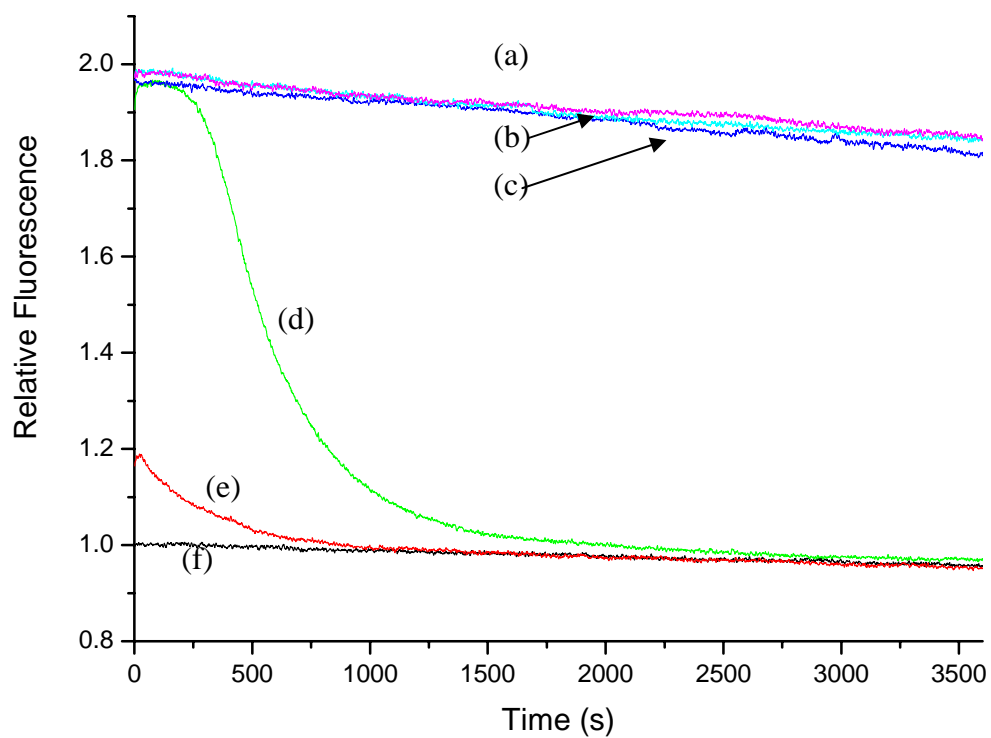


Figure 3.9 Time dependent fluorescence measurements of PenP N170Cb in the presence of penicillin G, (a) 10^{-4} M, (b) 10^{-5} M, (c) 10^{-6} M, (d) 10^{-7} M, (e) 10^{-8} M, and (f) free enzyme

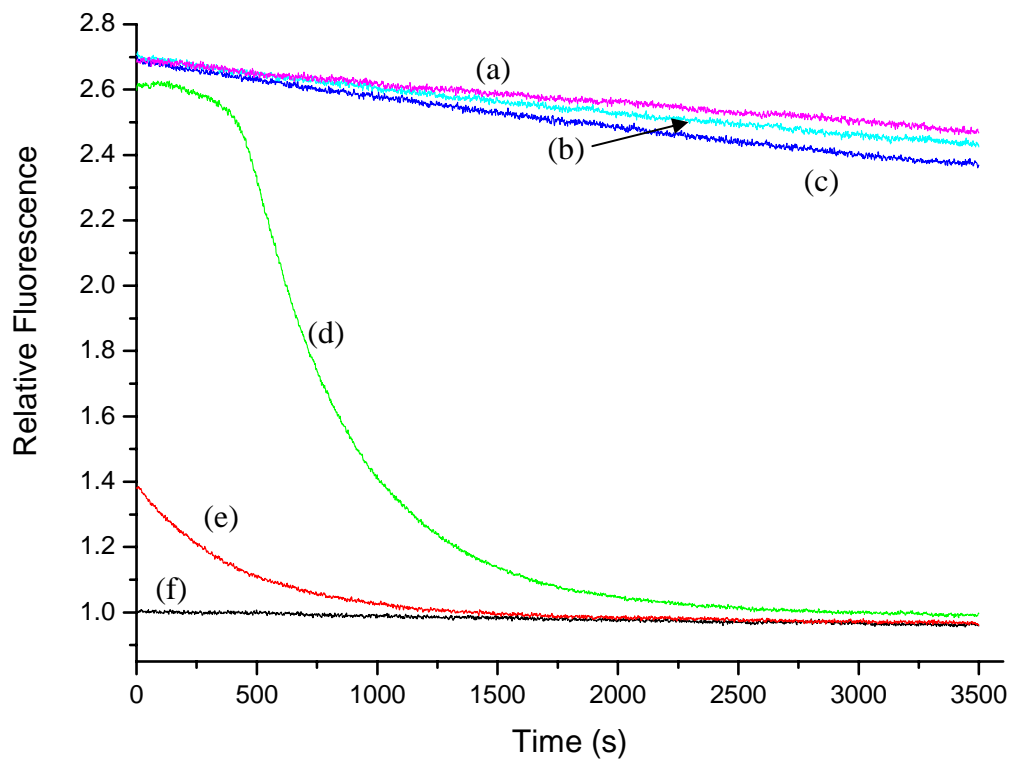


Figure 3.10 Time dependent fluorescence measurements of PenP N170Cb in the presence of penicillin V, (a) 10^{-4} M, (b) 10^{-5} M, (c) 10^{-6} M, (d) 10^{-7} M, (e) 10^{-8} M, (f) and free enzyme

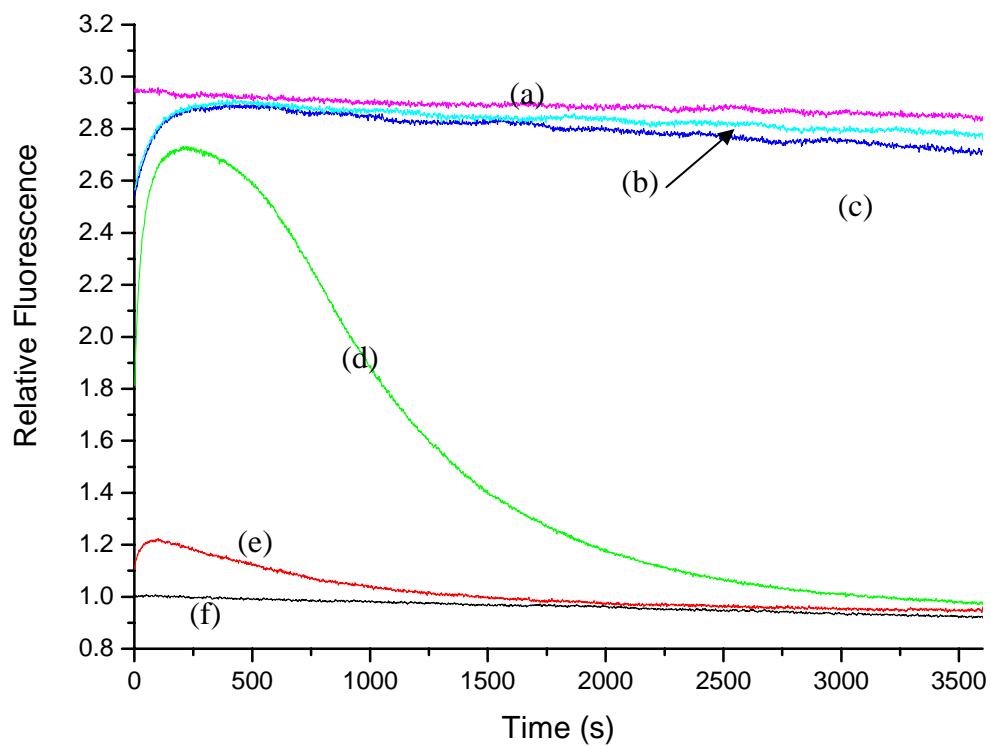


Figure 3.11 Time dependent fluorescence measurements of PenP N170Cb in the presence of ampicillin, (a) 10^{-4} M, (b) 10^{-5} M, (c) 10^{-6} M, (d) 10^{-7} M, (e) 10^{-8} M, and (f) free enzyme

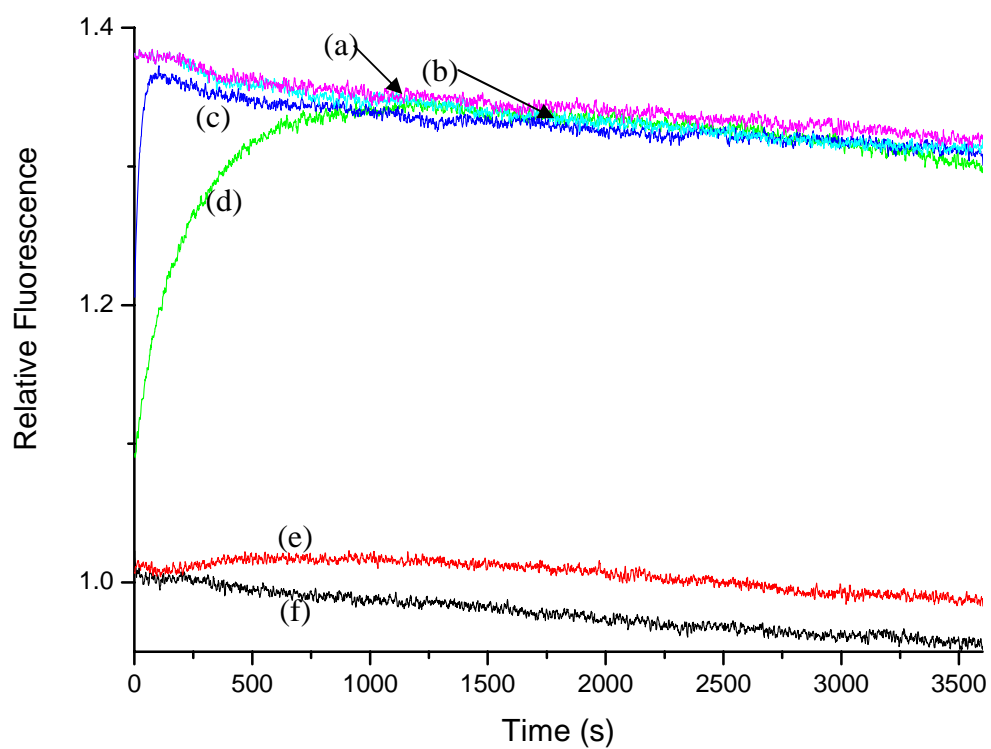


Figure 3.12 Time dependent fluorescence measurements of PenP N170Cb in the presence of cefuroxime, (a) 10^{-4} M, (b) 10^{-5} M, (c) 10^{-6} M, (d) 10^{-7} M, (e) 10^{-8} M, and (f) free enzyme

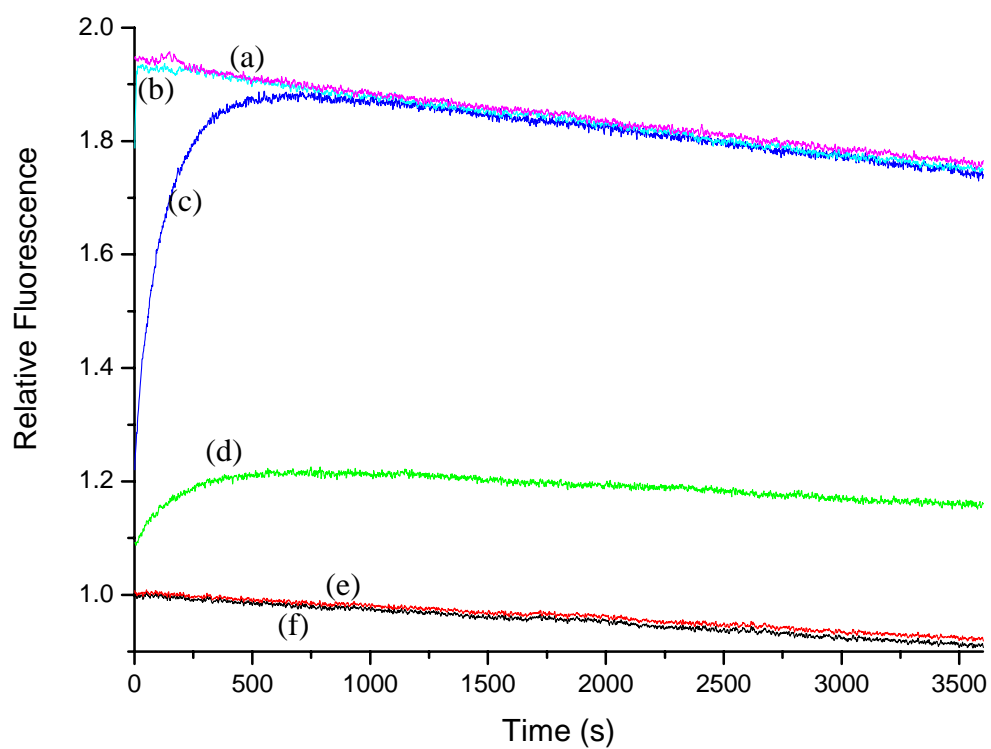


Figure 3.13 Time dependent fluorescence measurements of PenP N170Cb in the presence of cefoxitin, (a) 10^{-4} M, (b) 10^{-5} M, (c) 10^{-6} M, (d) 10^{-7} M, (e) 10^{-8} M, and (f) free enzyme

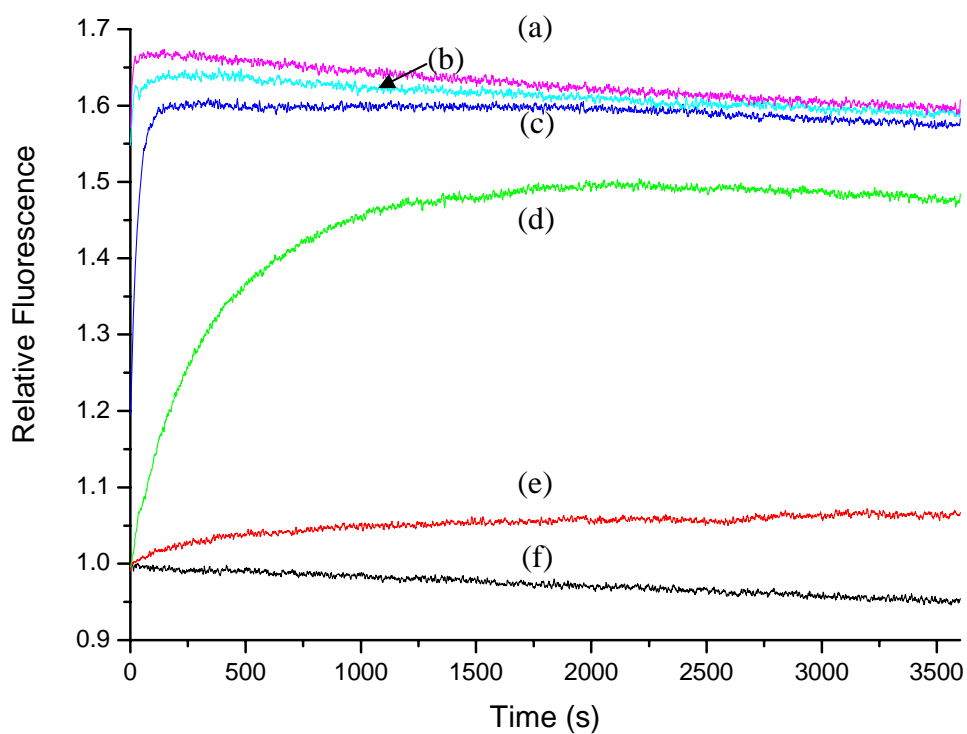


Figure 3.14 Time dependent fluorescence measurements of PenP N170Cb in the presence of moxalactam, (a) 10^{-4} M, (b) 10^{-5} M, (c) 10^{-6} M, (d) 10^{-7} M, (e) 10^{-8} M, and (f) free enzyme

3.4. Discussion

3.4.1. Fluorescence signal of the labeled MBP-PenP cysteine mutants

In the rational design of β -lactamase fluorescent biosensors, it is believed that the position and the orientation of the fluorophore label are very important to the fluorescence signal generation. The fluorophore should be close to and pointing towards the active site. In addition, the position at which the fluorophore located should be flexible for re-orientation upon substrate binding. Although the position of the cysteine-mutated residue with fluorophore label cannot be easily figured out, it is believed that these modifications would not greatly alter the configuration of the residue. Therefore, the position and orientation of the fluorophore label can be estimated from the X-ray crystal structure.

In this study, three amino acid residues on the flexible Ω -loop with different distances from the active site and side chain orientation were selected. The distance between the active site and amino acid residue were calculated (between C α of Ser70 and C α of amino acid residue, based on PenP crystal structure 4BLM) and listed in Table 3.2.

E176 is the furthest residue from the active site among the three selected residues, and the side chain is pointing towards the solvent. As expected, no fluorescence signal can be observed from all fluorophore-labeled E176C mutants. V172 is a residue closer to the active site but has little role in substrate binding and catalysis. The side chain of this residue is pointing towards the end of the Ω -loop and neither to the active site nor to the solvent. Indeed, the side chain is buried by surrounding residues and has not enough space to accommodate fluorescence label. Therefore, the conformation of Ω -loop should be changed after labeled with fluorophore at V172C. Interestingly, there are significant fluorescence signals in badan labeled V172C but only weak or no fluorescence signals were observed in FM and TMRM labeled V172C. A possible reason could be the relatively small size of badan which has only a mild steric effect on the Ω -loop and therefore may still accommodate the binding of substrates and hence experiencing conformation change without much disturbance of the active site. The larger size of FM and TMRM may totally disturb the conformation of the Ω -loop, forcing FM and TMRM label to stay outside the active site.

Although the side chain of N170 is pointing exactly to the active serine residue and is not buried by other residues, the nearby area is still relatively crowded. This area may accommodate the small badan but not the larger FM and TMRM. Actually,

the fluorescence signal of N170Cb is the largest among all these PenP cysteine mutants, but N170Cf and N170Cr give no fluorescence signal to penicillin G and only very weak signal to cefuroxime.

It should be noted that the fluorescence signal of PenP N170Cb is slightly better than PenP E166Cb, which has only about 80% increase in fluorescence intensity upon addition of penicillin G. In addition, the shift in emission maximum of both biosensors are similar. Before the addition of penicillin G, the emission maximum of both E166Cb and N170Cb are 513 nm, but that for N170Cb shifts to 498 nm and E166Cb to 500 nm. This difference in blue shift of emission maximum indicates that the badan in N170Cb might be slightly more hydrophobic than E166Cb. However, these still could not explain the difference in fluorescence signal between the two fluorescent biosensors. One possible reason is that the fluorescence of E166Cb is quenched by some amino acid residues which may be closer to badan at position 166 than at position 170.

Table 3.2 Distance of different residues from active residue Ser-70

| Residue | Distance from Ser70 (Å) |
|---------|-------------------------|
| E166 | 8.7 |
| N170 | 8.1 |
| V172 | 12.9 |
| E176 | 17.4 |

3.4.2. Time dependent fluorescence signal of MBP-PenP N170Cb

To evaluate the applicability of PenP N170Cb for the detection of β -lactam antibiotics, different penicillins and cephalosporins were used for time dependent fluorescence measurements. The overall time profile in these measurements is similar to E166Cb, which follows the Michaelis-Menten reaction mechanism and is characterized by a three phase profile. The initial rising phase is due to the increasing concentration of enzyme-substrate complex, of which the formation is responsible for generation of the fluorescence signals. In the case of penicillins, the rate of complex formation is so rapid that the rising phase cannot be observed. For cephalosporins the rising phase is also too rapid to be monitored at high substrate concentration but is observable at low substrate concentration. The second phase of the time dependent fluorescence measurements appears to be a plateau with no change in fluorescence during a certain period of time. This phase occurs after the fluorescence signal has reached the maximum level, at which the concentration of enzyme-substrate complex is equal to the total enzyme concentration. For convenience, "saturated" is used to describe the signal of this state. The length of this phase is dependent on the concentration of the substrate and also the rate of hydrolysis of the substrate by enzyme mutant.

In general, penicillins are hydrolyzed more rapidly, and therefore, the fluorescence signal leaves the plateau phase earlier than cephalosporins. The last phase is the declining phase, which indicates the concentration of antibiotics has decreased to a level that is comparable to N170Cb. Actually, at low concentration of penicillins (10^{-7} M), only the declining phase can be observed. It is because a significant portion of substrate is hydrolyzed and concentration of enzyme-substrate complex does not increase to saturated signal level. Although the fluorophore was labeled at different positions, the time profile of fluorescence signal of E166Cb and N170Cb are very similar. Both of them showed a fast declining phase for penicillins and a slow declining phase for cefuroxime. This indicates that the presence of fluorophore at different positions have little effect on the decrease in fluorescence.

However, the sensitivity of PenP N170Cb and PenP E166Cb (PenP N170Q E166Cb) towards different antibiotics are quite different. The overall fluorescence signal of PenP N170Cb are larger than PenP E166Cb, for example, the change in fluorescence in the presence of penicillin V is almost 3 folds that of PenP N170Cb, where PenP E166Cb and PenP N170Q E166Cb show not more than a 2 folds change. In addition, PenP E166Cb shows no fluorescence signal after mixing with cefoxitin and ampicillin, but both of them can be successfully detected by PenP N170Cb. The

difference indicate that the fluorescence signal of PenP N170Cb is less substrate dependent and is a more universal biosensor than PenP E166Cb and PenP N170Q E166Cb.

The difference in fluorescence intensity and emission maximum between the two biosensors in detecting ampicillin is quite interesting, because E166Cb give no signal but N170Cb give the strongest signal. This cannot be easily explained because the exact position of the fluorophore is not known, however, the structure of the antibiotic can provide some clues to this phenomenon. The only difference between ampicillin and penicillin G is the amino group on the 7α side-chain. This amino group should be positively charged in this environment (pH 7, 50 mM potassium phosphate buffer) which can affect the local conformation of the Ω -loop. P167 which is also positively charged is right next to E166C with the badan label in PenP E166Cb. The repulsion between the proline and ampicillin may hinder the badan fluorophore to approach the hydrophobic pocket and leave it in a more solvent exposed environment. In PenP N170Cb, the amino acid residues next to position 170 are leu-169 and glu-171 are not likely to have interaction with the positive charge on ampicillin. The hydrophobic and neutral-charge leu-169 should have only very weak interaction with the positive charge whereas glu-171 should have a large spatial distance from the bound

ampicillin as the side chain of glu-171 is pointing outward to the solvent environment. Therefore, there is no strong charge-charge interaction which might hinder the fluorophore to get into the less solvent exposed binding pocket. Furthermore, the additional positive charge on ampicillin could destabilize the excited state resulting in significantly larger fluorescence signal of N170Cb in detecting ampicillin than penicillin G.

3.5 Concluding remarks

Three different PenP β -lactamase mutants, E166A/N170C, E166A/V172C, E166A/E176C, have been successfully expressed, purified and labeled with badan, FM and TMRM. These nine labeled mutants were tested for fluorescence response to penicillin G and cefuroxime. The most sensitive labeled mutant, E166A/N170Cb, was selected for a more detail study.

Although attaching fluorophores at different positions on the Ω -loop of PenP β -lactamase did not result in a very significant improvement in fluorescence signal, it provides some important information for biosensor construction. PenP β -lactamase based fluorescent biosensor can be constructed by placing fluorophore at positions other than 166, and the fluorescence signal can be better than the labeled PenP E166C mutant. This modification may be applied to other β -lactamase based fluorescent biosensors. The site of the fluorophore labeling is also important to the behavior of the biosensor and positions other than 166 may only be suitable for some fluorophores (such as badan) but not the other (such as FM and TMRM). Therefore, careful selection and screening have to be conducted and there is a compromise between the position and the fluorophore size.

Chapter 4

Fluorescent biosensors based on some modified TEM β -lactamases

4.1 Introduction

The TEM β -lactamase family is probably the most important β -lactamase family, not just because of the largest number of mutants, but also of the wildly spread and clinical dominance [87-89]. The earliest member of this β -lactamase family, R-TEM, was identified from a female patient called Temoniera [90, 91], who was infected by penicillin-resistant *E. coli*. This β -lactamase was encoded in a transferable β -lactam resistance factor (R-factor or R-plasmid) [90, 92], and thus “R” was used to denote this enzyme’s location on the R-plasmid. Later, different β -lactam R-factors were identified. Another TEM β -lactamase showing a single point mutation from R-TEM but with different isoelectric point was identified in these new R-factors and designated as TEM-2 [93, 94]. R-TEM was therefore re-named as TEM-1. TEM-3 (CTX-1), the next member in this family reported in 1987, showed a high level hydrolytic activity on extended spectrum β -lactam antibiotics (third generation β -lactam antibiotics), and was the first identified TEM extended spectrum β -lactamase (ESBL) [95, 96]. After identifying these naturally occurring TEM mutants, more and more TEM family β -lactamases were isolated from different drug resistant pathogens [97-99].

Jacoby and Bush have listed out all the sequence of clinically isolated TEM β -lactamases at the Lahey Clinic website (<http://www.lahey.org/studies/temtable.asp>). The latest update in June 2008 listed 161 TEM β -lactamases (although some of them were duplicated). The emergence of a large number TEM mutants is a result of the abuse use of β -lactamase inhibitor or third generation β -lactam antibiotics (extended spectrum β -lactam antibiotics) [100, 101]. Many of these mutants are inhibitor resistant (thus named as Inhibitor Resistant TEM, IRT) or have a high activity on ceftazidime (CAZ) or cefotaxime (CTX) (named as extended spectrum β -lactamase, ESBL) [98]. The substrate profile and biochemical properties of each mutant have been studied in details and the references for each mutant are also listed in the Lahey Clinic website.

Among various TEM β -lactamases, the ESBLs have active sites that are enlarged to accommodate the much larger cephalosporins. Moreover, the enlarged active site may also allow the fluorophore to flip deeper into the enzyme if ESBLs are modified to be fluorescent biosensors. This might reduce the solvent exposure area and suppress the background fluorescence intensity of the biosensor before binding of β -lactam antibiotics. The crystal structure of TEM-52 with high resolution is available [102]. In TEM-52, mutation G238S alters the conformation of the loop between the

two β -stands (3β and 4β). This mutation provides new hydrogen bonds to the Ser 243 residue through the backbone amide and hydroxyl groups. This additional interaction pulls the loop 2.8 Å away from the original position. In addition, Glu 240 located in that loop, which is a major steric hindrance for the binding of bulky substrate to TEM-1, has rotated 155° leaving a large area for the sterically bulky cephalosporins. E104K of TEM-52 is related to the stabilization of the opened active site and M182T which is termed as “global suppressor” and is important in stabilizing the whole protein.

As discussed above, the TEM family is excellent for constructing β -lactamase fluorescent biosensors as there is a large pool of mutants with different substrate affinity and thermal stability. For example, the naturally occurring M182T mutation, which raises the protein stability, can be directly applied to the construction of TEM-based biosensor without further detailed study and characterization. Moreover, mutations which showed deteriorating effect on the protein can be avoided during the rational design of the biosensor. To check whether TEM β -lactamase is useful for biosensor construction, TEM-1 β -lactamase mutants were firstly modified and expressed. The his-tag was added at the N-terminal of the enzyme to facilitate nickel affinity chromatographic purification as described in the previous chapter. In addition,

the two cysteine residues at position 77 and 123 were mutated to be alanine to prevent multiple labeling. Two positions, E166 and V216, were selected for fluorophore labeling and the locations of the two residues in TEM-1 are shown in Figure 4.1. In addition, TEM-52 was also selected for biosensor construction in this study. Three mutations (E104K, M182T and G238S) that are characteristics of TEM-52 were added to the TEM-1 V216C mutant. The sensitivity and signal properties of the fluorophore labeled mutants were studied

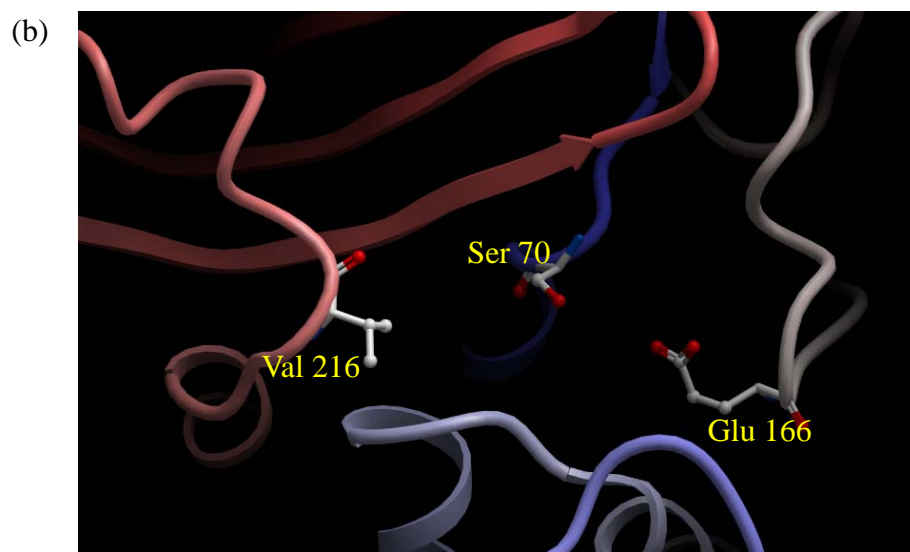
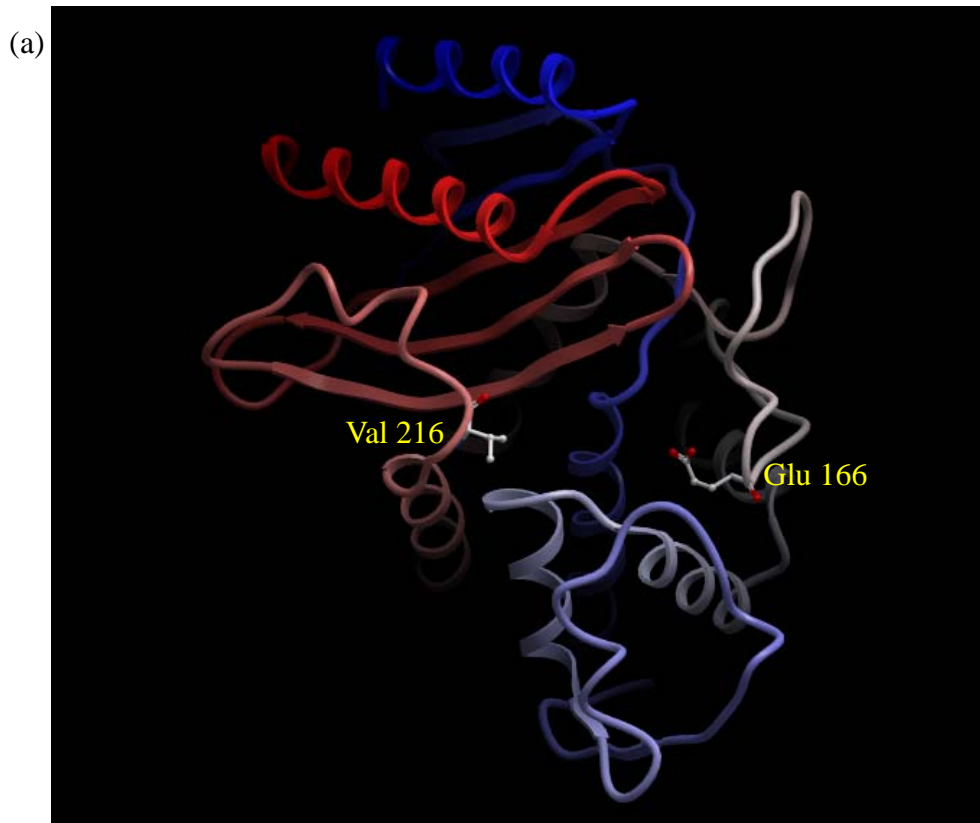


Figure 4.1 Locations of E166 and V216 in TEM-1 β -lactamase (a) and a closer view of the active site.

4.2 Methods

4.2.1 Site-directed mutagenesis and cloning of TEM cysteine mutants

pRsetK containing TEM-1 E166C and TEM-1 V216C β -lactamase mutants were obtained from Miss Kareena Tsang. In these two mutants, the two cysteine residues at position 77 and 123 were removed and replaced by alanine. Therefore, these two proteins contain no disulphide bond. To prepare TEM-52 V216C, three mutations, E104K, M182T and G238S, which are characteristic of TEM-52, were successively added to TEM-1 V216C which had previously been cloned into pRsetK as described in section 2.2.4 Primers used for these mutations are listed in Table 4.1. The vector obtained is denoted as pRsetK-TEM-52 V216C.

Table 4.1 Primers used for TEM-52 mutations

| Primers | Sequence | T _m (°C) |
|------------|---------------------------------|------------------------|
| TM-E104K-F | GAATGACTTGGTTAAATACTCACCAGTCAC | 57.9 |
| TM-E104K-R | GTGACTGGTGAGTATTTAACCAAGTCATTC | |
| TM-M182T-F | GAGCGTGACACCACGACCCCTGCAGCAATGG | 77.1 |
| TM-M182T-R | CCATTGCTGCAGGGGTCGTGGTGTCACGCTC | |
| TM-G238S-F | GATAAATCTGGAGCCAGCGAGCGTGGGTCTC | 71.4 |
| TM-G238S-R | GAGACCCACGCTCGCTGGCTCCAGATTTATC | |

4.2.2 Preparation and labeling of TEM cysteine mutants

The detailed protein expression and purification procedures were described in section 2.3 and the labeling procedures have been described in section 2.4 respectively.

4.2.3 Fluorometric measurement of the labeled TEM cysteine mutants

The steady state and time dependent fluorescence spectra of the labeled TEM mutants were recorded by the same procedures as described in section 2.5. Detailed procedures of lifetime measurement have been described in section 2.6.

4.2.4 Molecular modeling of TEM-52 V216f

Molecular modeling of TEM-52 V216Cf was performed using ICM-Pro 3.4-8a (Molsoft). TEM-52 (PDB code 1HTZ) was mutated so that the residue V216 was changed to cysteine. FM label was added to the cysteine residue afterward. All torsion angles of residues K104, Y105, K215, A217 (amino acid residues near the FM label) and also the V216C with the FM label were set to be variable. The biased probability

Monte Carlo (BPMC) minimization procedure was used for energy minimization. To figure out the position of FM label after penicillin G binding, the same BPMC minimization procedure was conducted on the model with penicillin G introduction to the active site.

4.3 Results

4.3.1 Preparation and labeling of the TEM cysteine mutants

Purification of the three mutants by nickel affinity column chromatography was monitored by SDS-PAGE and the gels are shown in Figure 4.2 - 4.4. The two proteins were purified with 95% purity. The labeling of two mutants with three fluorophores were confirmed by SDS-PAGE gel as shown in Figure 4.5 – 4.6

4.3.2 Fluorescence signals of the labeled TEM cysteine mutants

The fluorescence spectra of the labeled mutants were obtained in the presence of penicillin G and cefuroxime, which are shown in Figures 4.7 - 4.9. TEM-1 E166Cf show 60% increase in fluorescence upon addition of penicillin G and about 20% increase for cefuroxime. In the case of TEM-1 E166Cr, no significant signal can be obtained. TEM-1 V216Cf shows a better fluorescence response, even though it is only about 2 folds increase in the fluorescence intensity for detecting penicillin G. The fluorescence signal from TEM-1 V216Cr is slightly weaker than TEM-1 V216Cf.

TEM-52 V216Cb, similar to the TEM-1 V216Cb, showed no response to both penicillin G and cefuroxime. The TMRM labeled TEM-52 V216C also showed no significant change in fluorescence. TEM-52 V216Cf, however, showed the highest sensitivity with about 3.6 folds increase in fluorescence intensity in the presence of penicillin G and 1.6 folds increase in the presence of cefuroxime. This fluorescein-labeled mutant with the largest signal change was chosen for further study.

4.3.3 Fluorescence lifetimes of TEM-52 V216Cf

The fluorescence lifetimes of TEM-52 V216Cf was measured before and after the addition of penicillin G. The time-resolved fluorescence decay curves and fluorescence lifetimes are shown in Figure 4.10. The fluorescence decay can be fitted with a biexponential decay model, but addition of penicillin G significantly increases the lifetime of the shorter fluorescence decay component and also the amplitude of the longer fluorescence decay. This results in about a 3 folds increase in the average fluorescence lifetime.

4.3.4 Molecular models of TEM-52 V216Cf

The molecular model of TEM-52 V216Cf has been constructed. As shown in Figure 4.11, the FM label located in the active site is in close contact with Tyr-105. Upon binding with penicillin G, the FM label flips for about 90° and departs from the active site. This change not just results in the increase of solvent accessibility of the FM label, but also the departure of the FM label from Tyr-105.

4.3.5 Time dependent fluorescence signals of TEM-52 V216Cf

Six antibiotics (penicillin G, penicillin V, ampicillin, cefuroxime, cefoxitin and moxalactam) were chosen as substrates for TEM-52 V216Cf in order to study the time profile of fluorescence signal, which are shown in Figures 4.12 – 4.17. The fluorescence signal increased to a plateau for all cases. For penicillin type antibiotics, an increase in fluorescence was faster than the cephalosporin and was completed within 1000 s even for antibiotic concentration as low as 10^{-7} M. Unlike PenP N170Cb, no decrease in fluorescence was observed in TEM-52 V216Cf for penicillin type antibiotics except for ampicillin which showed a very slow decrease in signal at low concentration. The maximum change in fluorescence is about 3 folds in the

detection of penicillin V and ampicillin and 3.6 folds in the detection of penicillin G, where the detection limit of this class β -lactams was approximately 10^{-8} M. Cephalosporin type antibiotics showed a very slow increase in fluorescence, which lasted for the whole measurement period even at 10^{-4} M antibiotics. The maximum change in fluorescence is less than 2 folds in the case of cefuroxime, and about 2.6 folds for cefoxitin and moxalactam. The detection limit is about 10^{-6} M for cefuroxime and 10^{-7} M for cefoxitin and moxalactam.

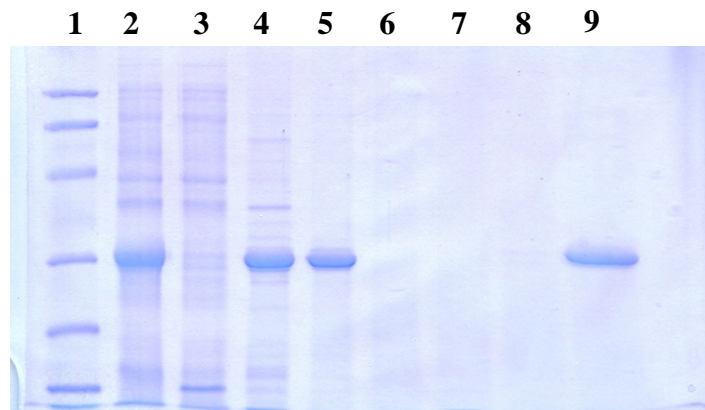


Figure 4.2 Purification profiles of TEM-1 E166C. Lane 1, low range molecular marker: rabbit muscle phosphorylase b (97400 Da), BSA (66200 Da), hen egg white ovalbumin (45000 Da), bovine carbonic anhydrase (31000 Da), soybean trypsin inhibitor (21500 Da), hen egg white lysozyme (14400 Da); lane 2, crude cell lysate; lane 3, soluble fraction of cell lysate; lane 4, insoluble fraction of cell lysate; lane 5, soluble fraction of re-folded inclusion body before loaded onto nickel-affinity column; lane 6, soluble fraction of re-folded inclusion body after passing through nickel-affinity column; lane 7, washed out by running buffer; lane 8, washed out by running buffer with 30 mM imidazole; lane 9, elution of TEM-1 E166C by elution buffer.

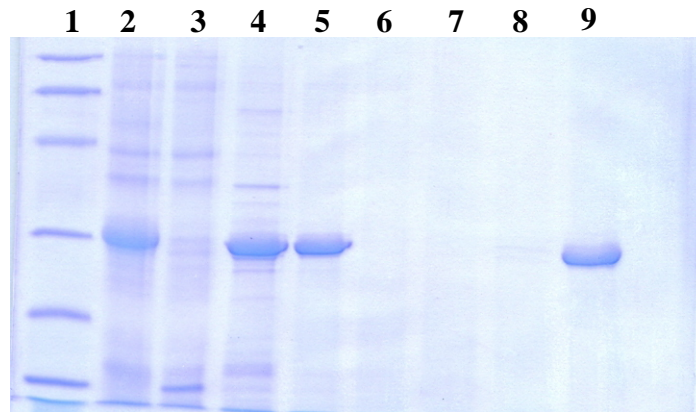


Figure 4.3 Purification profiles of TEM-1 V216C. Lane 1, low range molecular marker: rabbit muscle phosphorylase b (97400 Da), BSA (66200 Da), hen egg white ovalbumin (45000 Da), bovine carbonic anhydrase (31000 Da), soybean trypsin inhibitor (21500 Da), hen egg white lysozyme (14400 Da); lane 2, crude cell lysate; lane 3, soluble fraction of cell lysate; lane 4, insoluble fraction of cell lysate; lane 5, soluble fraction of re-folded inclusion body before loaded onto nickel-affinity column; lane 6, soluble fraction of re-folded inclusion body after passing through nickel-affinity column; lane 7, washed out by running buffer; lane 8, washed out by running buffer with 30 mM imidazole; lane 9, elution of TEM-1 E166C by elution buffer.

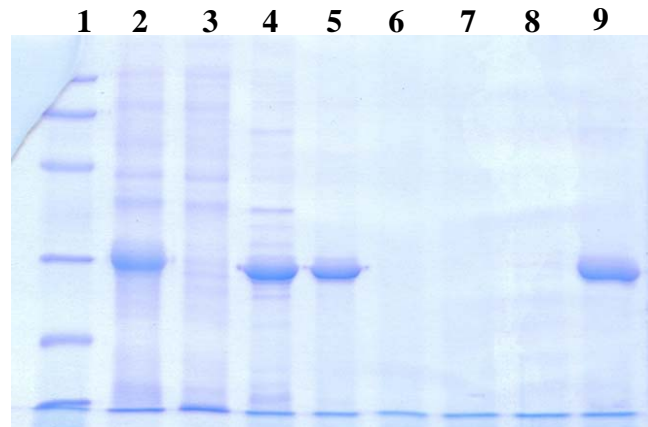


Figure 4.4 Purification profiles of TEM-52 V216C. Lane 1, low range molecular marker: rabbit muscle phosphorylase b (97400 Da), BSA (66200 Da), hen egg white ovalbumin (45000 Da), bovine carbonic anhydrase (31000 Da), soybean trypsin inhibitor (21500 Da), hen egg white lysozyme (14400 Da); lane 2, crude cell lysate; lane 3, soluble fraction of cell lysate; lane 4, insoluble fraction of cell lysate; lane 5, soluble fraction of re-folded inclusion body before loaded onto nickel-affinity column; lane 6, soluble fraction of re-folded inclusion body after passing through nickel-affinity column; lane 7, washed out by running buffer; lane 8, washed out by running buffer with 30 mM imidazole; lane 9, elution of TEM-52 V216C by elution buffer.

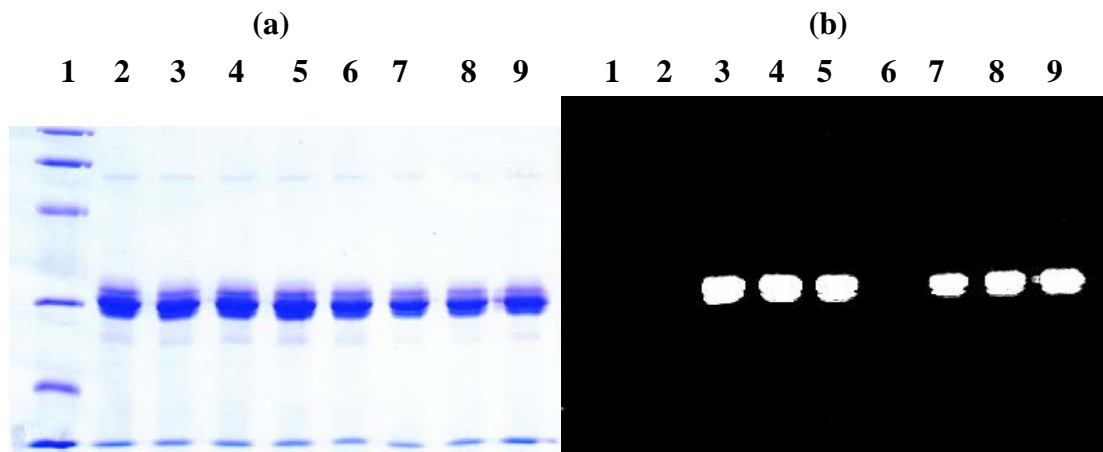


Figure 4.5 SDS-PAGE of fluorophore labeled TEM-1 E166C and V216C stained with Coomassie-blue (a) and under UV illumination (b). Lane 1, low range molecular marker: rabbit muscle phosphorylase b (97400 Da), BSA (66200 Da), hen egg white ovalbumin (45000 Da), bovine carbonic anhydrase (31000 Da), soybean trypsin inhibitor (21500 Da), hen egg white lysozyme (14400 Da); lane 2, TEM-1 E166C; lane 3, TEM-1 E166Cb; lane 4, TEM-1 E166Cf; lane 5, TEM-1 E166Cr; lane 6, TEM-1 V216C; lane 7, TEM-1 V216Cb; lane 8, TEM-1 V216Cf; lane 9, TEM-1 V216Cr.

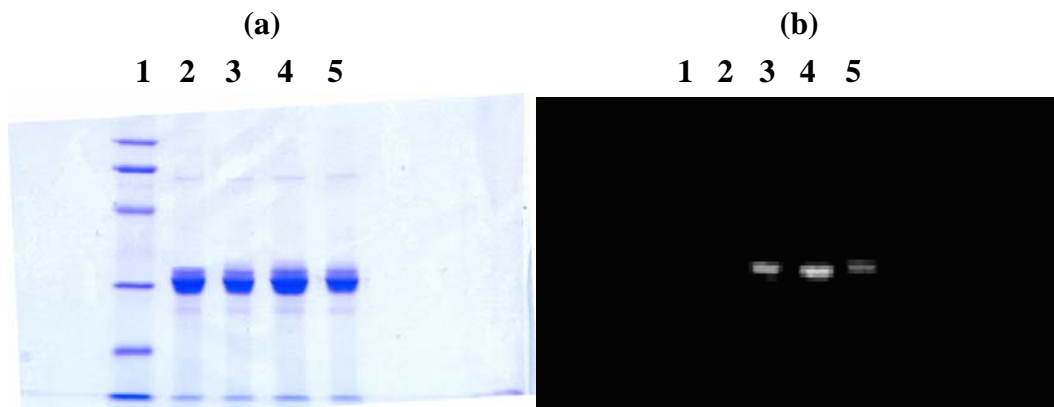


Figure 4.6 SDS-PAGE of fluorophore labeled TEM-52 V216C stained with Coomassie-blue (a) and under UV illumination (b). Lane 1, low range molecular marker: rabbit muscle phosphorylase b (97400 Da), BSA (66200 Da), hen egg white ovalbumin (45000 Da), bovine carbonic anhydrolase (31000 Da), soybean trypsin inhibitor (21500 Da), hen egg white lysozyme (14400 Da); lane 2, TEM-52 V216C; lane 3, TEM-52 V216Cb; lane 4, TEM-52 V216Cf; lane 5, TEM-52 V216Cr.

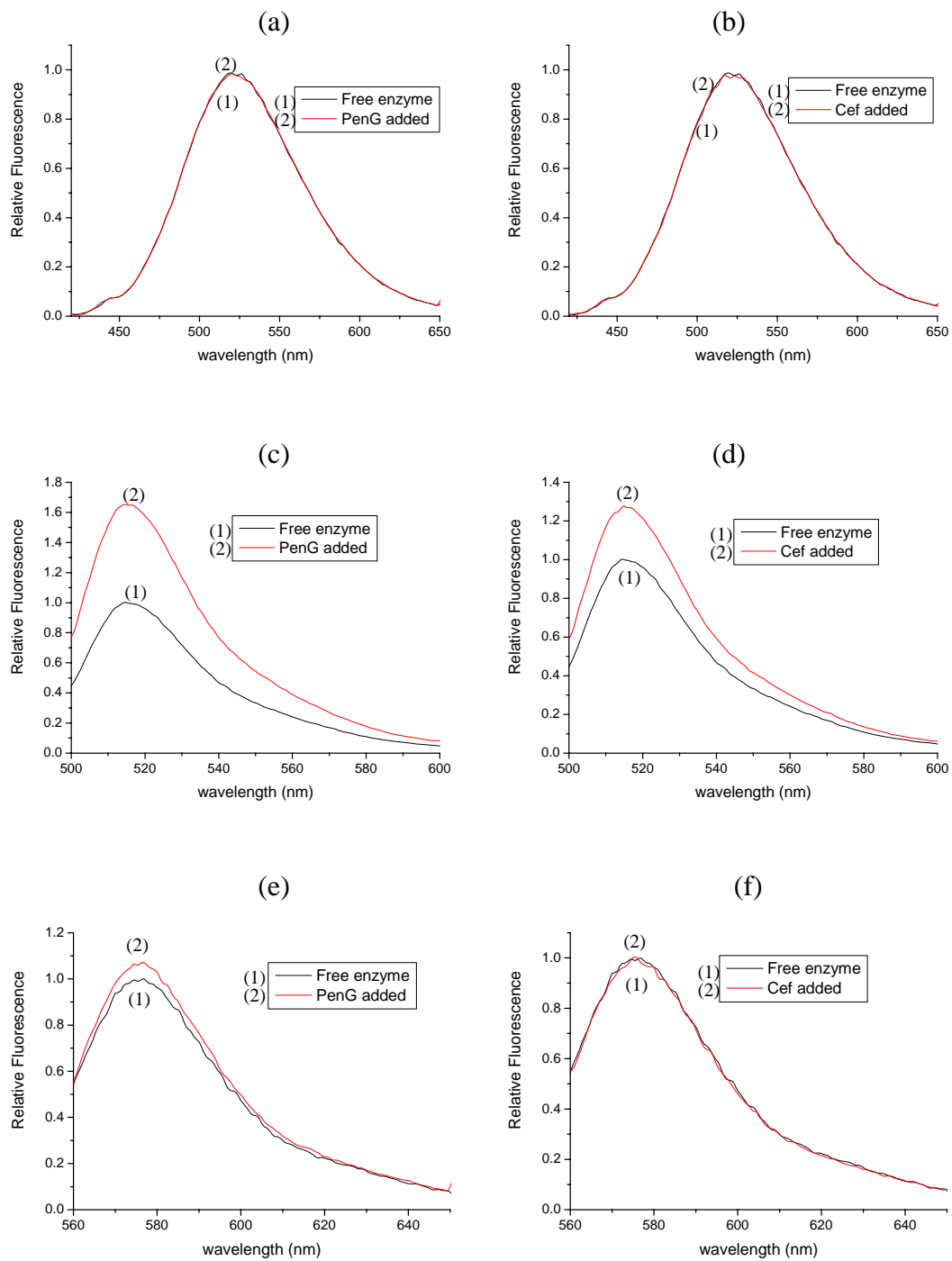


Figure 4.7. Fluorescence spectra of TEM-1 E166C labeled with badan ((a) and (b)), FM ((c) and (d)), and TMRM ((e) and (f)), in the presence of 2 mM penicillin G and cefuroxime.

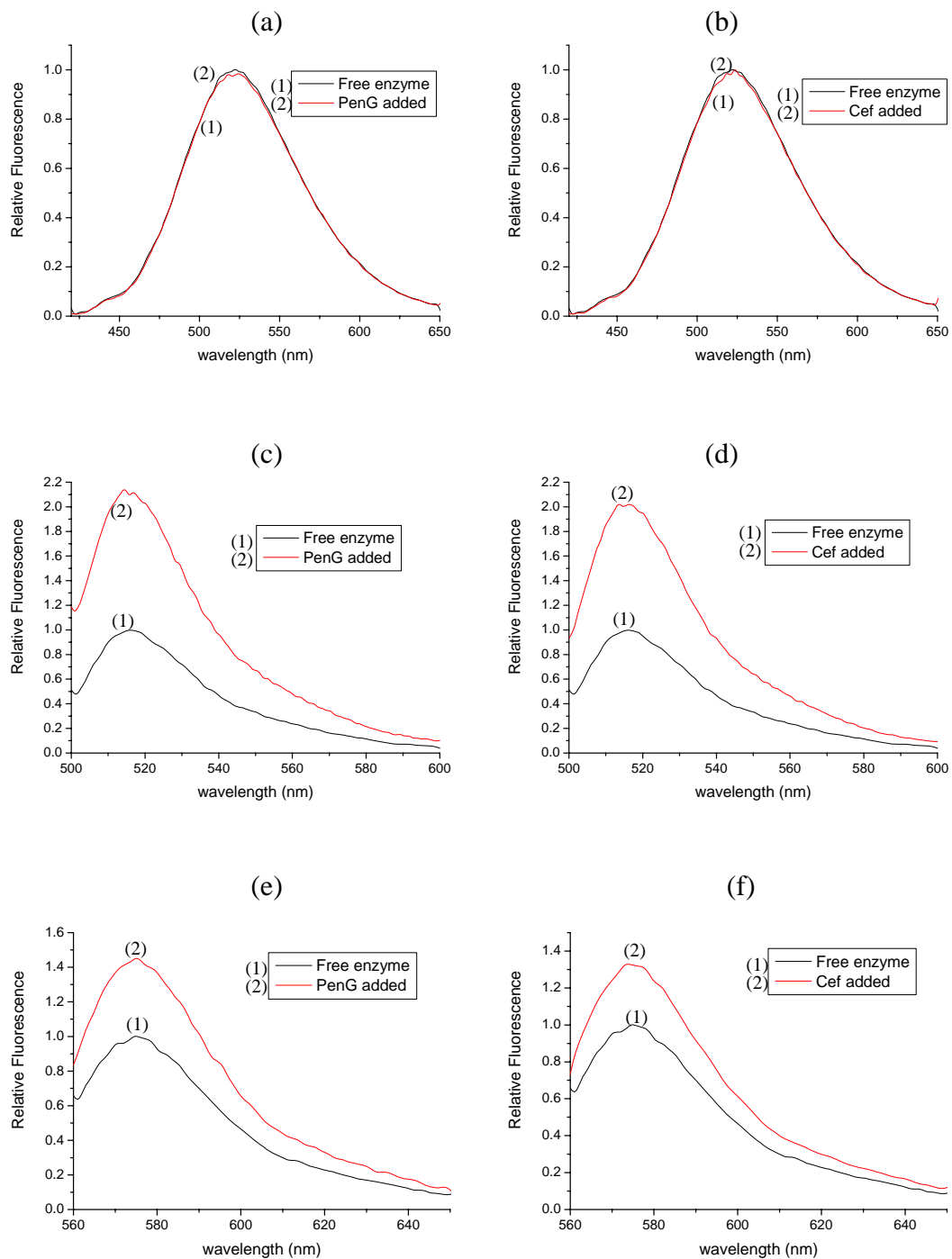


Figure 4.8. Fluorescence spectra of TEM-1 V216C labeled with badan ((a) and (b)), FM ((c) and (d)), and TMRM ((e) and (f)), in the presence of 2 mM penicillin G and cefuroxime.

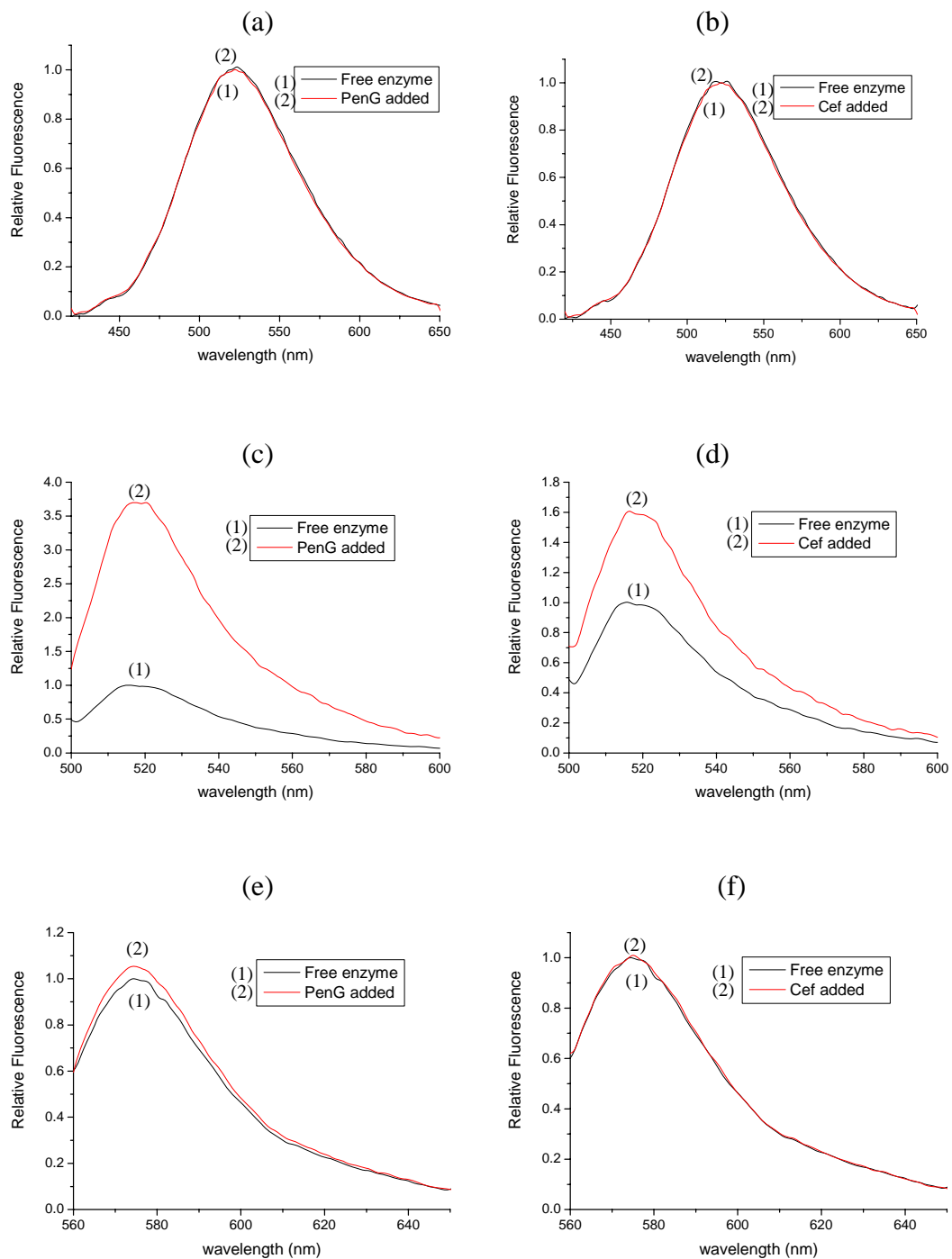


Figure 4.9. Fluorescence spectra of TEM-1 V216C labeled with badan ((a) and (b)), FM ((c) and (d)), and TMRM ((e) and (f)), in the presence of 2 mM penicillin G and cefuroxime

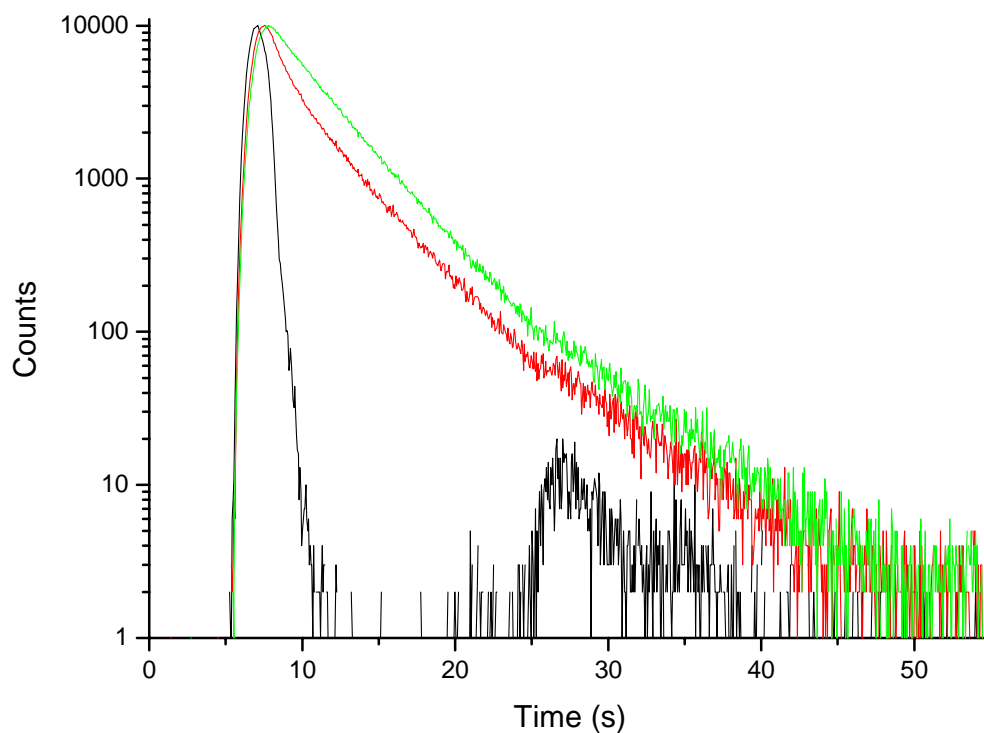


Figure 4.10 Time-resolved fluorescence decay curve of TEM-52 V216Cf in the absence (red) and presence (green) of penicillin G, the curve in black was the prompt (background scattering). Both curves were fitted with biexponential decay and the fluorescence lifetimes are tabulated below.

| | $\tau_1(\text{ns})/a_1$ | τ_2/a_2 | $\bar{\tau}$ | χ^2 |
|----------------------|-------------------------|--------------|--------------|----------|
| TEM-52 V216Cf | 0.73 / 0.71 | 3.82 / 0.29 | 1.11 | 1.34 |
| TEM-52 V216Cf + PenG | 1.77 / 0.27 | 3.93 / 0.73 | 3.35 | 1.05 |

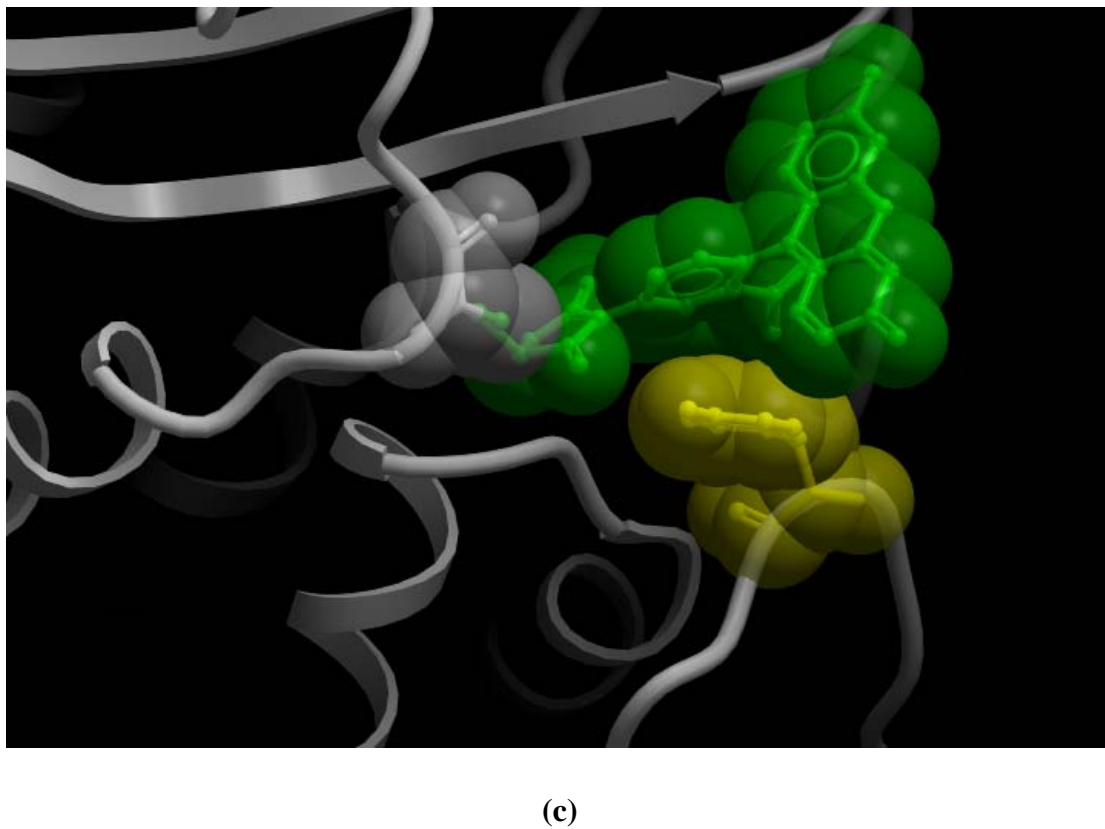
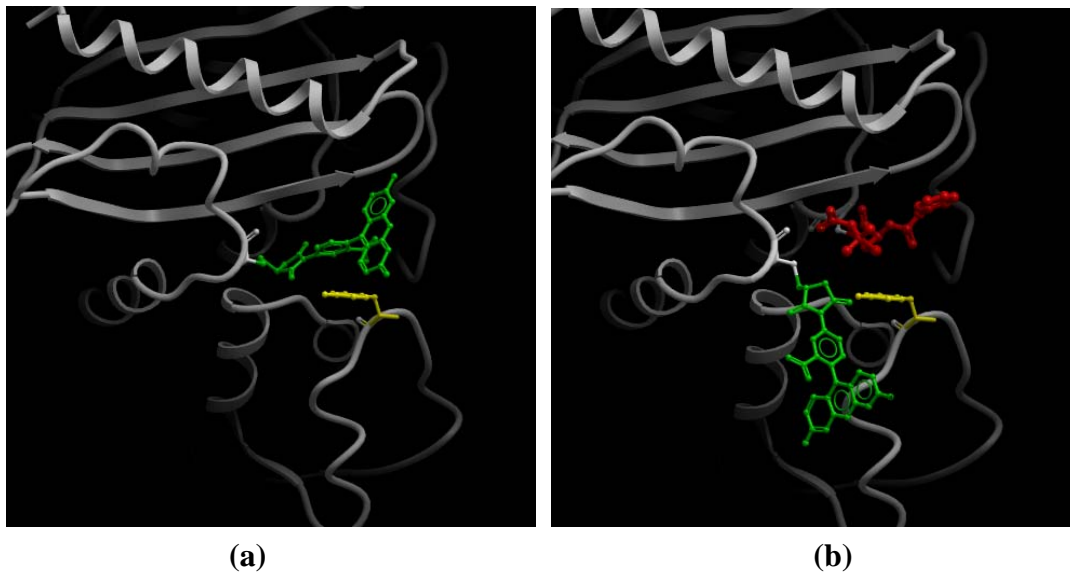


Figure 4.11 Molecular models of TEM-52 V216Cf before (a) and after (b) binding with penicillin G. (c) A closer look of FM label in the active site. The FM label, penicillin G and Tyr-105 were highlighted as green, red and yellow respectively.

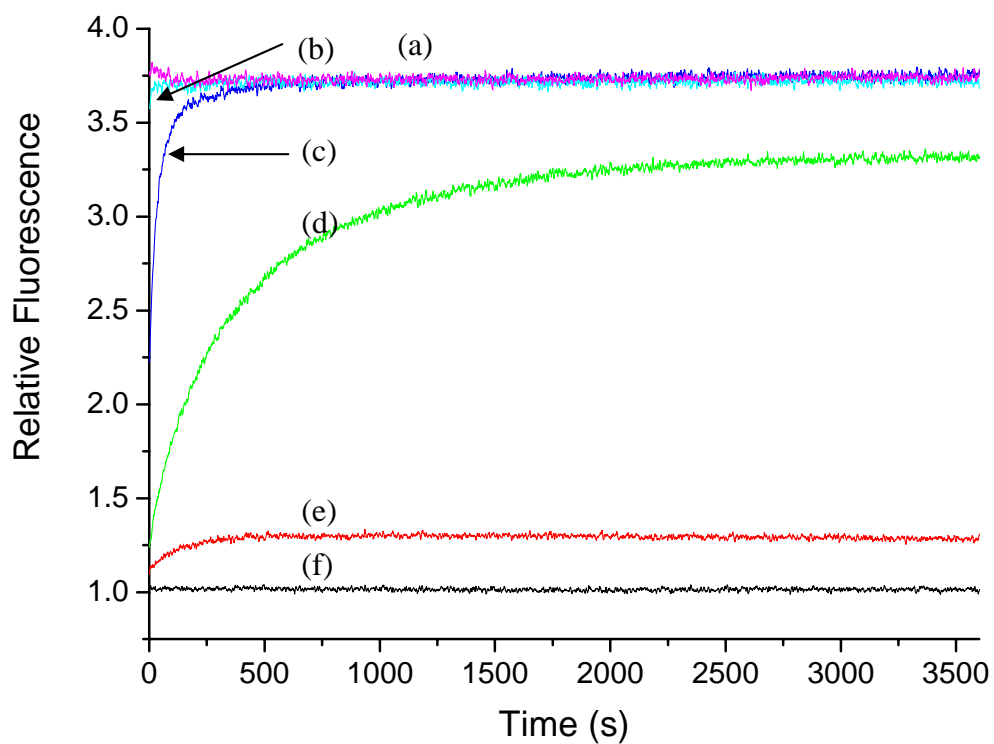


Figure 4.12 Time dependent fluorescence measurements of TEM-52 V216Cf in the presence of penicillin G, (a) 10^{-4} M, (b) 10^{-5} M, (c) 10^{-6} M, (d) 10^{-7} M, (e) 10^{-8} M, and (f) free enzyme

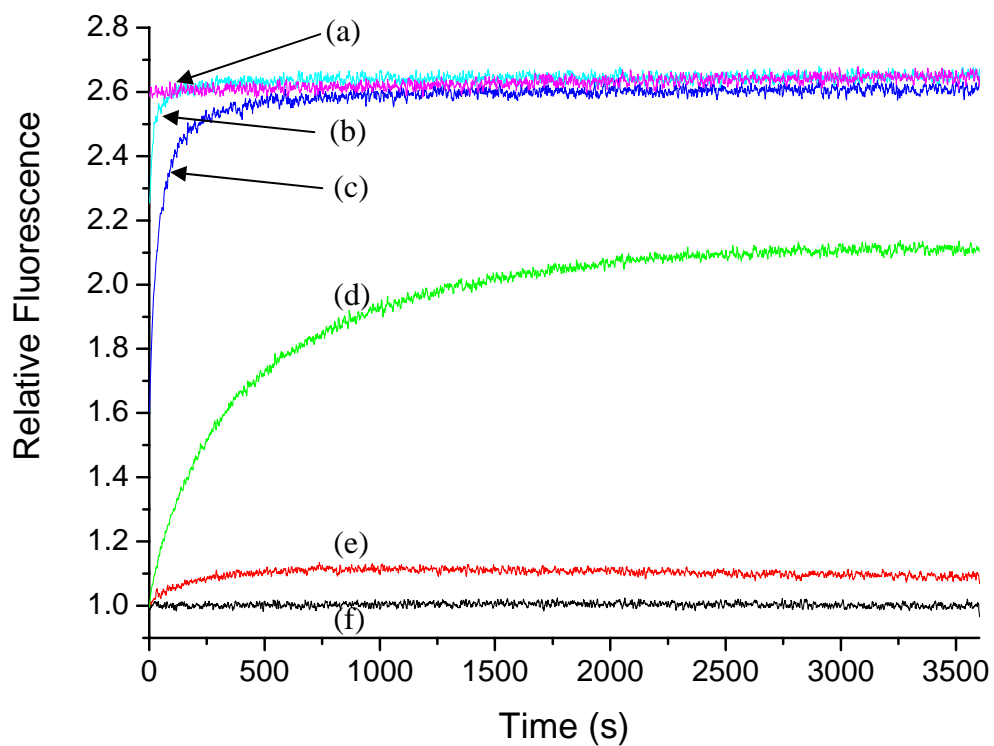


Figure 4.13 Time dependent fluorescence measurements of TEM-52 V216Cf in the presence of penicillin V, (a) 10^{-4} M, (b) 10^{-5} M, (c) 10^{-6} M, (d) 10^{-7} M, (e) 10^{-8} M, and (f) free enzyme

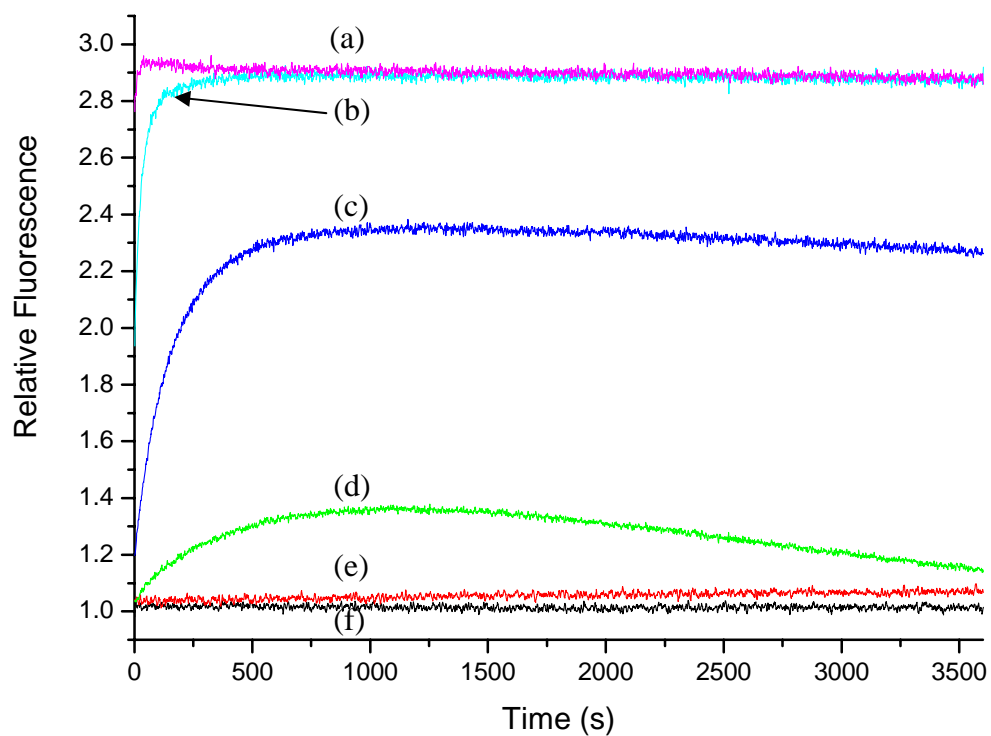


Figure 4.14 Time dependent fluorescence measurements of TEM-52 V216Cf in the presence of ampicillin, (a) 10^{-4} M, (b) 10^{-5} M, (c) 10^{-6} M, (d) 10^{-7} M, (e) 10^{-8} M, and (f) free enzyme

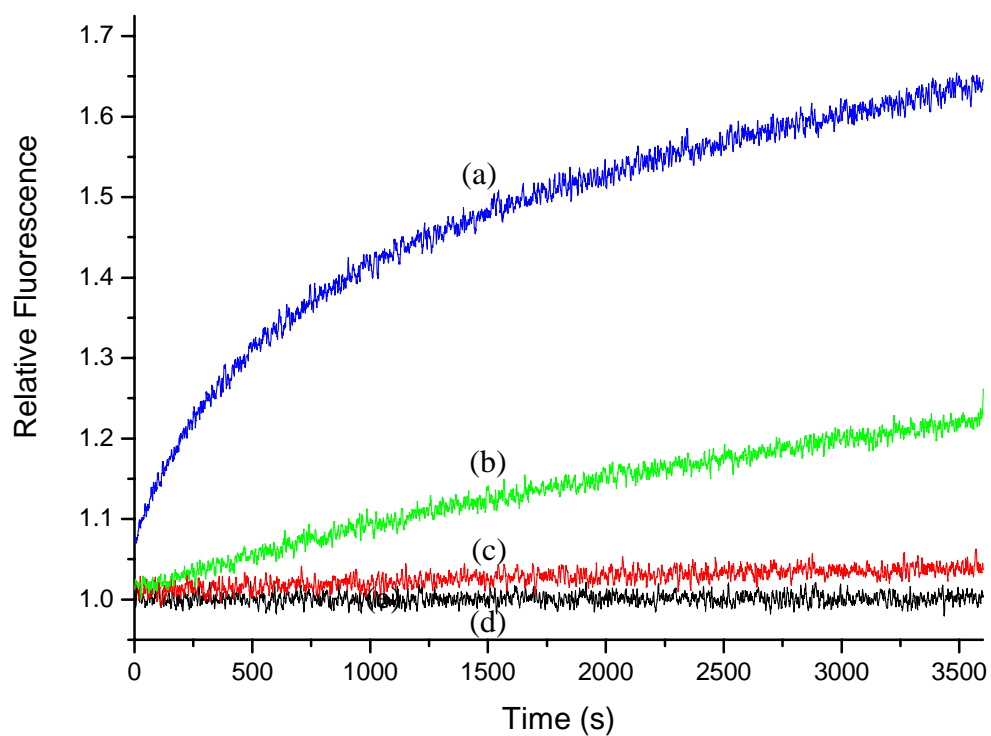


Figure 4.15 Time dependent fluorescence measurements of TEM-52 V216Cf in the presence of cefuroxime, (a) 10^{-4} M, (b) 10^{-5} M, (c) 10^{-6} M, and (d) free enzyme

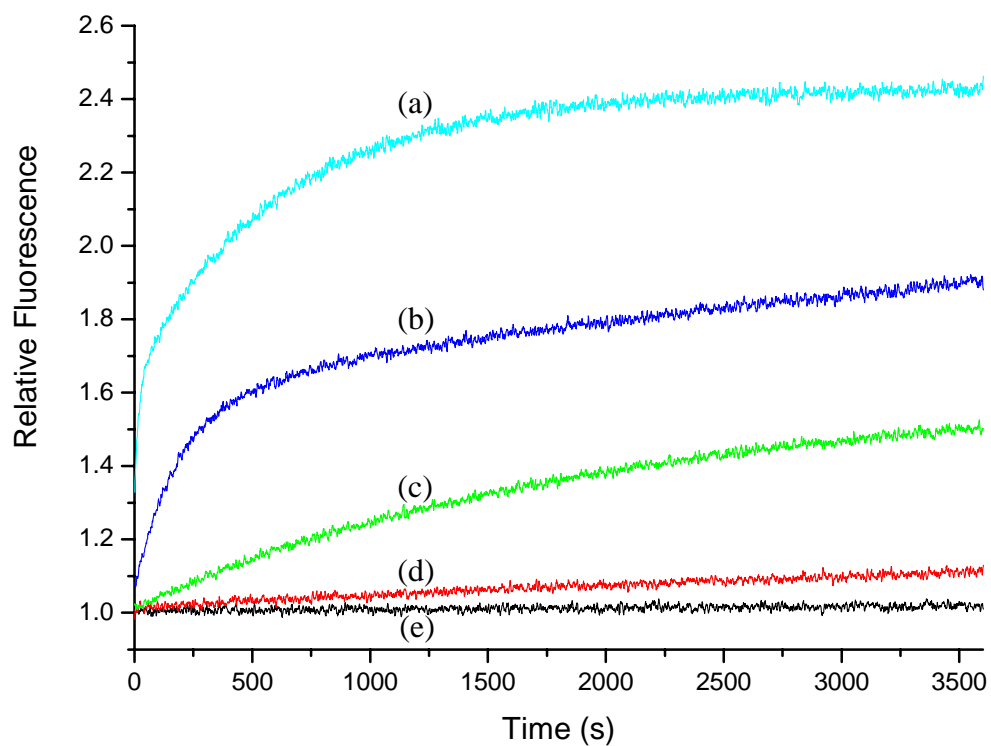


Figure 4.16 Time dependent fluorescence measurements of TEM-52 V216Cf in the presence of cefoxitin, (a) 10^{-4} M, (b) 10^{-5} M, (c) 10^{-6} M, (d) 10^{-7} M, and (e) free enzyme

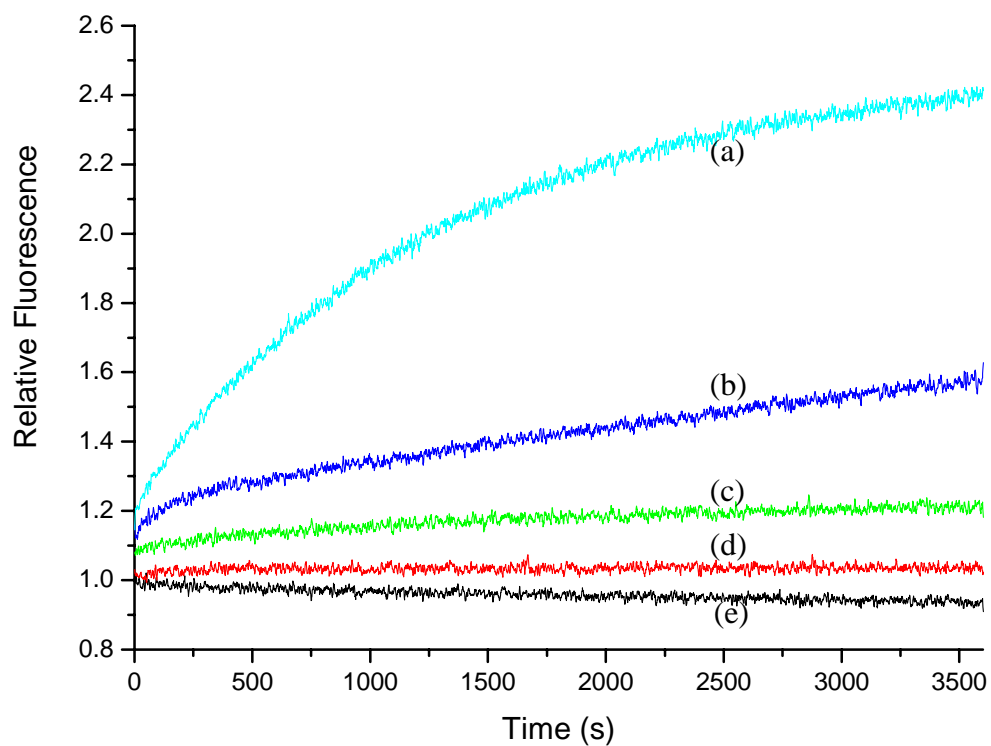


Figure 4.17 Time dependent fluorescence measurements of TEM-52 V216Cf in the presence of Moxalactam, (a) 10^{-4} M, (b) 10^{-5} M, (c) 10^{-6} M, (d) 10^{-7} M, and (e) free enzyme

4.4 Discussion

4.4.1 Fluorescence signals of the labeled TEM cysteine mutants

Unlike PenP and PenPC, TEM-1 β -lactamase are expressed as inclusion body in *E coli* in the absence of secretory signal peptide, which requires extended time for purification and therefore limits the throughput of screening different mutants. As a result, only a limited number of mutants were selected for optimization of TEM-based biosensors. E166C was selected because the analogous mutant in PenP and PenPC showed strong fluorescence signal. With similar 3-D configuration, the labeled TEM-1 E166C might also be able to give fluorescence signal. Position V216 was chosen for fluorophore labeling because it is pointing towards to the active site.

Most labeled mutants showed fluorescence signal except the badan labeled TEM-1 mutants. This is quite similar to the case of PenP N170C, that the selected position can give fluorescence signal only when it is labeled with a particular fluorophore. However, in the case of TEM-1, not just V216Cb, but also E166Cb give no fluorescence signal. This is in contrast to PenP E166C, which is suitable for labeling three fluorophores. Actually the micro-environment around E166 in TEM-1 is different from that of PenP, because of different amino acid residue nearby.

Moreover, fluorescence signal generated by TEM-1 V216Cf is larger than TEM-1 E166Cf. It is quite surprising because V216 is located at a less flexible loop between helix 10 and helix 11.

Fluorophores being labeled on this shorter loop with smaller degree of freedom may experience smaller change in solvent exposure area. Thus, the larger change in fluorescence of FM and TMRM labeled V216C than the E166Cf mutant could be rationalized by two possible reasons: (1) Attachment of the fluorophores onto the small loop could disrupt its conformation and make the loop more dynamic, and (2) Additional factors other than the dynamic of the loop and fluorophore on which the fluorophore is being attached can affect the fluorescence. The second possibility actually implies the change in fluorescence is not only depending on the solvent exposure area of the fluorophore. Indeed, fluorescein should show a shift in excitation and emission maximum (~15 nm) if the polarity of the environment changes significantly. Unlike the badan-labeled β -lactamase mutants, however, the shift in excitation and emission maximum of FM and TMRM labeled β -lactamase mutants are very small before and after the addition of antibiotics. The small change in excitation and emission maximum is an indirect evidence that the signal generation mechanism is more complicated than increase in solvent exposure of the fluorophore.

No matter what the signal generation mechanism is, the increase in fluorescence in the TEM-1 V216Cf is still relatively small, and therefore, further improvement on the TEM β -lactamase based biosensor is necessary. To do this, three mutations (E104K, M182T and G238S) were introduced to prepare TEM-52 V216C mutant.

Signal profiles of the labeled TEM-52 V216C mutants are quite similar to the labeled TEM-1 V216C mutants. Both mutants labeled with badan and TMRM result in no fluorescence response to penicillin G and cefuroxime and only those labeled with FM gives significant fluorescence signals. However, the much larger increase in fluorescence of TEM-52 V216Cf upon addition of penicillin G indicated the significant advantage of using TEM-52 as biosensor over TEM-1. This larger difference of the signal can be attributed to the suppression of the initial or background fluorescence intensity. It can be assumed that the fluorescence quantum yield of antibiotic bound TEM-1 V216Cf and TEM-52 V216Cf are the same because the fluorophore of both biosensors is then departed from the active site and exposed to solvent. Therefore, the suppression of initial fluorescence (i.e. in the absence of β -lactam) is the cause for the larger difference in fluorescence between the bound and unbound state. Actually, in the absence of β -lactam antibiotics, the fluorescence intensity of TEM-52 V216Cf is significantly lower than TEM-1 V216Cf under the

same conditions (data not shown).

Such suppression of initial fluorescence in TEM-52 could be a result of interaction of mutated residue(s) with FM or the difference in active site topology between TEM-1 and TEM-52 which caused a different orientation and solvent exposure area of the fluorophore. The first possibility is less likely because FM labeled TEM-1 V216C with additional M182T and M182T/E104K mutations did not show such a large increase in fluorescence, and the M182T/E104K mutations even slightly reduce the fluorescence change (data not shown). Although the effect of G238S alone was not examined, the additional serine side chain should have little effect on the fluorescence, because the hydroxyl group on the serine residue can only interact with the oxyanion on the xanthene ring, which would rather have increased the fluorescence quantum yield of FM. Moreover, the crystal structure of native TEM-52 β -lactamase suggested that the hydroxyl group of G283S is pointing towards the B4 β -strand rather than the active site, making it less likely to interact with FM which is located in the active site. The crystal structure of TEM-52 β -lactamase also reveals that the active site is enlarged by the G238S mutation. This enlarged active site could accommodate the xanthene moiety of the FM more than the TEM-1 active site, resulting in smaller solvent accessible area of the FM molecule.

4.4.2 Signal generation mechanism and fluorescence lifetimes of TEM-52 V216Cf

It was proposed that the increase in fluorescence of FM labeled PenPC based biosensor was due to the gain in solvent accessible area of the fluorophore [76]. However, this postulation cannot completely explain the observations in the TEM-52 biosensor. The most important clue to the signal generation mechanism in FM-labeled TEM biosensor is from studies of fluorescence quenching mechanism of fluorescein through binding to anti-fluorescein antibody [103, 104], in which tryptophan in the binding pocket of anti-fluorescein antibody was proved to be important for the fluorescence quenching of fluorescein. A more recent study conducted by Wolfrum revealed that tryptophan and tyrosine which have the highest reduction potential among the 20 amino acids can significantly quench the fluorescence of many organic dyes, including fluorescein, by photoinduced electron transfer (PET) [105]. Interestingly, a highly conserved tyrosine residue is present in all class A β -lactamase at position 105. This conserved Tyr-105 located in the active site is likely to interact with the FM label in TEM-52 V216Cf. The enlarged active site of TEM-52 can therefore allow the labeled fluorescein to stay in the active site, providing a large contact surface area between Tyr-105 and the fluorescein label.

The fluorescence lifetimes of TEM-52 V216Cf cannot provide direct evidence of

PET fluorescence quenching in this case, but the change in fluorescence lifetimes and their amplitude can be easily rationalized by PET quenching mechanism. Before the binding of penicillin G, the two component fluorescence decays can be interpreted as two different species present in the solution. The dominant species with sub-nanosecond lifetime (0.73 ns) could be TEM-52 V216Cf with the FM molecule in close contact with and heavily quenched by Tyr-105. The longer lifetime species (3.82 ns) could be the one with FM located far away from the active site without direct contact with the tyrosine residue. The binding of penicillin G makes the FM label to depart from the active site resulting at a longer distance from Tyr-105. As a result, the relative proportion of the longer lifetime component is significantly increased (from 0.29 to 0.73), and the shorter lifetime component becomes less dominant. Moreover, the increase in the lifetime of the short component (from 0.73 ns to 1.77 ns) indicates the reduction in fluorescence quenching, which can be explained by shielding of Tyr-105 from the fluorophore by the penicillin G molecule.

The lifetime measurements not just provided indirect evidence of the occurrence of PET quenching in the biosensing processing, but also revealed further information on the mode of fluorescence quenching. The dynamic quantum yield is the ratio between the rate of radiative relaxation and the overall rate of excited state

depopulation:

$$QY_{dyn} = \frac{k_r}{k_r + k_{nr} + k_q[Q]} \quad (1)$$

where k_r and k_{nr} are the rate constant of radiative and non-radiative decay, and $k_q[Q]$ is the rate constant of excited state depopulation by collision quenching. This equation can be rewritten as

$$QY_{dyn} = \frac{\bar{\tau}}{\tau_n} \quad (2)$$

where $\bar{\tau}$ and τ_n are the average fluorescence lifetime and intrinsic fluorescence lifetime of the fluorescence species respectively.

The intrinsic fluorescence lifetime is independent on the quenching agent and therefore remains constant before and after penicillin G (or with and without quenched by Tyr-105). The ratio of the dynamic quantum yield between penicillin-bound and free enzyme state is thus the ratio of the average lifetime of these two states

$$\frac{QY_{dyn,bound}}{QY_{dyn,free}} = \frac{\bar{\tau}_{bound} / \tau_n}{\bar{\tau}_{free} / \tau_n} = \frac{\bar{\tau}_{bound}}{\bar{\tau}_{free}} \quad (3)$$

i.e. the ratio of the dynamic quantum yield is $3.35 \text{ ns} / 1.11 \text{ ns} = 3.02$

The steady state quantum yield, QY_{ss} , is directly proportional to the fluorescence intensity. As a result, the ratio between steady state quantum yield of bound-state and free biosensor is equal to the ratio of the fluorescence intensity (denoted as “relative fluorescence” here)

$$\frac{QY_{ss, bound}}{QY_{ss, free}} = \frac{I}{I_0} = 3.6$$

The steady state quantum yield and dynamic quantum yield can be related by the following equation,

$$QY_{ss} = QY_{dyn} \times QY_{stat} \quad (4)$$

where QY_{stat} is the portion of fluorescence species without being quenched by quencher through static quenching mechanism:

$$QY_{stat} = \frac{[F_o] - [F \cdot Q]}{[F_o]} = \frac{F}{F_o}$$

where $[F_o]$ is the total concentration of fluorescence species and $[F \cdot Q]$ is the non-fluorescence complex of fluorescence species and quencher.

In the following equation, the ratio of static quantum yield between the bound and free biosensor can be calculated as:

$$\frac{QY_{ss,bound}}{QY_{ss,free}} = \frac{QY_{dyn,bound}}{QY_{dyn,free}} \times \frac{QY_{stat,bound}}{QY_{stat,free}} \quad (5)$$

$$3.6 = 3.02 \times \frac{QY_{stat,bound}}{QY_{stat,free}}$$

$$\frac{QY_{stat,bound}}{QY_{stat,free}} = 1.19$$

That the values of $QY_{dyn, bound} / QY_{dyn, free}$ and $QY_{stat, bound} / QY_{stat, free}$ are greater than 1.0 implies that the binding of penicillin G to TEM-52 V216Cf reduces both dynamic and static quenching efficiency. In addition, $QY_{dyn, bound} / QY_{dyn, free}$ is significantly larger than $QY_{stat, bound} / QY_{stat, free}$, indicating that the increase in fluorescence is dominant by the change in dynamic quenching process, and the amount of non-fluorescence FM-quencher complex (most likely FM - Tyr-105 complex) before and after the binding of penicillin G is quite similar.

On the other hand, molecular modeling can also provide some hints on the signal generation mechanism. Binding of penicillin G resulted in conformational change on the FM label but had little effect on the two residues next to V216C (K215 and A217).

This is contrary to the molecular models of PenPC E166Cf, in which part of the Ω -loop moved outside, allowing the FM label to expose to a more hydrophilic environment [76, 86]. In other words, the movement of FM label in TEM V216Cf is smaller than that of PenPC E166Cf upon penicillin G binding. Moreover, the FM label is significantly separated from the Tyr-105 upon penicillin binding, which is consistent with the proposed signal generation mechanism.

4.4.3 Time dependent fluorescence signals of TEM-52 V216Cf

Although TEM-52 V216Cf gives a 3.6 folds increase in fluorescence intensity upon the addition of penicillin G, the sensitivity towards other β -lactam antibiotics are significantly lower. For example, penicillin V and ampicillin gave a less than 3 folds increase in fluorescence intensity. However, the sensitivity of this biosensor is significantly improved over TEM-1 V216Cf, which has only about 2 folds increase in fluorescence signal. An attractive feature of this biosensor is the steady fluorescence signal. In PenP and PenPC based biosensors, the fluorescence signals drop rather rapidly due to hydrolysis of the bound β -lactam antibiotic. TEM-52 V216Cf gives a much more stable fluorescence signal, which indicates that the enzyme-substrate complex is much more stable than those of PenP and PenPC based biosensors. Indeed, the hydrolysis of the six antibiotics as monitored by UV-vis spectrometry indicated that the hydrolytic activity of TEM-52 V216Cf is negligible (result not shown).

However, the slow rising phase of the fluorescence signal in the presence of cephalosporin type antibiotics limits the applicability of this biosensor to the detection of this class of antibiotics. The slow binding of cephalosporin type antibiotics is unexpected because TEM-52 is classified as ESBL which should have a higher

catalytic efficiency, and probably better binding, to cephalosporins. Nevertheless, the E166N mutation and FM label at the active site would affect the binding of β -lactams, and the three mutations added to the biosensor cannot completely overcome these deteriorate effect.

4.5 Concluding remarks

Two amino acid residues, E166 and V216, on TEM β -lactamase were mutated to cysteine for fluorophore labeling. These two mutants were successfully expressed and labeled with different fluorophores. It was found that labeling with FM onto V216C gives the largest increase in fluorescence signal among all labeled mutants. Further optimization of this biosensor was done by introduction of 3 additional mutations as those in TEM-52 ESBL. This mutant was denoted as TEM-52 V216C and the FM labeled mutant is a much more sensitive biosensor, giving a 3.6 folds increase in fluorescence signal in the detection of penicillin G. This improved signal can be attributed to the suppression of the background fluorescence of the free biosensor, which might be the result of the interaction of the FM molecule with Tyr-105 in the active site. Fluorescence lifetime measurement reveals that the static and dynamic quantum yield of the pen G bound biosensor is about 1.2 and 3 folds higher than the free biosensor, suggesting that the change in fluorescence is due to a change of the dynamic quenching environment. Time dependent fluorescence measurements showed that TEM-52 V216Cf is suitable for detection of penicillin type antibiotics, because of the absence in deacylation of substrate which gives a stable fluorescence signal. However, the response time in detecting cephalosporins is much longer than

penicillin, which limits the applicability of this biosensor.

Chapter 5

Fluorescent biosensors based on modified PenPC β -lactamase

5.1. Introduction

β -Lactamase I from *B. cereus* 569/H, of which the gene was denoted as *penPC* [106], is one of the most early discovered [31], purified [107, 108] and structurally determined [26, 109] “penicillin-inactivating enzyme”. The “ I ” after β -lactamase denotes that there are several different β -lactamase genes encoded in the genome of *B. cereus* 569/H and I, II and III are used to differentiate them [108, 110]. β -Lactamase II is a zinc containing class B β -lactamase, and β -lactamase I and III, which have similar DNA sequence, belong to class A. Unlike other clinically important β -lactamases (e.g. TEM-1), these enzymes are not accompanied with transferable elements like transposon or R-plasmid, and are therefore subjected to relatively lower attention from medical researchers.

However, this early discovered enzyme is an excellent β -lactamase model for studying enzyme activities [111, 112], enzyme-inhibitor interaction [113-116] and structure homology and protein expression / secretion [106, 117, 118]. One of the most important findings based on PenPC β -lactamase is the identification of the three dimensional structure of “penicillin reorganization protein” [26], which shares common structural feature among all serine type β -lactamases and transpeptidases /

carboxypeptidases. Another major finding based on this enzyme is the hydrolytic mechanism of class A β -lactamase. The carboxylate group dependence of penicillins hydrolysis was firstly identified by chemical modification of PenPC β -lactamase [119, 120]. Further mutation studies revealed that glu-166 is largely responsible for the hydrolysis in class A β -lactamase. More details, like the appropriate distance of the carboxylate group of this residue from the active site, were also studied [49, 51]. Indeed, Gibson and Leung showed that either decrease or increase the distance between the carboxylate group and the α carbon atom of residue 166 will reduce the activity of this enzyme [49, 51]. In Leung's experiment, E166 was mutated to cysteine and the protein expressed was labeled with iodoacetic acid on this residue [49, 51]. Actually, this mutant and expression system was used for the construction of the fluorescent biosensor PenPC E166Cf [76, 86].

Although PenPC E166Cf is sensitive enough to detect low concentration of β -lactam antibiotics down to 10^{-8} M, it is possible that the sensitivity can be further improved by methodology as demonstrated in previous chapters. These methods were therefore applied to PenPC β -lactamase and the results are discussed in this chapter. The effect of the arrangement of affinity tag on fluorophore labeled PenPC E166C, the optimization of fluorescence signal by labeling the fluorophore at different

locations, and effect of Y105W mutation on the fluorescence signal will be discussed.

Selection of affinity tag for purification of PenPC biosensors

The successful improvement of PenP and TEM based fluorescent biosensors suggested that placing fluorophore at different position can be a possible strategy to improve the sensitivity of PenPC based biosensor. Unlike PenP and TEM, however, the crystal structure of PenPC is not available, and the exact orientation of amino acid residues and loop conformation are not known. Thus, more mutants should be prepared in order to make sure an optimized position was selected. The original expression and purification system for PenPC E166C mutant can produce highly pure protein [76, 86] but it is relatively time consuming and is not suitable for screening of multiple mutants. Expression of protein with fused affinity tag and purification by corresponding affinity chromatography may reduce the time in protein preparation and thus allows more mutants to be expressed.

Maltose binding protein (MBP) which was fused with PenP mutants is a popular affinity tag for recombinant proteins. This tag can increase the solubility and assist the folding of fusion partner, which could increase the stability of PenPC mutants.

However, the speed of purification is still limited because of the long column generation and regeneration time. Polyhistidine tag (his-tag) coupled with metal affinity chromatography is ideal in terms of speed and purity. Therefore, his-tag was added to PenPC E166C to the N-terminal and the C-terminal respectively (for convenience the two proteins were named as H-PenPC E166C and PenPC-H E166C), and the expression system for producing these two proteins was constructed based on expression vector pRsetK. To take advantage of MBP, a his-tag containing MBP was fused to PenPC E166C (in short, H-MBP-PenPC E166C), and the expression vector used for producing this fusion protein was constructed and named as pHMal-c2xK. These 3 proteins were successfully expressed and labeled with fluorescein for assessing the performance of the biosensors.

Optimization of PenPC biosensors by labeling different fluorophores at different locations

After selecting the expression – purification protocol, different cysteine mutants of PenPC β -lactamase can be constructed. As discussed before, the crystal structure of PenPC is not available. However, the high sequence homology between PenP and PenPC β -lactamase and the available PenP β -lactamase crystal structure do provide

some clues to the selection of fluorophore labeling positions [83, 121]. Firstly, positions 170, 172 and 176, which were selected for fluorophore labeling in PenP β -lactamase were also selected in this case for comparison. With similar local environment and flexibility, the residues next to E166 and N170, which are F165, T167 and L169, may also be suitable for fluorophore labeling. F165 is very close to the active site, but it is not a conserved residue and the side chain is pointing in an opposite direction to the active site. The equivalent residue of T167 of PenPC in PenP is P167. The crystal structure of PenP β -lactamase showed that the side chain of P167 has large contact area with the bound substrate [121]. Therefore, there is a chance that the labeled fluorophore may locate closely to the active site and depart away upon substrate binding [121]. Another selected residue, L169, though has no important role in catalysis, is a highly conserved residue in class A β -lactamase. The side chain of this residue is pointing exactly towards ser-70 and is thus selected for fluorophore labeling. The locations of residues on PenP which are equivalent to F165, E166, T167, L169, N170, A172 and D176 on PenPC are shown in Figure 5.1.

Similar to the procedures in chapter 3, these selected positions were mutated to cysteine after the changing the glutamate acid at 166 position to alanine. These mutants were then labeled with the three fluorophores, badan, FM and TMRM, and

the fluorescence signals were recorded and discussed.

Studying and optimizing fluorescence signal of fluorophore labeled PenPC E166C

As discussed in chapter 4, the signal generation mechanism could be more complex than previously proposed. The spectral properties of free and penicillin bound TEM-52 based biosensor suggested that the different degree of fluorescence quenching may be an additional basis of signal generation. Most probably, the quenching mechanism is due to PET between fluorophore and the tyrosine 105 residue in the active site. Binding of β -lactam molecule caused departure of the fluorescein label from Tyr-105 and have raised the fluorescence intensity because of reduction in quenching efficiency.

Indeed, this mechanism may occur in other β -lactamase based biosensor, like PenPC E166Cf. To prove this idea, as well as to improve the sensitivity of this biosensor, Tyr-105 was mutated to tryptophan. Tryptophan, similar to tyrosine, is an aromatic and hydrophobic residue, but with a different reduction potential. The reduction potential should be a factor affecting the sensitivity of the biosensor because PET efficiency is highly dependent on the reduction potential of the excited state

fluorophore and quencher. If PET is present in the biosensing process, the tryptophan mutant should have improved signal because the tryptophan residue should quench the fluorescence intensity much more than tyrosine.

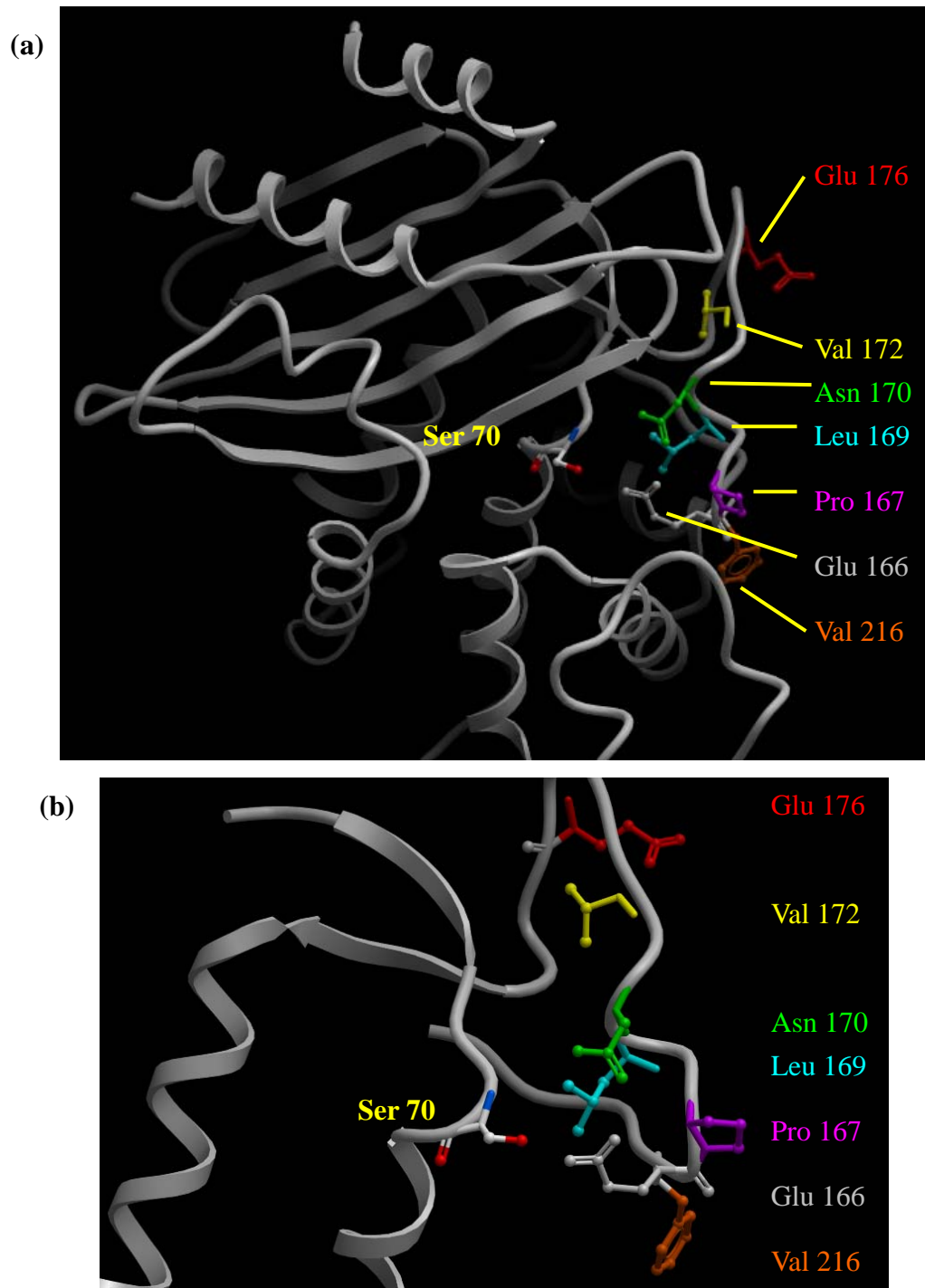


Figure 5.1 Location of residues (F165, E166, P167, L169, N170, V172 and E176) on PenP which are equivalent to F165, E166, T167, L169, N170, A172 and D176 on (a) PenPC, and (b) another view of those residues

5.2 Methods

5.2.1 Construction of pHMal-c2xK

pHMal-c2xK was modified from pMal-c2xK by addition of nine codons, which encoded MGSHHHHHH, to the N-terminal of maltose binding protein (MBP). The insertion of the nine codons was done by following the protocol from QuickChange® II Site-Directed Mutagenesis Kits (Stratagene) but in two separated reactions. The first reaction was used for inserting four histidines before the methionine of the MBP by using two primers, His-add-1F and His-add-1R (Table 5.1). The reaction was performed in a 50 µl solution which was made up of 5 µl of 10X reaction buffer, 1 µl each of the two primers (125 ng), 1 µl of pMAL-c2xK (50 ng), 1 µl of dNTP mix, 1 µl of *PfuTurbo* DNA polymerase (2.5 U/µl) and 40 µl sterile water. The PCR cycling condition was pre-denaturation at 95 °C for 5 min, 18 cycles at 95 °C for 30 s, 57 °C for 1 min, and 68 °C for 7 min. To remove pMal-c2xK in the mixture, 1 µl DpnI (10 U/µl) was added and the solution was incubated at 37 °C for 1 hour. After DpnI digestion, a 10 µl of the product was transformed into *E. coli* XL-1 Blue for plasmid preparation. Plasmid designated as pMal-c2xK-hf was extracted and analyzed by DNA sequencing to confirm the successful addition of four histidines.

The second reaction, which made use of His-add-2F and His-add-2R, was used to insert MGS_{HH} before the four histidines just added. The reaction condition was the same except that the template of the reaction was pMal-c2xK-hf rather than pMal-c2xK, and the PCR cycling condition was slightly modified – pre-denaturation at 95 °C for 5 min, 18 cycles of 95 °C for 30 s, 60 °C for 1 min and 68 °C for 7 min. Different PenPC E166C β-lactamase mutants were cloned into the product plasmid as described in the following sections.

Table 5.1 DNA sequence of primers used for addition of his-tag to MBP and PenPC

| Primers | Sequence | T _m (°C) |
|-------------|---|------------------------|
| His-add-1F | CTTCACCAACAAGGACCATAGATT <u>CACCATCACCATAT</u> | 79.0 |
| His-add-1R | GAAAATCGAAGAAGGTAAACTG CAGTTTACCTTCTTCGATTTTCATATGGTGATGGTGAAT CTATGGTCCTTGTGGTGAAG | |
| His-add-2F | CTTCACCAACAAGGACCATAGATTATGGGATCTCACCA | 82.0 |
| His-add-2R | <u>TCACCATCACCATATGAAAATCGAAG</u> CTTCGATTTTCATATGGTGATGGTGATGGTGAGATCCCA <u>TAATCTATGGTCCTTGTGGTGAAG</u> | |
| PC-BamH1-F | CAGTTGGATCCCAAAAATCAGGCAACGCATAAAG | 74.2 |
| PC-Hind3-R | TCGATAAGCTTACCTAAGAGCCTTAACTATAACTTTAG | 60.4 |
| HPC-Nde1-F | TCGATCATATGCATCACCATCACCAT | 80.5 |
| | CACAAAATCAGGCAACGCATAAAG | |
| PCH-Hind3-R | TCGATAAGCTTAGTGATGGTGATGGTGATG | 76.3 |
| | CCTAAGAGCCTTAACTATAACTTTAGTTGC | |

5.2.2 Subcloning of PenPC β -lactamase genes with and without his-tag into pRsetK and pHMal-c2xK

To prepare PenPC E166C with his-tagged MBP, the gene of PenPC E166C was cloned into pHMal-c2xK. The gene of PenPC E166C was obtained by PCR from pYCL-18 using two primers, PCBamH1-F and PCHind3-R (Table 5.1), flanked by BamHI and HindIII restriction sites respectively. The PCR profile was set as follows: pre-denaturation at 94 °C for 3 min, 25 cycles amplification at 94 °C for 1 min, 56 °C for 1 min, 72 °C for 1 min, and final elongation at 72 °C for 10 min. The PCR product was purified by PCR Product Purification Kit (Roche). The vector pHMal-c2xK and purified PCR product were digested with BamHI and HindIII restriction enzymes at 37 °C overnight. The digested fragments were purified by agarose gel electrophoresis and Agarose Gel DNA Extraction Kit (Roche). The digested pHMal-c2xK and PenPC gene were mixed in a ratio of 1:3 and was ligated by using Quick Ligation Kit (Roche). The ligation product was transformed into *E. coli* XL-1 Blue as described. Plasmid was extracted and analyzed by DNA sequencing. The obtained vector was designated as pHMal-c2xK-PenPC E166C.

To add his-tag to the N/C-terminal of PenPC E166C, the PenPC gene was obtained by PCR using two pair of primers, HPC-Nde1-F / PC-Hind3-R, and PC-Nde1-F / PCH-Hind3-R (Table 5.1). The PCR products were digested by NdeI and HindIII and the subsequent cloning procedures were the same as described above. The two vectors obtained were designated as pRsetK-H-PenPC E166C and pRsetK-PenPC-H E166C respectively.

5.2.3 Site-directed mutagenesis and cloning of H-MBP-PenPC cysteine mutants

Six selected amino acid residues (F165, T167, L169, N170, A172 and D176) were mutated to cysteine for fluorophore labeling and to compare with the labeled E166C. To prepare the six mutants, E166A was firstly prepared by using primers E166A-F and E166A-R, and the product pHMal-c2xK-PenPC E166A was used for subsequent mutagenesis. The procedures were the same as described in section 2.2.3 and the primers used are listed in Table 5.2. The PCR cycling conditions were 95 °C for 5 min, 16 cycles of 95 °C for 30 s, x °C for 1 min and 68 °C for 7.5 min, where x is the T_m of the primers pair minus 5 °C.

Table 5.2 DNA sequence of primers used for cysteine mutation

| Primer pairs | Sequence | T _m (°C) |
|----------------------|---|---------------------|
| E166CA-F E166CA-R | GTCCTAATCGCTTTGCAACAGAATTAACG CGTTTAATTCTGTTGCAAAGCGATTAGAC | 62.2 |
| F165C-F F165C-R | CTATGTCTAATCGCTGTGCAACAGAATTAAC GTTTAATTCTGTTGCACAGCGATTAGACATAG | 60.7 |
| T167C-F T167C-R | CTAATCGCTTTGCATGCGAATTAACGAAG CTTCGTTTAATTCGCATGCAAAGCGATTAG | 65.0 |
| L169C-F L169C-R | GCTTTGCAACAGAATGCAACGAAGCTATTC GAATAGCTTCGTTGCATTCTGTTGCAAAGC | 65.4 |
| N170C-F N170C-R | GCAACAGAATTATGCGAAGCTATTCCAGG CCTGGAATAGCTTCGCATAATTCTGTTGC | 63.7 |
| A172C-F A172C-R | CAGAATTAACGAATGTATTCCAGGAGAC GTCTCCTGGAATACATTCGTTTAATTCTG | 57.9 |
| D176C-F D176C-R | GAAGCTATTCCAGGATGTATTTCGTGACACTAG CTAGTGTCACGAATACATCCTGGAATAGCTTC | 61.6 |

5.2.4 Introduction of Y105W mutation by site-directed mutagenesis.

Y105W mutation was introduced into pHMal-c2xK-PenPC E166C by site directed mutagenesis. The procedures were those described in section 2.2.4. The primers used for the mutagenesis are shown in Table 5.3.

Table 5.3 DNA sequence of primers used for Y105W mutation

| Primer | Sequence | T _m (°C) |
|---------|------------------------------|------------------------|
| Y105W-F | GATCTTGTAAGACTGCAACCCGATTACG | 60.0 |
| Y105W-R | CGTAATCGGGTTGCAGTTTACAAGATC | 60.0 |

5.2.5 Preparation and labeling different PenPC cysteine mutants

All mutants were expressed and purified under the same procedures as described in section 2.3. PenPC E166C mutants with different tagging were labeled with fluorescein only and all other mutants (including H-MBP- PenPC E166C) were labeled with 3 different fluorophores, badan, FM and TMRM as described in section 2.4.

5.2.6 Fluorometric measurement of labeled PenPC cysteine mutants

Fluorescence spectra and time dependent fluorescence measurements were carried out on the labeled PenPC mutants with penicillin G and cefuroxime. Detailed procedures are the same as those described in section 2.5

Fluorescence lifetimes of free TMRM and H-MBP-PenPC Y105W/E166Cr were measured as described in section 2.6. The quantum yield of free TMRM, H-MBP-PenPC E166Cr and Y105W/E166Cr were measured using the method described previously, and rhodamine B in methanol reported with a quantum yield of 0.70 was used as standard.

Briefly, rhodamine B solutions were prepared at suitable concentration with absorbance lower than 0.1 (5×10^{-8} M, 1×10^{-7} M, 2×10^{-7} M and 3×10^{-7} M). The fluorescence spectra of the rhodamine B solutions were measured and recorded with the excitation wavelength set at 545 nm. The UV-vis absorbance spectra and the absorbance at 545 nm of these solutions were also recorded. A plot of the area under the fluorescence spectrum versus that absorbance of the corresponding solution was obtained, from which the slope of the curve was calculated. This procedure was

repeated with free TMRM, H-MBP-PenPC E166Cr and Y105W/E166Cr (with and without addition of penicillin G), but at different concentrations (1×10^{-7} M, 2×10^{-7} M, 3×10^{-7} M and 5×10^{-7} M).

The quantum yield of each sample was calculated using the equation

$$\Phi_{sample} = \Phi_{standard} \frac{Slope_{sample}}{Slope_{standard}}$$

where $\Phi_{standard}$ and Φ_{sample} are the quantum yield of the standard and sample,

$Slope_{standard}$ and $Slope_{sample}$ represent the slope calculated from the plot of fluorescence spectral area v.s. absorbance at 545 nm.

5.3 Results

5.3.1 Preparation and labeling of TEM cysteine mutants

All the mutants were successfully expressed and purified by using nickel column chromatography. All purified proteins were analyzed by SDS-PAGE. Three tagged PenPC mutants are shown in Figure 5.2 - 5.4. The six mutants, F165C, T167C, L169C, N170C, A172C and D176 were shown in Figures 5.6 - 5.11. H-MBP-PenPC Y105W/E166C was shown in Figure 5.16. The purity of all the mutants was higher than 95%. The purified mutants were successfully labeled with FM and were analyzed by SDS-PAGE (Figure 5.5, Figure 5.12 - 5.15 and Figure 5.17)

5.3.2 Fluorescence signals of different tagged PenPC E166Cf

The fluorescence spectra of the three tagged PenPC E166Cf in the presence / absence of penicillin G and cefuroxime are shown in Figure 5.18. In the presence of 5×10^{-4} M antibiotics, all PenPC E166Cf molecules in the solution should be bound with substrates, and therefore, maximum fluorescence signals were obtained. It can be seen that all of them have similar fluorescence signal, but H-PenPC E166Cf and PenPC-H E166Cf have a slightly lower sensitivity than H-MBP-PenPC E166Cf.

5.3.3 Fluorescence signals of the labeled H-MBP-PenPC mutants

The fluorescence spectral changes of different labeled mutants upon substrate addition are shown in figures 5.19 – 5.25. Most of the labeled mutants gave weak or even no fluorescence signal to antibiotics, and none of labeled mutants have more than 2 folds increase in fluorescence intensity. The largest increase in fluorescence occurred in FM and TMRM labeled E166C, which has 2 folds and about 1.7 folds increase in fluorescence upon addition of antibiotics. The FM labeled N170C also showed about 1.4 folds increase in fluorescence and the other xanthene labeled mutants, T167Cr, L169Cr, N170Cr, A172Cf and A172Cr have about 1.2 folds increase. It should be pointed out that the emission maximum of all these FM and TMRM labeled mutants are very similar, and substrate addition only causes less than 2 nm shift in the wavelength. A larger difference in emission maximum can be observed between different mutants, the largest difference is 4 nm between F165Cf (513 nm) and L169Cf (518 nm). In the case of badan labeled mutants, three of them showed fluorescence change upon the addition of antibiotic. E166Cb showed a large increase in fluorescence, with about 2 folds increase at 475 nm upon the addition of penicillin G. L169Cb also showed an increase in fluorescence upon addition of cefuroxime, with the largest change (1.6 folds increase) at 450 nm. The most distinct

labeled mutant is N170Cb, which is the only labeled mutant that showed a large decrease (3.1 folds) in fluorescence. Addition of penicillin G caused a 2 nm red shift, and cefuroxime caused a 7 nm blue shift. The relative change in fluorescence are shown in Table 5.4.

5.3.4 Fluorescence signals of labeled H-MBP-PenPC Y105W/E166C

The fluorescence signals of three labeled mutants were studied using penicillin G and cefuroxime as substrate. The spectral change was recorded and shown in figure 5.26. H-MBP-PenPC Y105W/E166Cb showed a similar emission, indicating that the badan labeled experience a similar solvent exposure as in E166Cb. However, the change in intensity and bathochromic shift of Y105W/E166Cb is smaller than E166Cb. Y105W/E166Cf has a significantly enhanced fluorescence signal with, 3 folds increase in fluorescence intensity. The largest change occurred in TMRM labeled Y105W/E166C, which has a 4 folds increase in fluorescence intensity.

5.3.5 Fluorescence lifetimes and quantum yields of H-MBP-PenPC Y105W/E166Cr

The quantum yield of various species are shown in Table 5.5. The quantum yield of H-MBP-PenPC Y105W/E166Cr is the lowest, and conjugation with H-MBP-PenPC E166C has little effect on the quantum yield. This indicates that the Y105W mutation can cause extensive quenching to the TMRM label. Addition of penicillin G caused a significant increase in quantum yield, in both H-MBP-PenPC E166Cr and H-MBP-PenPC Y105W/E166Cr.

Table 5.5 The fluorescent quantum yield of TMRM H-MBP-PenPC E166Cr and Y105W/E166Cr

| Sample | Quantum yield |
|--|---------------|
| TMRM | 0.44 ± 0.02 |
| H-MBP-PenPC E166Cr | 0.41 ± 0.05 |
| H-MBP-PenPC E166Cr + 1×10^{-4} M penG | 0.67 ± 0.06 |
| H-MBP-PenPC Y105W/E166Cr | 0.16 ± 0.04 |
| H-MBP-PenPC Y105W/E166Cr + 1×10^{-4} M penG | 0.65 ± 0.05 |

The fluorescence lifetime decay curves of free TMRM and Y105W/E166Cr are shown in Figure 5.27. The decay curve of TMRM is well fitted with mono-exponential decay model and Y105W/E166Cr shows a biexponential decay pattern. Addition of penicillin G to Y105W/E166Cr slightly increased the fluorescence lifetimes.

5.3.6 Time dependent fluorescence signals of H-MBP-PenPC Y105W/E166Cr

Six antibiotics were used as substrates for H-MBP-PenPC Y105W/E166Cr to study the time profile of fluorescence signal, which are shown in figures 5.28 - 5.33. Similar to TEM-52 V216Cf, all these profiles show a fast increasing phase of fluorescence upon addition of penicillin type antibiotics. The fluorescence change is about 3.6 folds for penicillin V and ampicillin. The fluorescence intensity drops rather rapidly in the decreasing phase at low antibiotic concentration. Ampicillin showed a slightly faster decay of fluorescence at a concentration of 10^{-7} M. Cephalosporin showed only the increasing phase during the whole period of measurement. Unlike TEM-52 V216Cf, the increase in fluorescence is much more rapid and the detection limit can be down to 10^{-7} M.

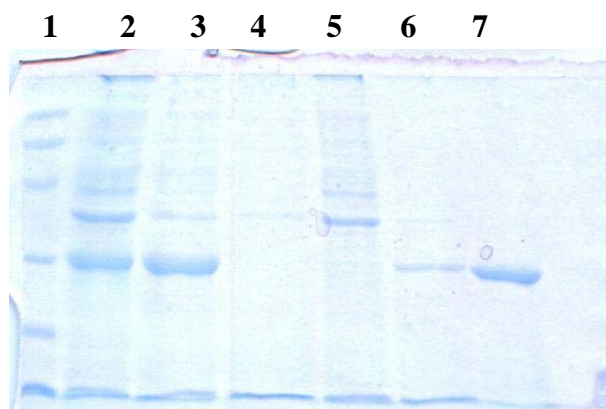


Figure 5.2 Purification profiles of H-PenPC E166C.

Lane 1, low range molecular marker: rabbit muscle phosphorylase b (97400 Da), BSA (66200 Da), hen egg white ovalbumin (45000 Da), bovine carbonic anhydrase (31000 Da), soybean trypsin inhibitor (21500 Da), hen egg white lysozyme (14400 Da);

Lane 2, crude cell lysate;

Lane 3, soluble part of cell lysate;

Lane 4, cell lysate after passing through nickel-affinity column;

Lane 5, non-specific binding washed out by running buffer;

Lane 6, non-specific binding washed out by running buffer with 30 mM imidazole;

Lane 7, elution of H-PenPC E166C by elution buffer.

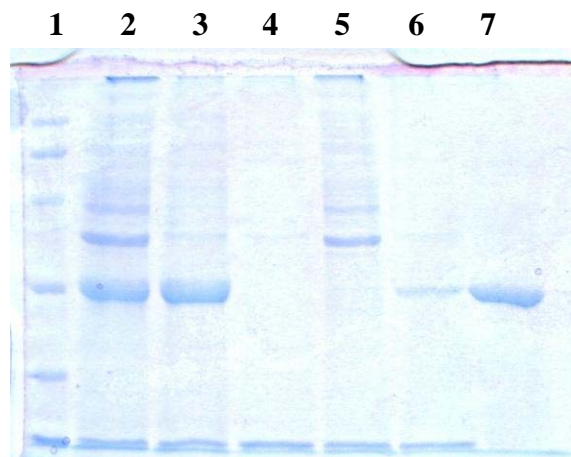


Figure 5.3 Purification profiles of PenPC-H E166C.

Lane 1, low range molecular marker: rabbit muscle phosphorylase b (97400 Da), BSA (66200 Da), hen egg white ovalbumin (45000 Da), bovine carbonic anhydrase (31000 Da), soybean trypsin inhibitor (21500 Da), hen egg white lysozyme (14400 Da);

Lane 2, crude cell lysate;

Lane 3, soluble part of cell lysate;

Lane 4, cell lysate after passing through nickel-affinity column;

Lane 5, non-specific binding washed out by running buffer;

Lane 6, non-specific binding washed out by running buffer with 30 mM imidazole;

Lane 7, elution of PenPC-H E166C by elution buffer

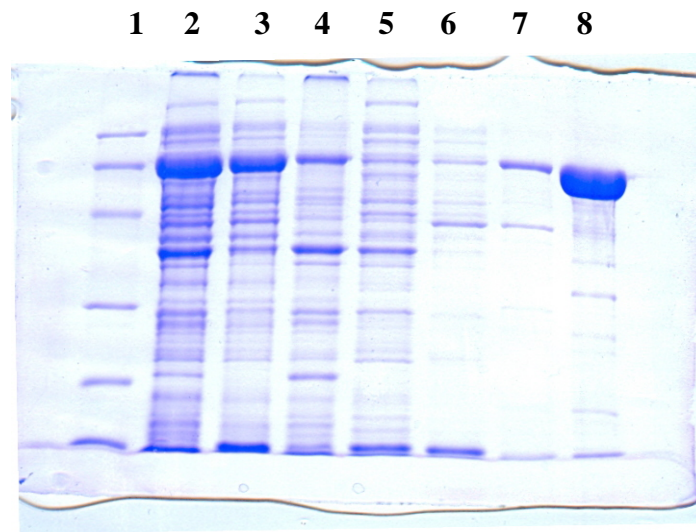


Figure 5.4 Purification profiles of H-MBP-PenPC E166C.

Lane 1, low range molecular marker: rabbit muscle phosphorylase b (97400 Da), BSA (66200 Da), hen egg white ovalbumin (45000 Da), bovine carbonic anhydrase (31000 Da), soybean trypsin inhibitor (21500 Da), hen egg white lysozyme (14400 Da);

Lane 2, crude cell lysate;

Lane 3, soluble part of cell lysate;

Lane 4, insoluble part of cell lysate

Lane 5, cell lysate after passing through nickel-affinity column;

Lane 6, non-specific binding washed out by running buffer;

Lane 7, non-specific binding washed out by running buffer with 30 mM imidazole

Lane 8, elution of H-MBP-PenPC E166C by elution buffer

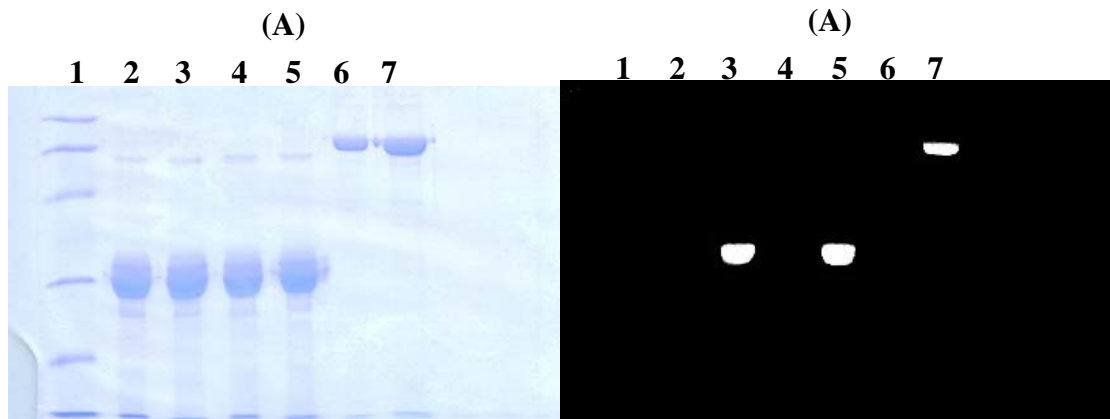


Figure 5.5 SDS-PAGE of FM labeled H-PenPC E166C, PenPC-H E166C and H-MBP-PenPC E166C stained with Coomassie-blue (A) and under UV illumination (B).

Lane 1, low range molecular marker: rabbit muscle phosphorylase b (97400 Da), BSA (66200 Da), hen egg white ovalbumin (45000 Da), bovine carbonic anhydrase (31000 Da), soybean trypsin inhibitor (21500 Da), hen egg white lysozyme (14400 Da);

Lane 2, H-PenPC E166C;

Lane 3, H-PenPC E166Cf;

Lane 4, PenPC-H E166C;

Lane 5, PenPC-H E166Cf;

Lane 6, H-MBP-PenPC E166C;

Lane 7, H-MBP-PenPC E166Cf;

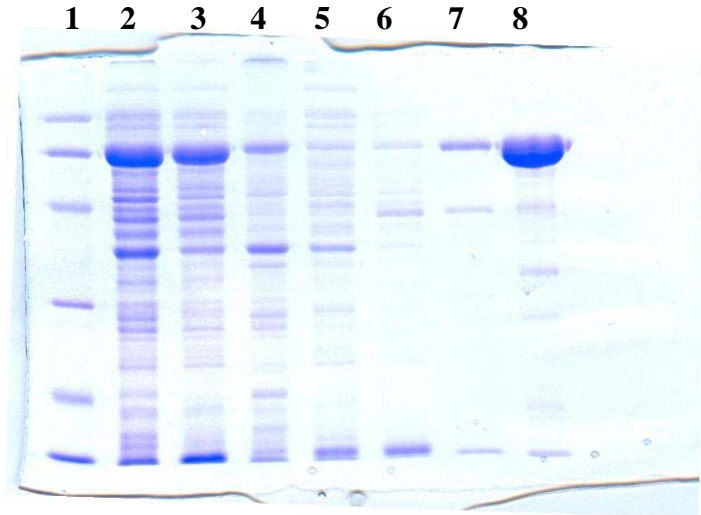


Figure 5.6 Purification profiles of H-MBP-PenPC F165C.

Lane 1, low range molecular marker: rabbit muscle phosphorylase b (97400 Da), BSA (66200 Da), hen egg white ovalbumin (45000 Da), bovine carbonic anhydrase (31000 Da), soybean trypsin inhibitor (21500 Da), hen egg white lysozyme (14400 Da);

Lane 2, crude cell lysate;

Lane 3, soluble part of cell lysate;

Lane 4, insoluble part of cell lysate

Lane 5, cell lysate after passing through nickel-affinity column;

Lane 6, non-specific binding washed out by running buffer;

Lane 7, non-specific binding washed out by running buffer with 30 mM imidazole

Lane 8, elution of H-MBP-PenPC F165C by elution buffer

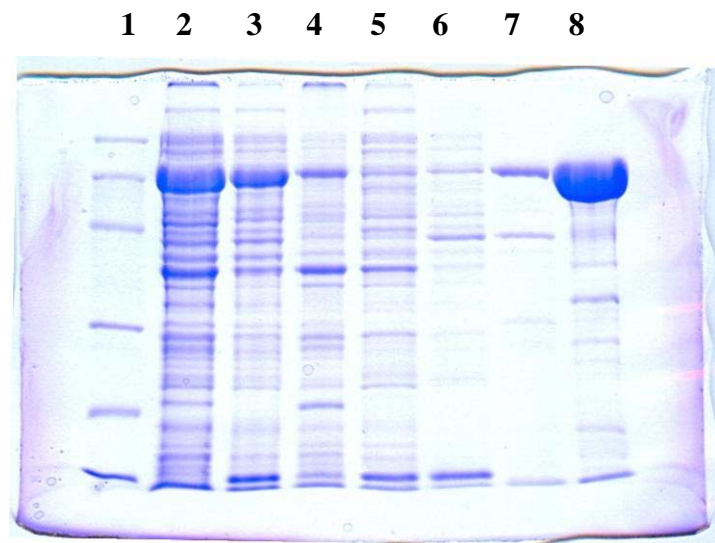


Figure 5.7 Purification profiles of H-MBP-PenPC T167C.

Lane 1, low range molecular marker: rabbit muscle phosphorylase b (97400 Da), BSA (66200 Da), hen egg white ovalbumin (45000 Da), bovine carbonic anhydrase (31000 Da), soybean trypsin inhibitor (21500 Da), hen egg white lysozyme (14400 Da);

Lane 2, crude cell lysate;

Lane 3, soluble part of cell lysate;

Lane 4, insoluble part of cell lysate

Lane 5, cell lysate after passing through nickel-affinity column;

Lane 6, non-specific binding washed out by running buffer;

Lane 7, non-specific binding washed out by running buffer with 30 mM imidazole

Lane 8, elution of H-MBP-PenPC T167C by elution buffer

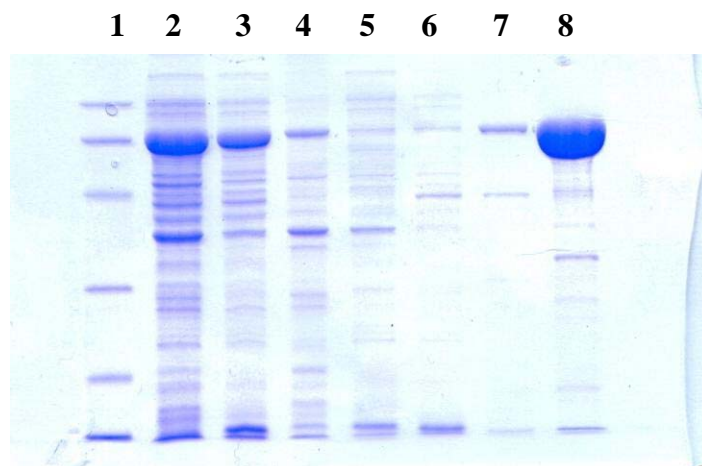


Figure 5.8 Purification profiles of H-MBP-PenPC L169C.

Lane 1, low range molecular marker: rabbit muscle phosphorylase b (97400 Da), BSA (66200 Da), hen egg white ovalbumin (45000 Da), bovine carbonic anhydrase (31000 Da), soybean trypsin inhibitor (21500 Da), hen egg white lysozyme (14400 Da);

Lane 2, crude cell lysate;

Lane 3, soluble part of cell lysate;

Lane 4, insoluble part of cell lysate

Lane 5, cell lysate after passing through nickel-affinity column;

Lane 6, non-specific binding washed out by running buffer;

Lane 7, non-specific binding washed out by running buffer with 30 mM imidazole

Lane 8, elution of H-MBP-PenPC L169C by elution buffer

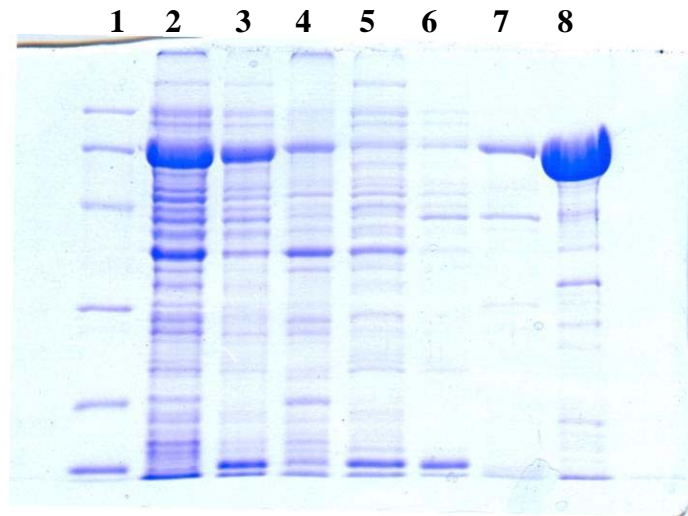


Figure 5.9 Purification profiles of H-MBP-PenPC N170C.

Lane 1, low range molecular marker: rabbit muscle phosphorylase b (97400 Da), BSA (66200 Da), hen egg white ovalbumin (45000 Da), bovine carbonic anhydrase (31000 Da), soybean trypsin inhibitor (21500 Da), hen egg white lysozyme (14400 Da);

Lane 2, crude cell lysate;

Lane 3, soluble part of cell lysate;

Lane 4, insoluble part of cell lysate

Lane 5, cell lysate after passing through nickel-affinity column;

Lane 6, non-specific binding washed out by running buffer;

Lane 7, non-specific binding washed out by running buffer with 30 mM imidazole

Lane 8, elution of H-MBP-PenPC N170C by elution buffer

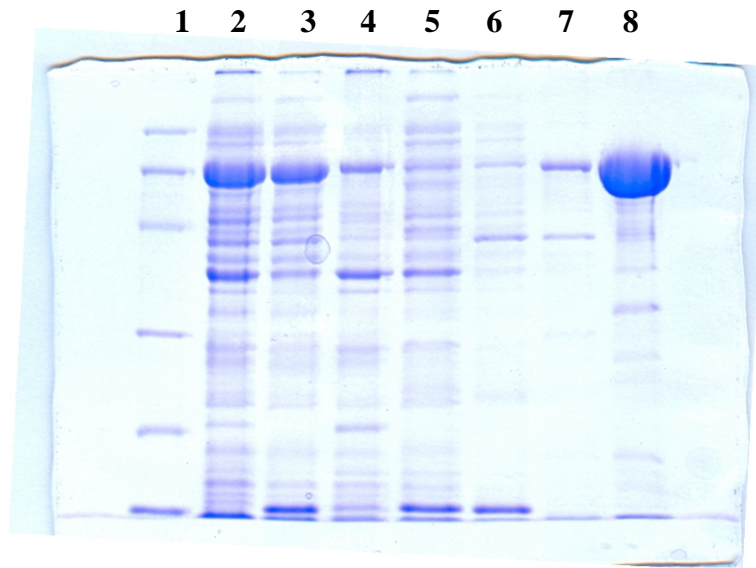


Figure 5.10 Purification profiles of H-MBP-PenPC A172C.

Lane 1, low range molecular marker: rabbit muscle phosphorylase b (97400 Da), BSA (66200 Da), hen egg white ovalbumin (45000 Da), bovine carbonic anhydrase (31000 Da), soybean trypsin inhibitor (21500 Da), hen egg white lysozyme (14400 Da);

Lane 2, crude cell lysate;

Lane 3, soluble part of cell lysate;

Lane 4, insoluble part of cell lysate

Lane 5, cell lysate after passing through nickel-affinity column;

Lane 6, non-specific binding washed out by running buffer;

Lane 7, non-specific binding washed out by running buffer with 30 mM imidazole

Lane 8, elution of H-MBP-PenPC A172C by elution buffer

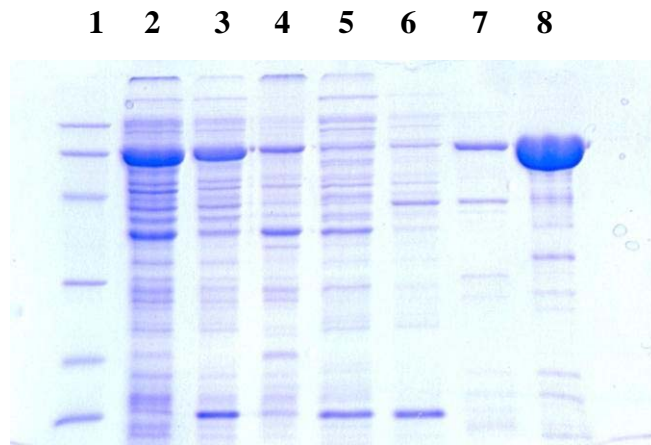


Figure 5.11 Purification profiles of H-MBP-PenPC D176C.

Lane 1, low range molecular marker: rabbit muscle phosphorylase b (97400 Da), BSA (66200 Da), hen egg white ovalbumin (45000 Da), bovine carbonic anhydrase (31000 Da), soybean trypsin inhibitor (21500 Da), hen egg white lysozyme (14400 Da);

Lane 2, crude cell lysate;

Lane 3, soluble part of cell lysate;

Lane 4, insoluble part of cell lysate

Lane 5, cell lysate after passing through nickel-affinity column;

Lane 6, non-specific binding washed out by running buffer;

Lane 7, non-specific binding washed out by running buffer with 30 mM imidazole

Lane 8, elution of H-MBP-PenPC D176C by elution buffer

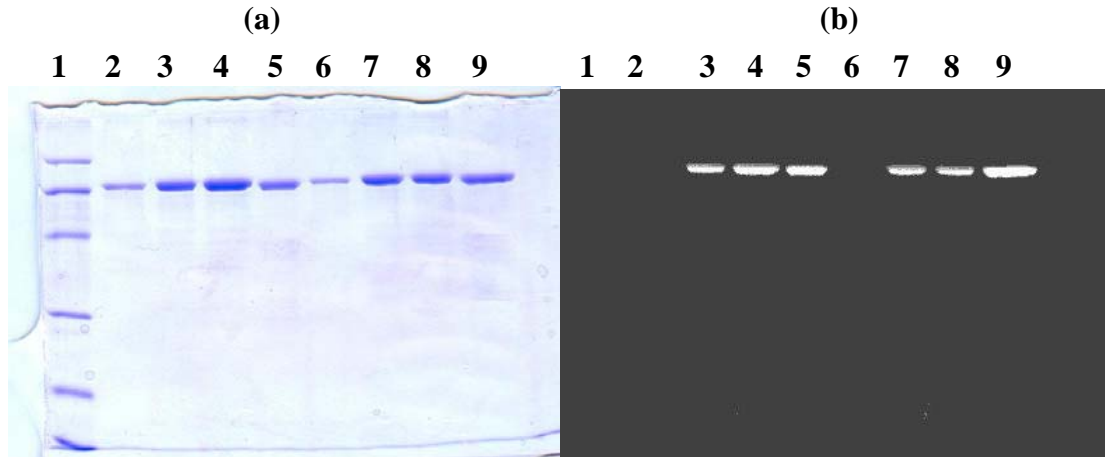


Figure 5.12 SDS-PAGE of fluorophore labeled H-MBP-PenPC F165C and H-MBP-PenPC E166C stained with Coomassie-blue (a) and under UV illumination (b).

Lane 1, low range molecular marker: rabbit muscle phosphorylase b (97400 Da), BSA (66200 Da), hen egg white ovalbumin (45000 Da), bovine carbonic anhydrase (31000 Da), soybean trypsin inhibitor (21500 Da), hen egg white lysozyme (14400 Da);

Lane 2, H-MBP-PenPC F165C;

Lane 3, H-MBP-PenPC F165Cb;

Lane 4, H-MBP-PenPC F165Cf;

Lane 5, H-MBP-PenPC F165Cr;

Lane 6, H-MBP-PenPC E166C;

Lane 7, H-MBP-PenPC E166Cb;

Lane 8, H-MBP-PenPC E166Cf;

Lane 9, H-MBP-PenPC E166Cr.

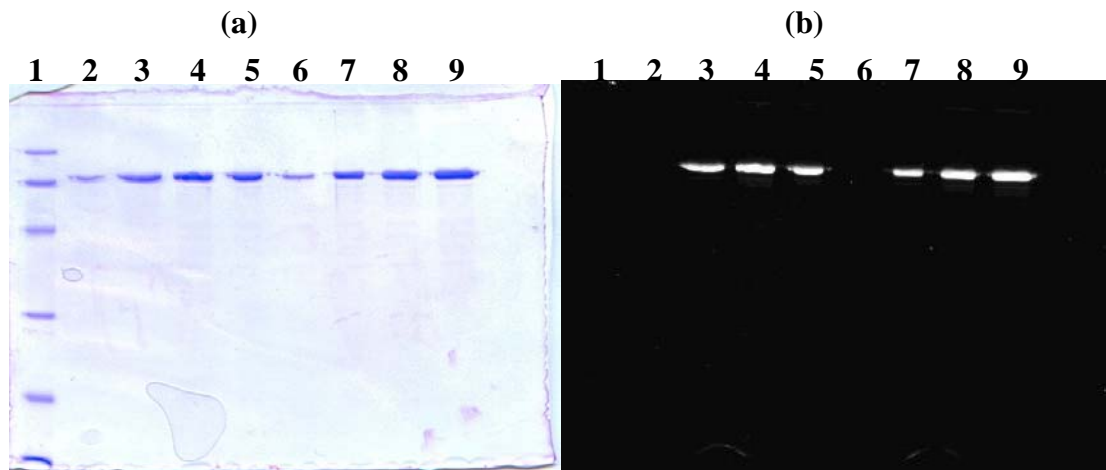


Figure 5.13 SDS-PAGE of fluorophore labeled H-MBP-PenPC T167C and H-MBP-PenPC L169C stained with Coomassie-blue (a) and under UV illumination (b). Lane 1, low range molecular marker: rabbit muscle phosphorylase b (97400 Da), BSA (66200 Da), hen egg white ovalbumin (45000 Da), bovine carbonic anhydrase (31000 Da), soybean trypsin inhibitor (21500 Da), hen egg white lysozyme (14400 Da);

Lane 2, H-MBP-PenPC T167C;

Lane 3, H-MBP-PenPC T167Cb;

Lane 4, H-MBP-PenPC T167Cf;

Lane 5, H-MBP-PenPC T167Cr;

Lane 6, H-MBP-PenPC L169C;

Lane 7, H-MBP-PenPC L169Cb;

Lane 8, H-MBP-PenPC L169Cf;

Lane 9, H-MBP-PenPC L169Cr.

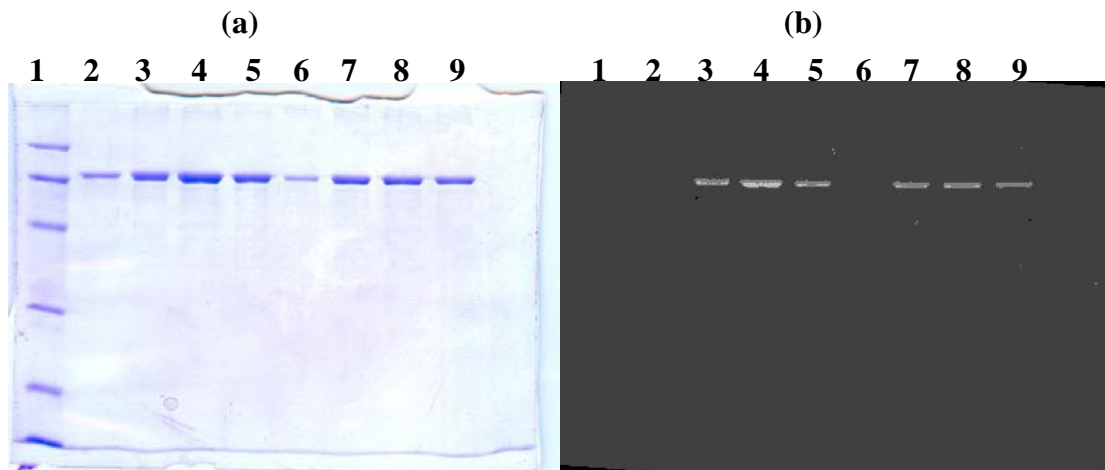


Figure 5.14 SDS-PAGE of fluorophore labeled H-MBP-PenPC N170C and H-MBP-PenPC A172C stained with Coomassie-blue (a) and under UV illumination.

(b)

Lane 1, low range molecular marker: rabbit muscle phosphorylase b (97400 Da), BSA (66200 Da), hen egg white ovalbumin (45000 Da), bovine carbonic anhydrase (31000 Da), soybean trypsin inhibitor (21500 Da), hen egg white lysozyme (14400 Da);

Lane 2, H-MBP-PenPC N170C;

Lane 3, H-MBP-PenPC N170Cb;

Lane 4, H-MBP-PenPC N170Cf;

Lane 5, H-MBP-PenPC N170Cr;

Lane 6, H-MBP-PenPC A172C;

Lane 7, H-MBP-PenPC A172Cb;

Lane 8, H-MBP-PenPC A172Cf;

Lane 9, MBP-PenPC A172Cr.

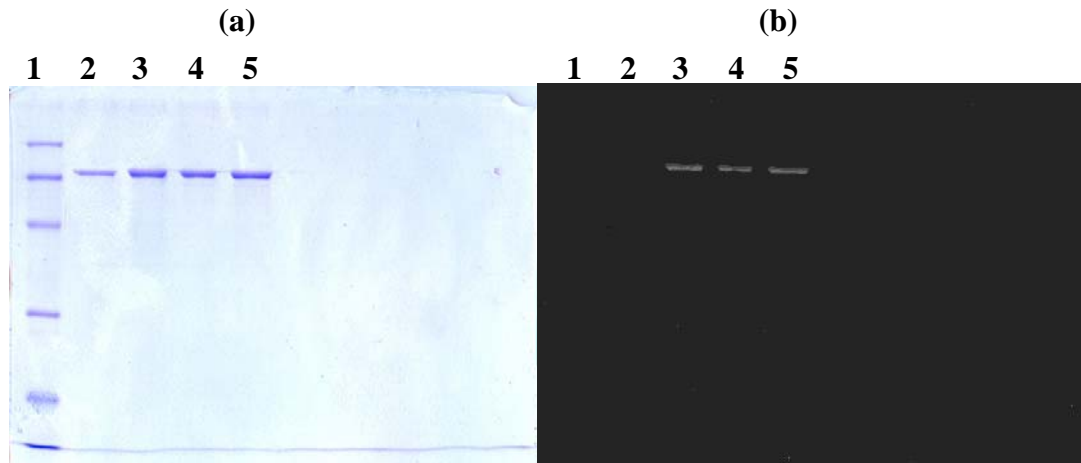


Figure 5.15 SDS-PAGE of fluorophore labeled H-MBP-PenPC D176C stained with Coomassie-blue (a) and under UV illumination. (b)

Lane 1, low range molecular marker: rabbit muscle phosphorylase b (97400 Da), BSA (66200 Da), hen egg white ovalbumin (45000 Da), bovine carbonic anhydrase (31000 Da), soybean trypsin inhibitor (21500 Da), hen egg white lysozyme (14400 Da);

Lane 2, H-MBP-PenPC D176C;

Lane 3, H-MBP-PenPC D176Cb;

Lane 4, H-MBP-PenPC D176Cf;

Lane 5, H-MBP-PenPC D176Cr.

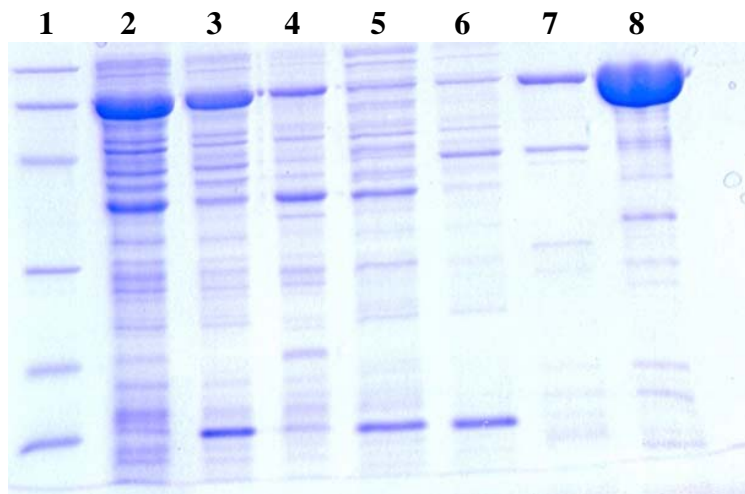


Figure 5.16 Purification of H-MBP-PenPC Y105W/E166C

Lane 1, low range molecular marker: rabbit muscle phosphorylase b (97400 Da), BSA (66200 Da), hen egg white ovalbumin (45000 Da), bovine carbonic anhydrase (31000 Da), soybean trypsin inhibitor (21500 Da), hen egg white lysozyme (14400 Da);

Lane 2, crude cell lysate;

Lane 3, soluble part of cell lysate;

Lane 4, insoluble part of cell lysate

Lane 5, cell lysate after passing through nickel-affinity column;

Lane 6, non-specific binding washed out by running buffer;

Lane 7, non-specific binding washed out by running buffer with 30 mM imidazole

Lane 8, elution of H-MBP-PenPC E166C by elution buffer

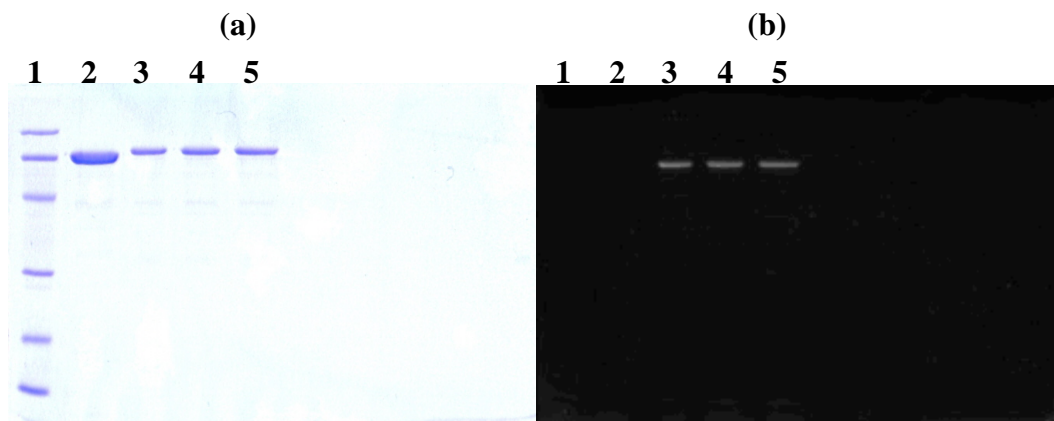


Figure 5.17 SDS-PAGE of fluorophore labeled H-MBP-PenPC Y105W/E166C stained with Coomassie-blue (a) and under UV illumination. (b)

Lane 1, low range molecular marker: rabbit muscle phosphorylase b (97400 Da), BSA (66200 Da), hen egg white ovalbumin (45000 Da), bovine carbonic anhydrase (31000 Da), soybean trypsin inhibitor (21500 Da), hen egg white lysozyme (14400 Da);

Lane 2, H-MBP-PenPC Y105W/E166C,

Lane 3, H-MBP-PenPC Y105W/E166Cb,

Lane 4, H-MBP-PenPC Y105W/E166Cf,

Lane 5, H-MBP-PenPC Y105W/E166Cr

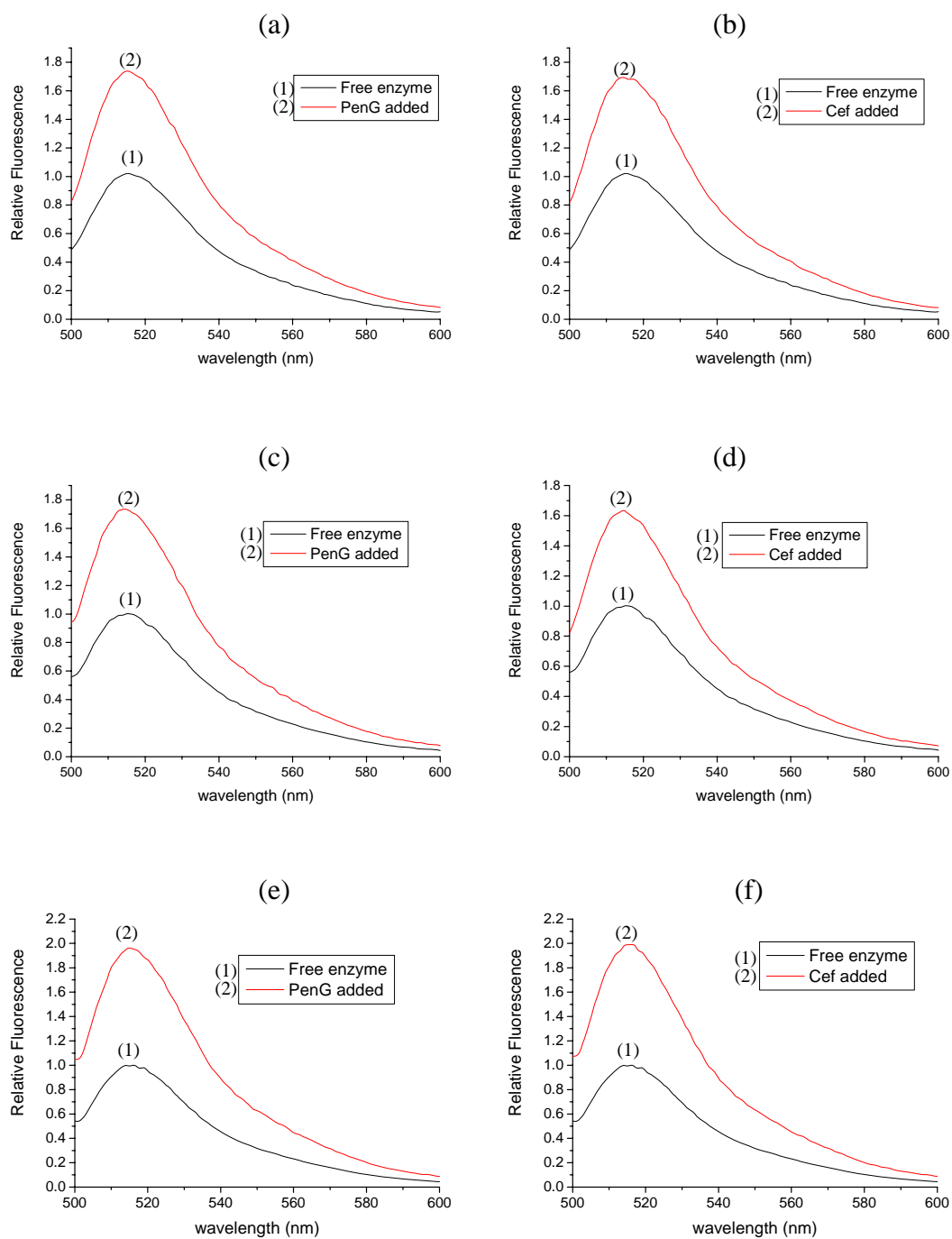


Figure 5.18 Fluorescent spectra of H-PenPC E166Cf ((a) and (b)), PenPC-H E166Cf ((c) and (d)), and H-MBP-PenPC E166Cf ((e) and (f)), in the present of 2 mM penicillin G and cefuroxime.

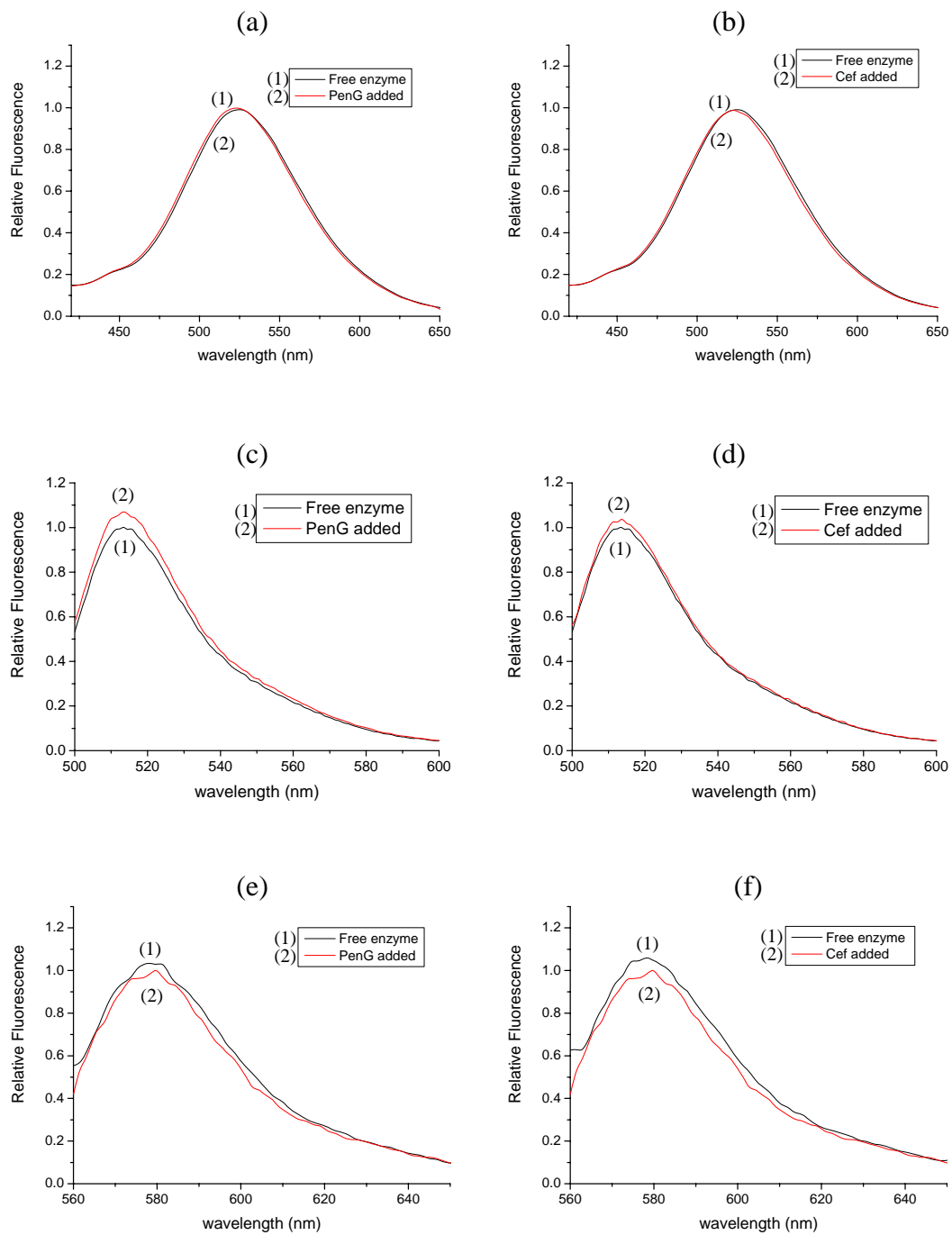


Figure 5.19 Fluorescence spectra of H-MBP-PenPC F165C labeled with badan ((a) and (b)), FM ((c) and (d)), and TMRM ((e) and (f)), in the presence of 2 mM penicillin G and cefuroxime.

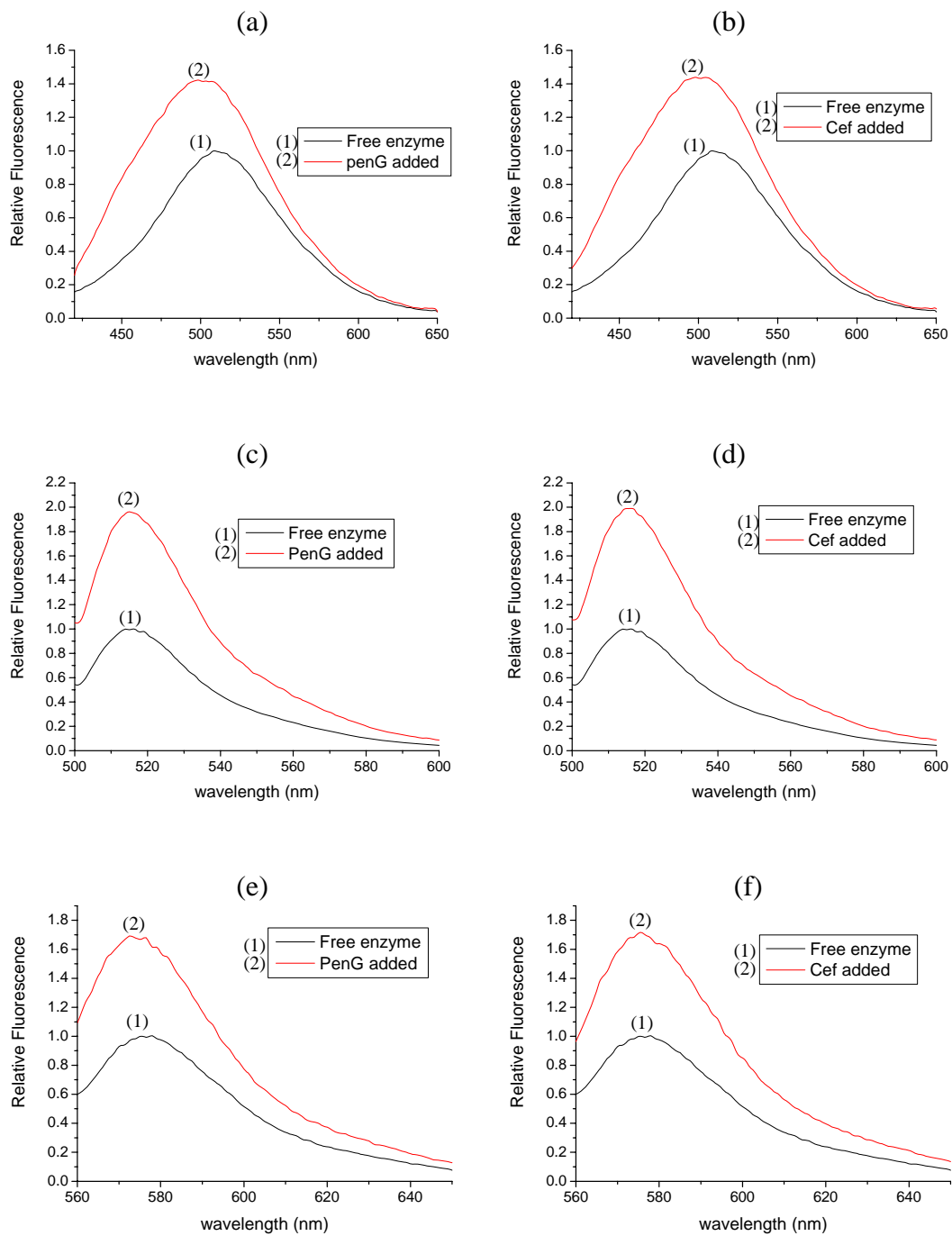


Figure 5.20 Fluorescence spectra of H-MBP-PenPC E166C labeled with badan ((a) and (b)), FM ((c) and (d)), and TMRM ((e) and (f)), in the presence of 2 mM penicillin G and cefuroxime.

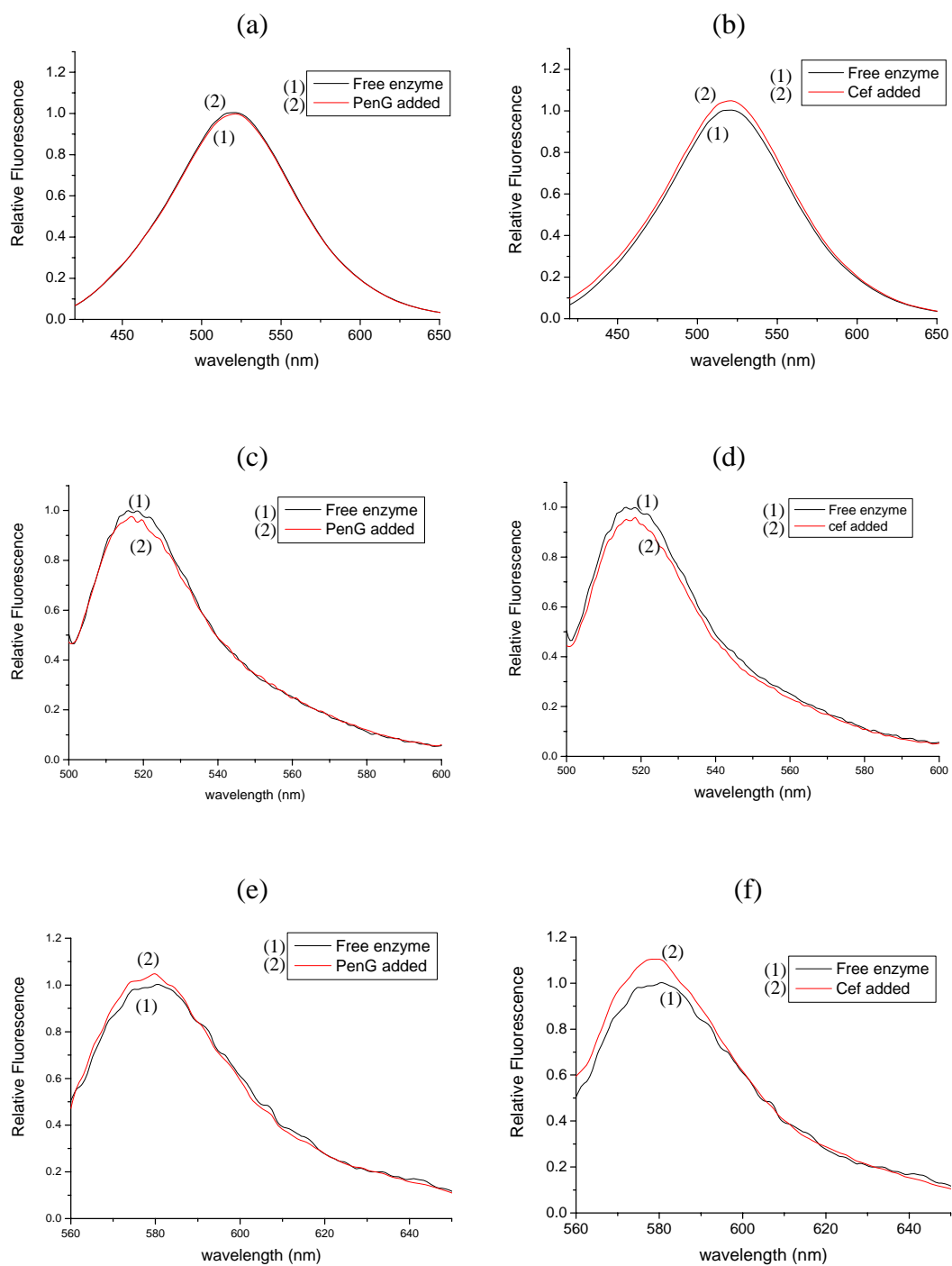


Figure 5.21 Fluorescence spectra of H-MBP-PenPC T167C labeled with badan ((a) and (b)), FM ((c) and (d)), and TMRM ((e) and (f)), in the presence of 2 mM penicillin G and cefuroxime.

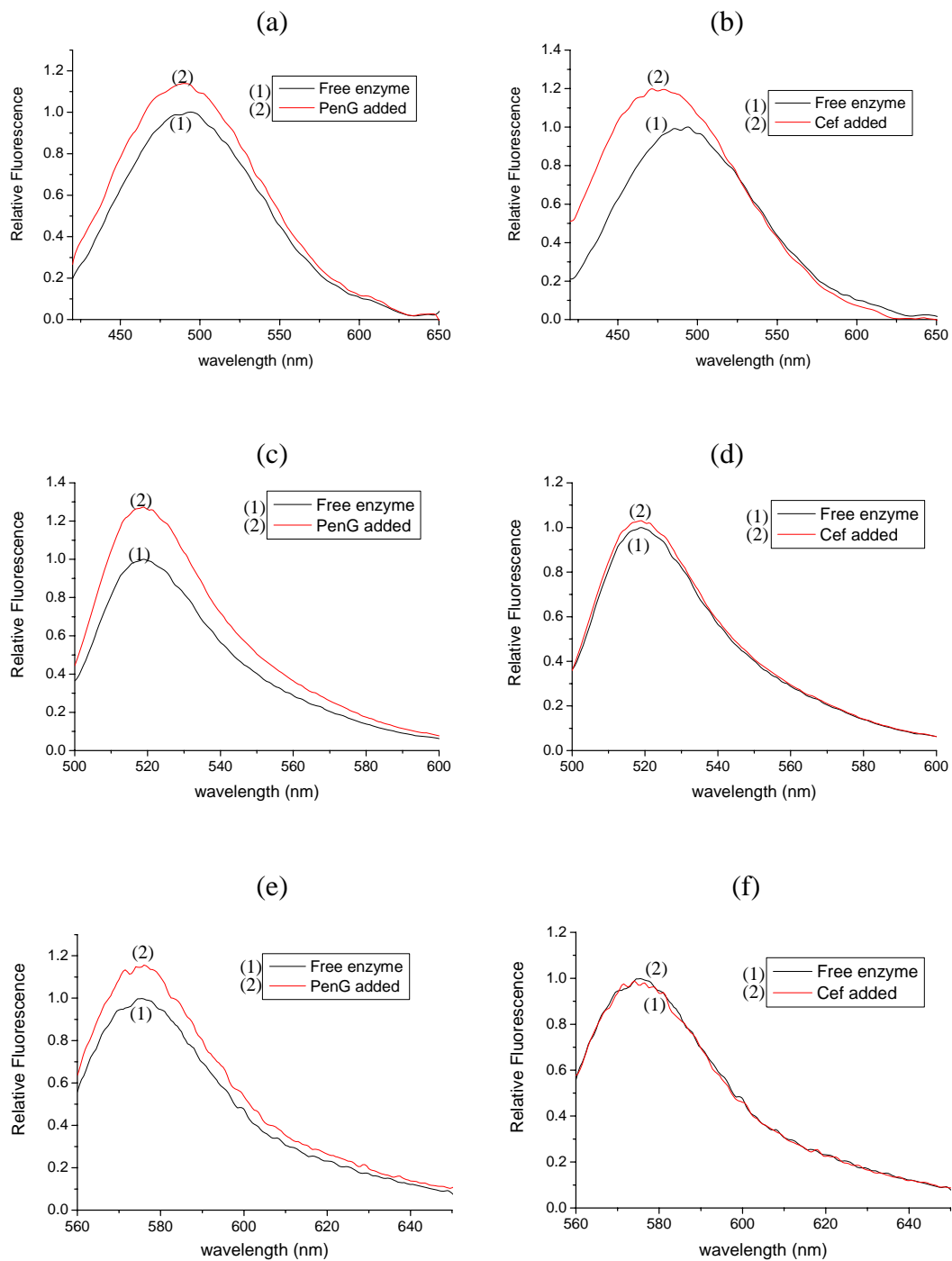


Figure 5.22 Fluorescence spectra of H-MBP-PenPC L169C labeled with badan ((a) and (b)), FM ((c) and (d)), and TMRM ((e) and (f)), in the presence of 2 mM penicillin G and cefuroxime.

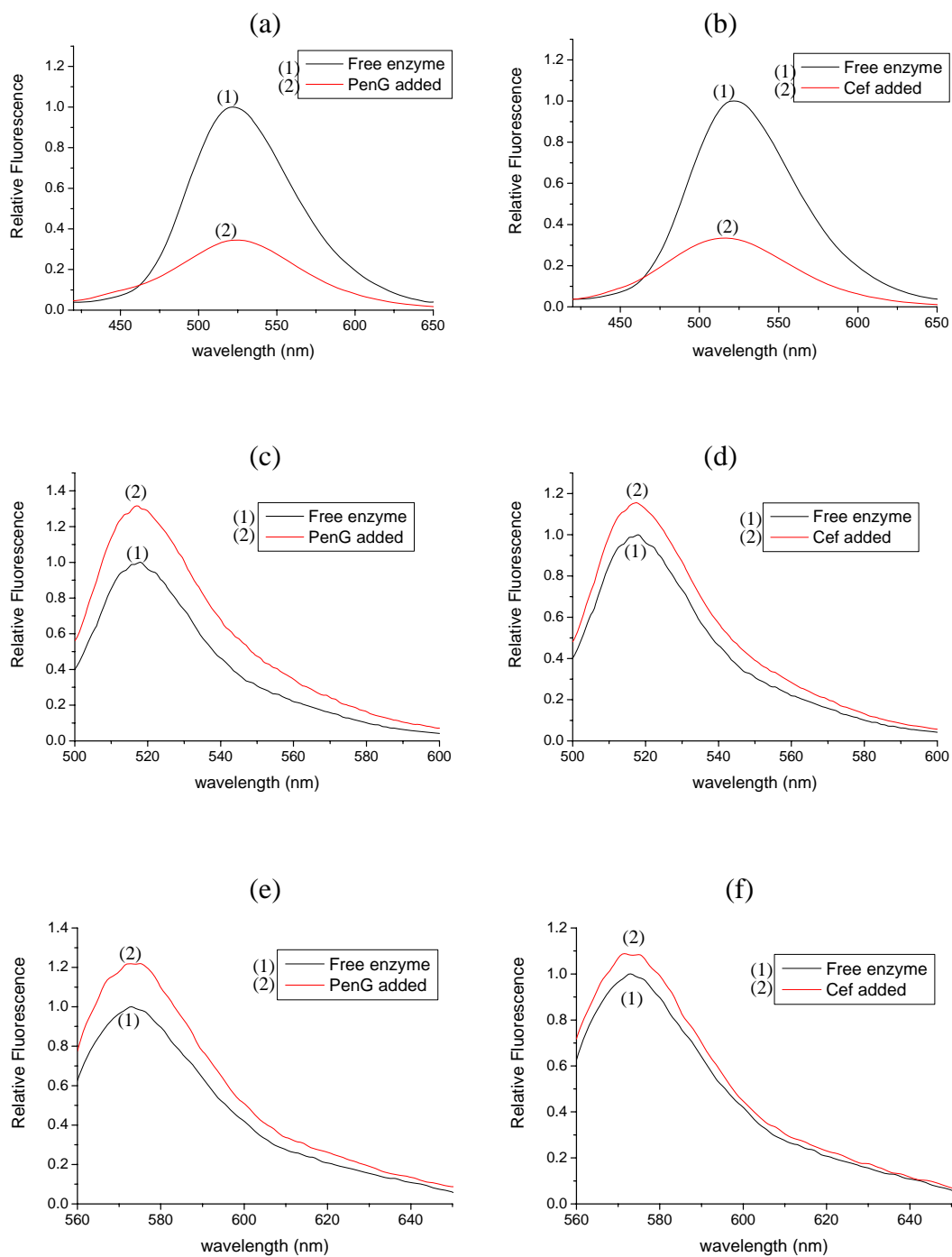


Figure 5.23 Fluorescence spectra of H-MBP-PenPC N170C labeled with badan ((a) and (b)), FM ((c) and (d)), and TMRM ((e) and (f)), in the presence of 2 mM penicillin G and cefuroxime.

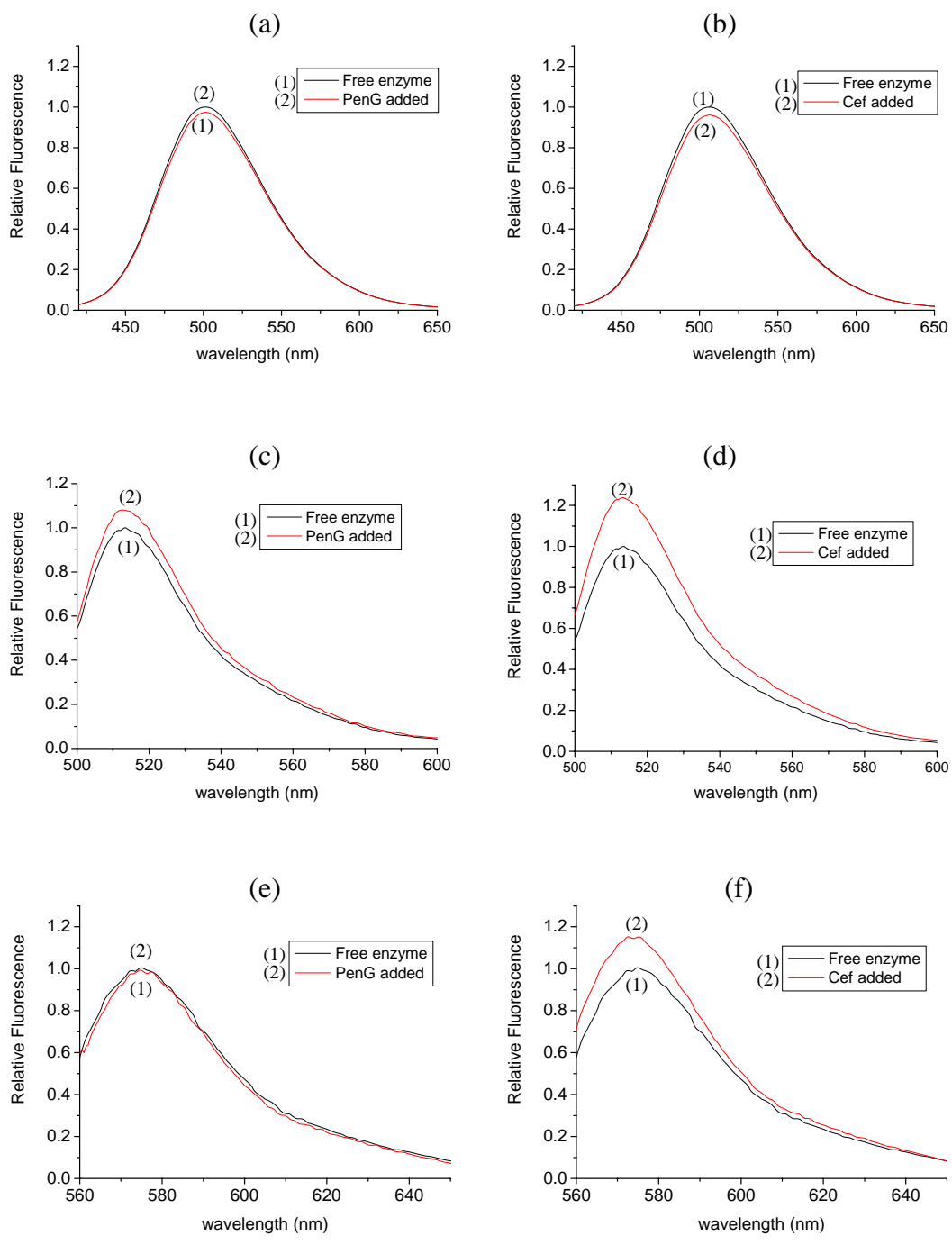


Figure 5.24 Fluorescence spectra of H-MBP-PenPC A172C labeled with badan ((a) and (b)), FM ((c) and (d)), and TMRM ((e) and (f)), in the presence of 2 mM penicillin G and cefuroxime.

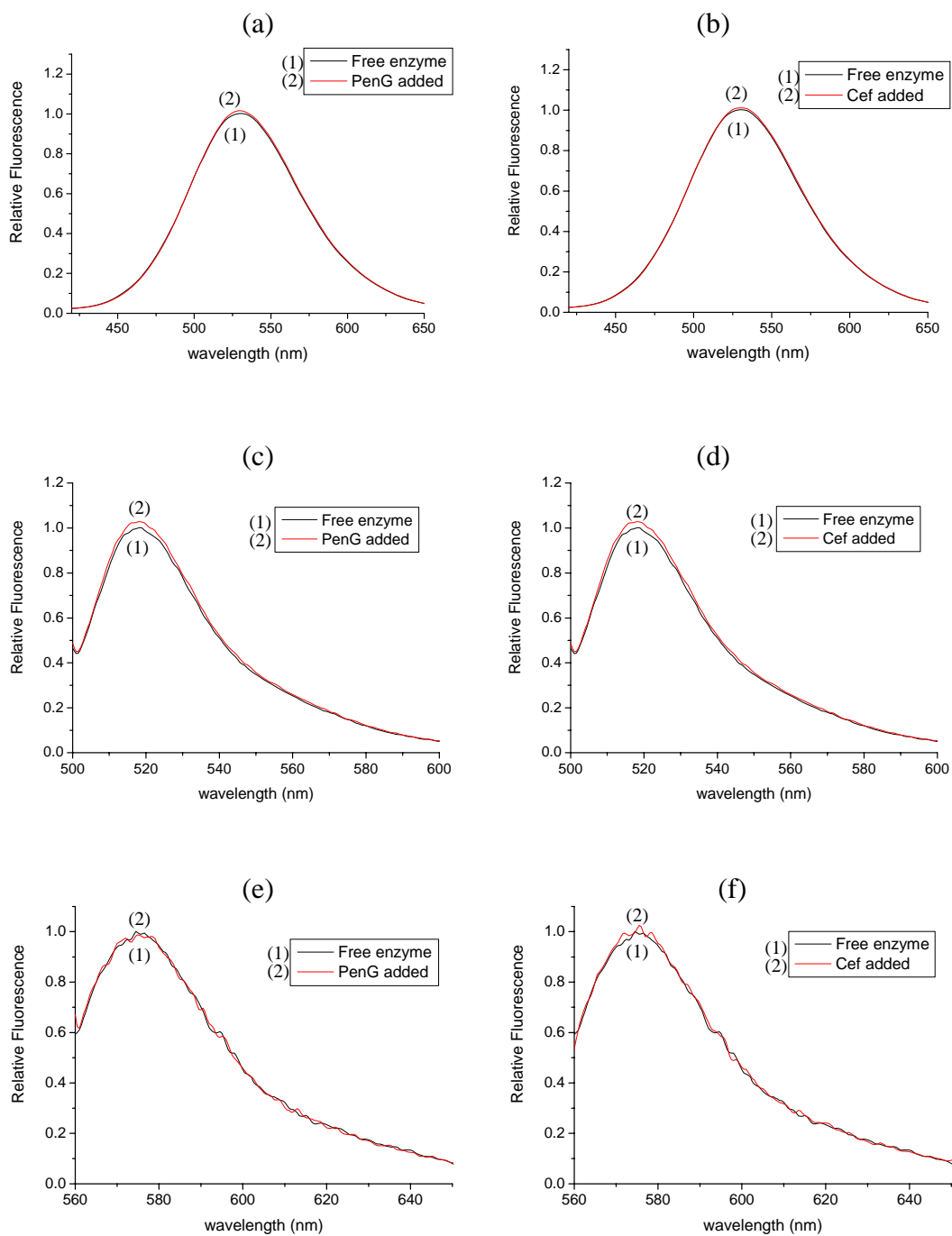


Figure 5.25 Fluorescence spectra of H-MBP-PenPC D176C labeled with badan ((a) and (b)), FM ((c) and (d)), and TMRM ((e) and (f)), in the presence of 2 mM penicillin G and cefuroxime.

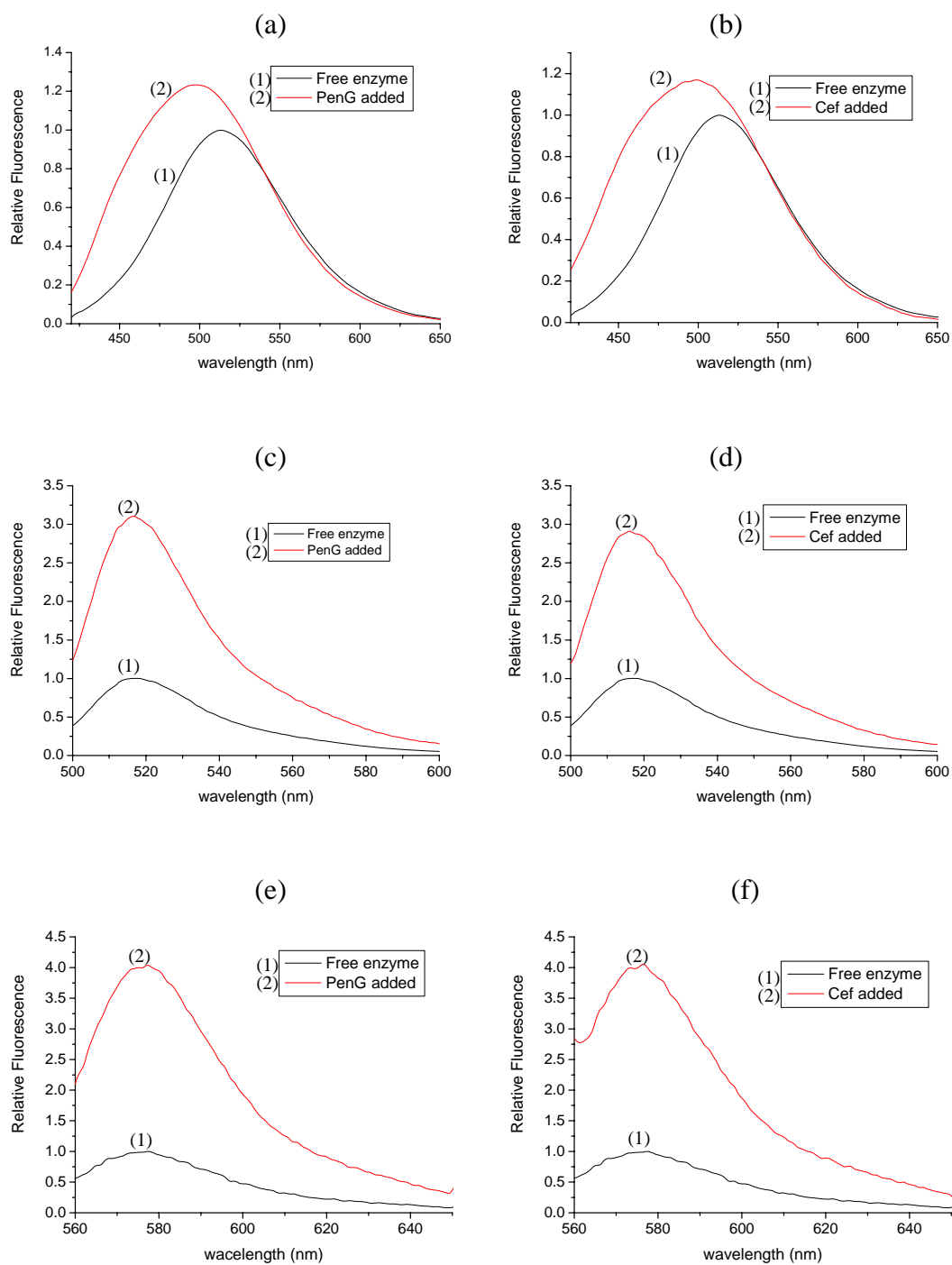


Figure 5.26 Fluorescence spectra of H-MBP-PenPC Y105W/E166C labeled with badan ((a) and (b)), FM ((c) and (d)), and TMRM ((e) and (f)), in the presence of 2 mM penicillin G and cefuroxime.

Table 5.4 Fluorescence signal of (a) badan, (b) FM and (c) TMRM labeled

H-MBP-PenPC mutants

(a)

| Position | Relative change in fluorescence | |
|----------|---------------------------------|------------|
| | Penicillin G | Cefuroxime |
| 165 | 1.0 | 1.0 |
| 166 | 2.0 | 1.9 |
| 167 | 1.0 | 1.0 |
| 169 | 1.6 | 1.6 |
| 170 | 0.3 | 0.3 |
| 172 | 1.2 | 1.1 |
| 176 | 1.0 | 1.0 |

(b)

| Position | Relative change in fluorescence | |
|----------|---------------------------------|------------|
| | Penicillin G | Cefuroxime |
| 165 | 1.0 | 1.0 |
| 166 | 2.0 | 2.0 |
| 167 | 1.0 | 1.0 |
| 169 | 1.0 | 1.0 |
| 170 | 1.3 | 1.2 |
| 172 | 1.2 | 1.1 |
| 176 | 1.0 | 1.0 |

(c)

| Position | Relative change in fluorescence | |
|----------|---------------------------------|------------|
| | Penicillin G | Cefuroxime |
| 165 | 1.0 | 1.0 |
| 166 | 1.7 | 1.7 |
| 167 | 1.0 | 1.0 |
| 169 | 1.1 | 1.0 |
| 170 | 1.2 | 1.1 |
| 172 | 1.2 | 1.0 |
| 176 | 1.0 | 1.0 |

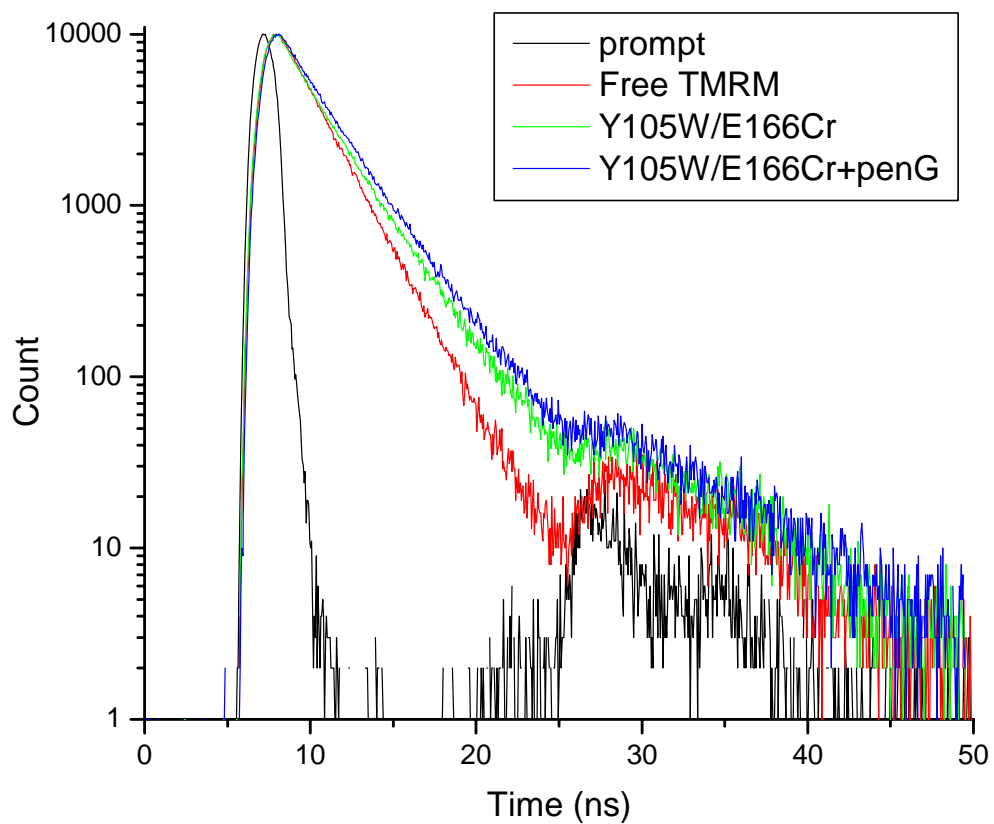


Figure 5.27 Time resolved decay curves of prompt (black), free TMRM (red), H-MBP-PenPC Y105W/E166Cr (green) and penicillin G bound H-MBP-PenPC Y105W/E166Cr (blue). The lifetime of each species are shown below:

| | $\tau_1(\text{ns})/a_1$ | τ_2/a_2 | $\bar{\tau}$ | χ^2 |
|------------------------------------|-------------------------|--------------|--------------|----------|
| TMRM | 2.33 / 1 | – | 2.33 | 1.02 |
| H-MBP-PenPC Y105W/E166Cr | 1.48 / 0.38 | 3.12 / 0.62 | 2.50 | 1.12 |
| H-MBP-PenPC Y105W/E166Cr + penG | 2.14 / 0.58 | 3.65 / 0.42 | 2.77 | 1.18 |

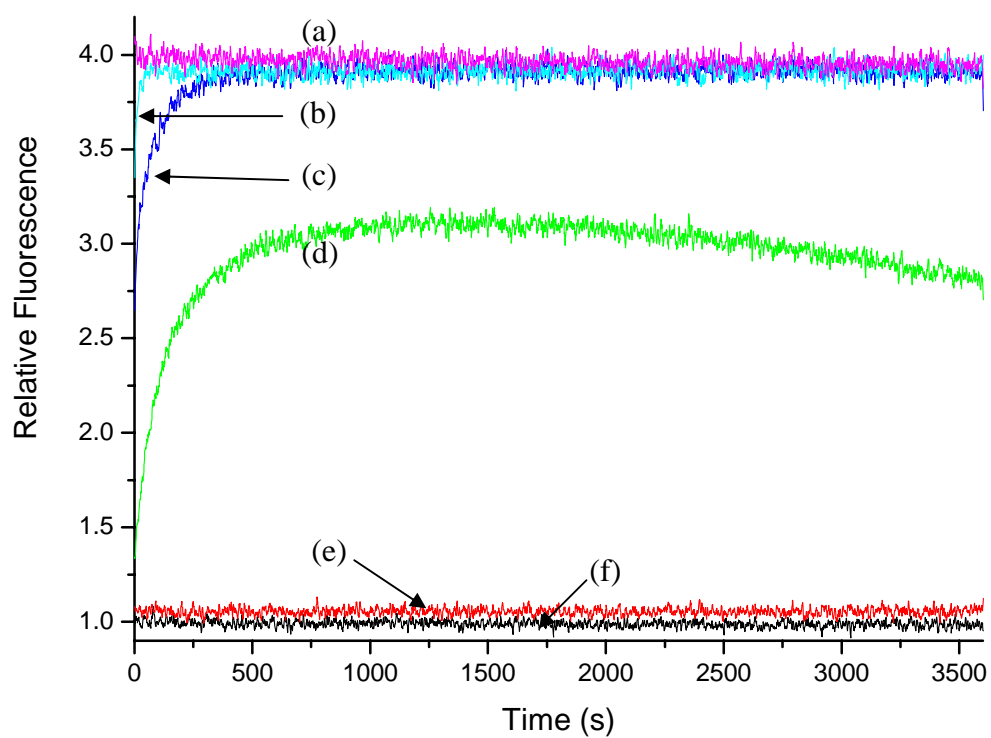


Figure 5.28 Time dependent fluorescence measurements of H-MBP-PenPC Y105W/E166Cr in the presence of penicillin G, (a) 10^{-4} M, (b) 10^{-5} M, (c) 10^{-6} M, (d) 10^{-7} M, (e) 10^{-8} M, and (f) free enzyme

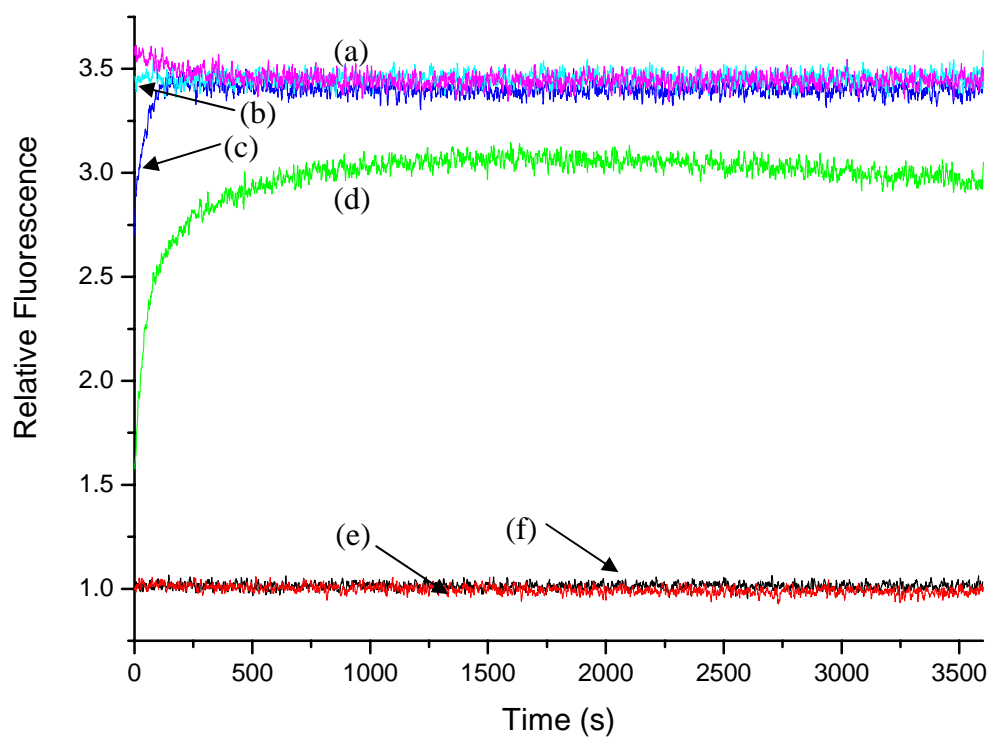


Figure 5.29 Time dependent fluorescence measurements of H-MBP-PenPC Y105W/E166Cr in the presence of penicillin V, (a) 10^{-4} M, (b) 10^{-5} M, (c) 10^{-6} M, (d) 10^{-7} M, (e) 10^{-8} M, and (f) free enzyme

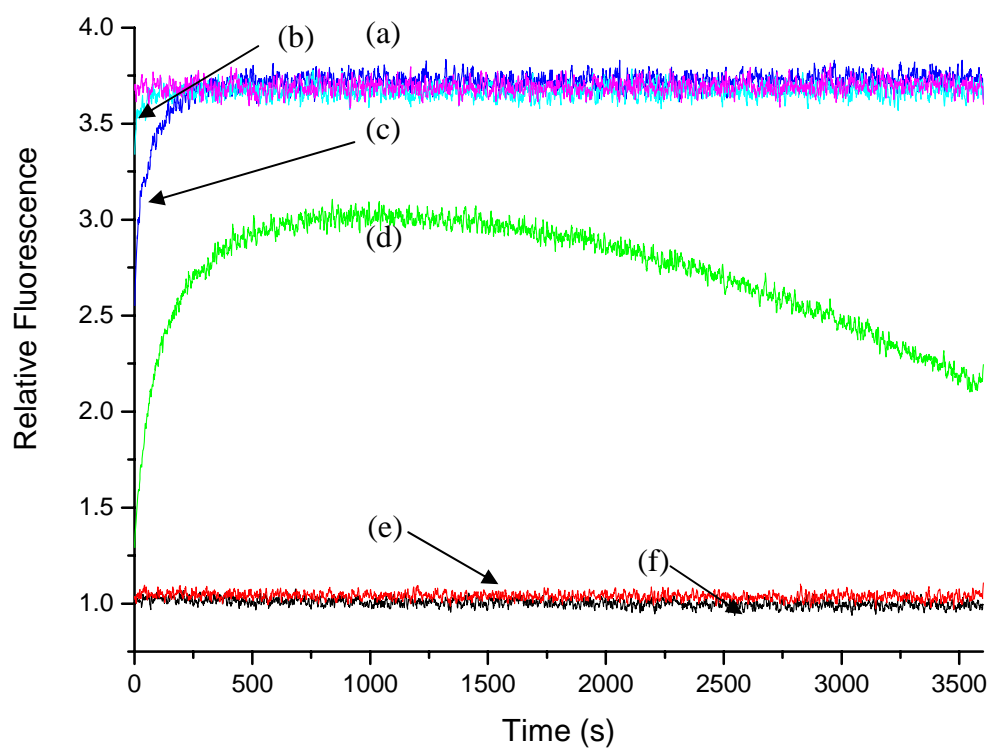


Figure 5.30 Time dependent fluorescence measurements of H-MBP-PenPC Y105W/E166Cr in the presence of ampicillin, (a) 10^{-4} M, (b) 10^{-5} M, (c) 10^{-6} M, (d) 10^{-7} M, (e) 10^{-8} M, and (f) free enzyme

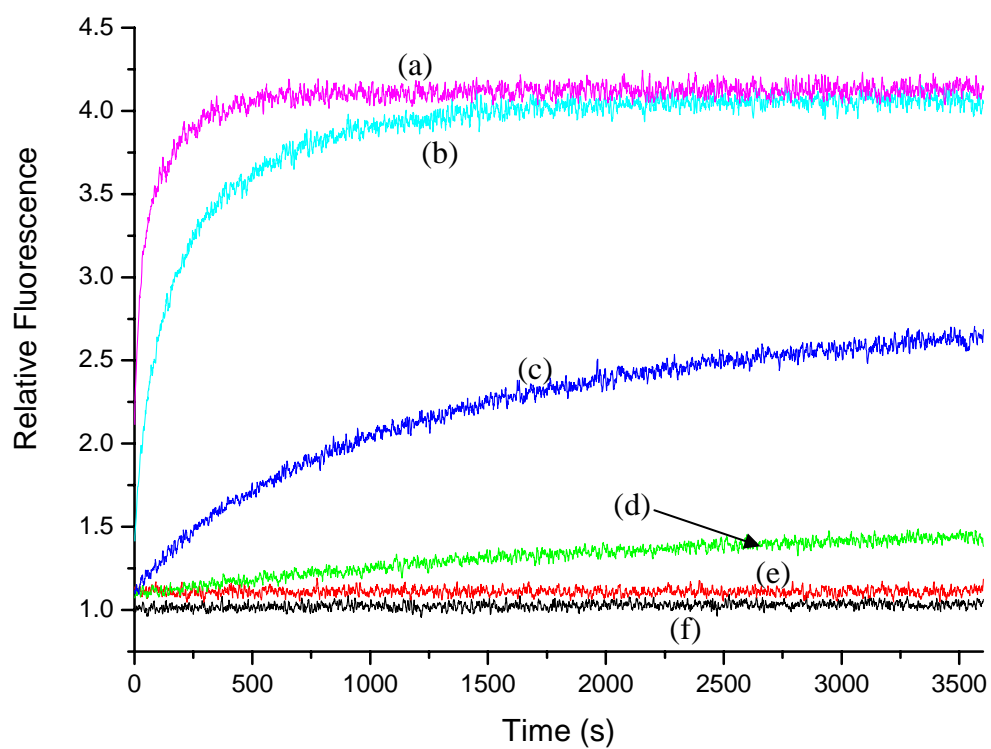


Figure 5.31 Time dependent fluorescence measurements of H-MBP-PenPC Y105W/E166Cr in the presence of cefuroxime, (a) 10^{-4} M, (b) 10^{-5} M, (c) 10^{-6} M, (d) 10^{-7} M, (e) 10^{-8} M, and (f) free enzyme

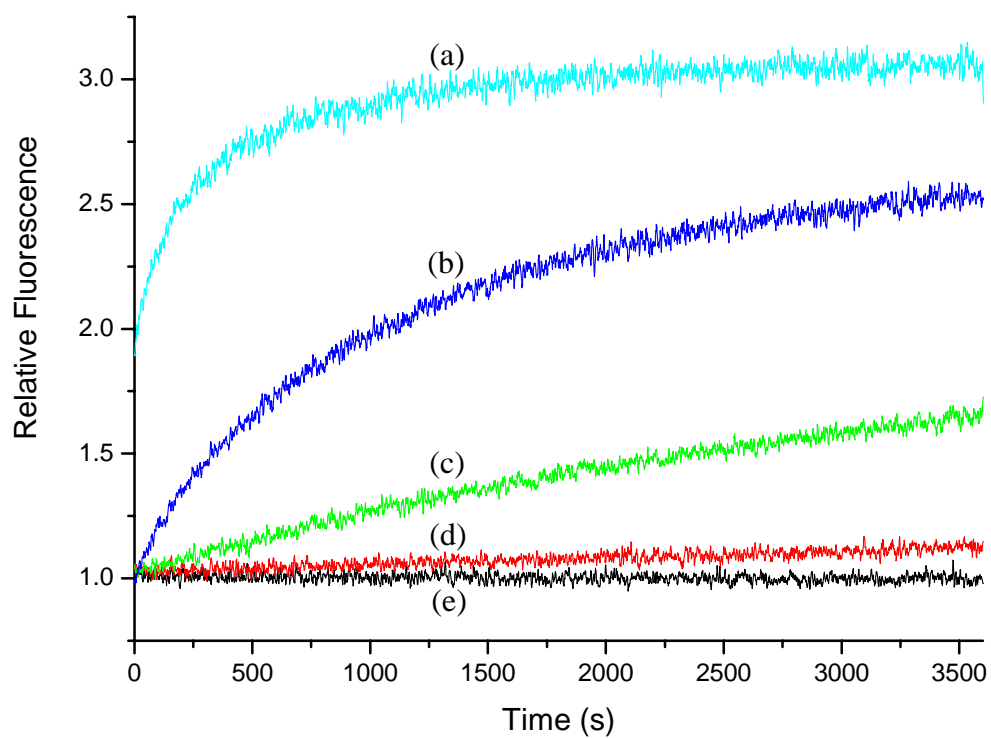


Figure 5.32 Time dependent fluorescence measurements of H-MBP-PenPC Y105W/E166Cr in the presence of cefoxitin, (a) 10^{-4} M, (b) 10^{-5} M, (c) 10^{-6} M, (d) 10^{-7} M, and (e) free enzyme

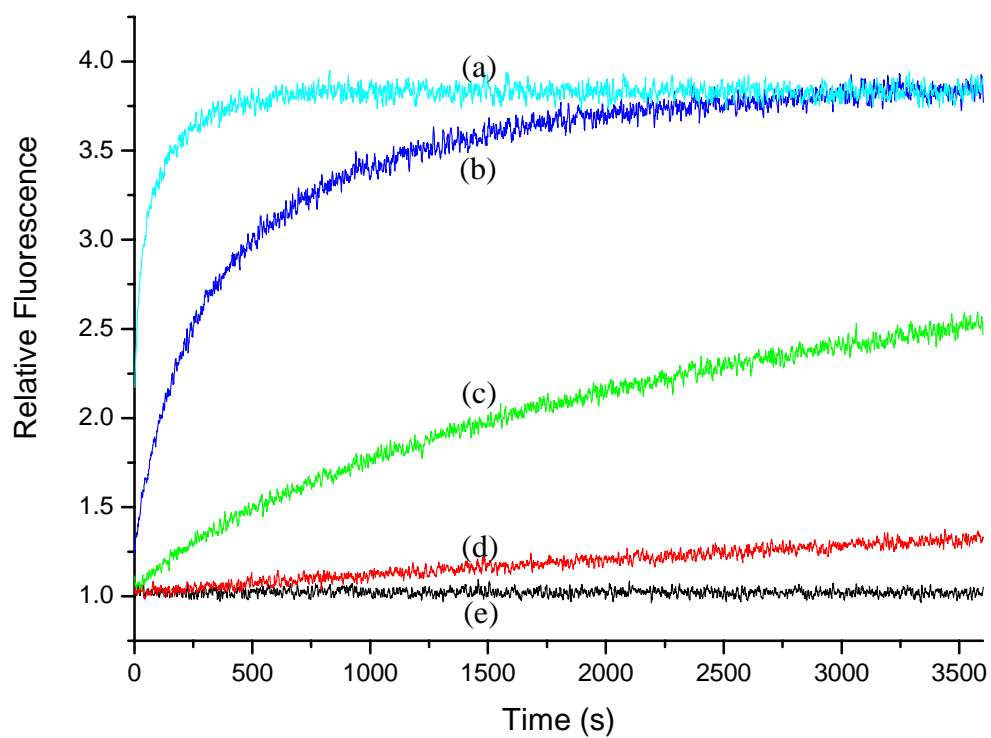


Figure 5.33 Time dependent fluorescence measurements of H-MBP-PenPC Y105W/E166Cr in the presence of moxalactam, (a) 10^{-4} M, (b) 10^{-5} M, (c) 10^{-6} M, (d) 10^{-7} M, and (e) free enzyme

5.4 Discussion

5.4.1 Effect of affinity tags on PenPC biosensors

The successful preparation of recombinant proteins rely heavily on the purification of target proteins from the protein matrix of expression host. Metal affinity chromatography for his-tag proteins is one of the most popular one-step purification strategies [122, 123]. This method is popular because it can be applied to a large number of different proteins and the small size of his-tag has minimal effect on the tertiary structure of most recombinant proteins. In the case of PenPC β -lactamase, the purification of protein can be done within one day and the purity obtained was quite satisfactory, which is much less time consuming than the previous expression and purification protocol.

However, this tag was reported to affect the activities of some proteins significantly. Indeed, Frere reported that the activity and also the folding of PenP β -lactamase can be impaired by addition of his-tag to the C-terminal [52]. Thus, although the addition of his-tag to PenPC β -lactamase mutants enable fast and simple purification, the effect of this tag should be figured out before the recombinant protein was used as biosensor. Indeed, the his-tag on β -lactamase not only affected the

activity of PenP β -lactamase, but also the fluorescence signal of fluorophore labeled PenPC mutants. The fluorescence change of H-PenPC E166Cf and PenPC-H E166Cf upon addition of penicillin G and cefuroxime was about 1.7 folds, which is significantly lower than the original PenPC E166Cf. Interestingly, the large size MBP fused to the N-terminal of PenPC E166Cf has no significant effect on the fluorescence signal. This could partly be attributed to the flexible linker between MBP and PenPC (GGSGS), which minimized the interaction between MBP and PenPC. Another possible reason for this difference could be the direct effect of his-tag on the protein structure. Addition of multiple positive charges to the protein may destabilize some secondary structure. In this case, the interaction with the dipole moment of the α -helix at the N-terminal is one possibility. The structure of the protein may become less stable and the FM label become more dynamic, resulting in a smaller degree of change in solvent accessible area upon β -lactam binding.

5.4.2 Fluorescence signals of PenPC biosensors with different fluorophore labeling locations

Different fluorophores had been labeled on different positions of the Ω -loop, and, the fluorescence signals of the labeled mutants were compared. Labeled F165C and

D176C showed no fluorescence increase in the presence of penicillin G and cefuroxime. However, based on all known β -lactamase crystal structures, residue 165 is much closer to the active site than residue 176. This suggests that the distance from the active site may not be the major determining factor of signal generation. The other obvious factor affecting the signal is the orientation of the fluorophore. Although the actual orientations of fluorophores are not known, both equivalent residues are not pointing towards the active site in the available crystal structures. Moreover, the emission maximum of F165Cb and D176Cb is significantly red shifted compared to other badan labeled mutants, implying that the location of labeled fluorophores (at least badan) is pointing outward to the solvent side. However, it is also possible that this modification impairs the substrate binding ability of the enzyme, and as a result, no signal can be generated.

L169C gave a significant increase in fluorescence when labeled with badan and FM. The emission maximum of L169Cb is blue shifted by an additional 10 nm compared to E166Cb, indicating the initial fluorophore environment is more hydrophobic than E166Cb. Actually, the highly conserved L169 is buried by other amino acid residues, the small badan label may locate in a similar position. Interestingly, the magnitude of bathochromic shift and fluorescence enhancement

caused by penicillin G is smaller than cefuroxime, which may result from the larger sized cefuroxime molecule. In contrast to L169Cb, L169Cf and L169Cr showed increase in fluorescence signal after the addition of penicillin G but not cefuroxime. This increase in fluorescence intensity cannot be explained by reduction in solvent exposure area. This rise in fluorescence without a significant change in emission maximum may result from the departure of fluorophore from quenching amino acid residues as proposed in chapter 4.

The other two positions, 170 and 172, were also selected for fluorophore labeling in the optimization of PenP based biosensor. The residue in position 172 is not conserved but is preferred for its hydrophobic environment (e.g. Val in PenP and Ala in PenPC). Similar to L169, X-ray crystal structure shows that the side chain of V172 is also buried by other residues. It is probable that the residue of A172C in PenPC has similar flexibility as V172C in PenP. In fact, all labeled 172 cysteine mutants behave similarly, all of them give a relatively small increase in fluorescence, which makes it useless for β -lactam biosensing. H-MBP-PenPC N170C is, on the contrary, more interesting. Although FM and TMRM labeled H-MBP-PenPC N170C show little fluorescence change to penicillin G and cefuroxime, the fluorescence of badan labeled mutant is largely reduced by the two substrates. This is opposite to PenP N170Cb, as

the fluorescence is largely enhanced by the presence of β -lactams. It showed that the signal behavior can be totally different for different β -lactamase even an equivalent and highly conserved residue were mutated and labeled with the same fluorophore. Moreover, the addition of penicillin G and cefuroxime to N170Cb also have unexpected effect to the fluorescence. Penicillin G – bound N170Cb has emission maximum slightly red shifted than the free N170Cb (from 521 nm to 523 nm). This small red shift is, however, incoherent with the large reduction of fluorescence intensity. More unexpected is the blue shift in emission maximum, which indicated that the environment surrounding the fluorophore had become more hydrophobic. In both cases, the excitation spectra resemble that of free N170Cb, indicating that the presence of another non-radiative relaxation process occur in the bound state of N170Cb. In addition, the quenching processing upon addition of cefuroxime is much stronger than penicillin G, because the rise in fluorescence by reduction of solvent accessibility (as indicated by the blue shifted emission maximum) was offset.

5.4.3 Fluorescence signals of fluorophore labeled H-MBP-PenPC Y105W/E166C

Although it is well known that Y105 is a highly conserved residue in class A β -lactamase [50], the role of this residue on protein structure and activity is still not

completely understood [124, 125]. Indeed, mutating this position into other amino acids, such as tryptophan, will not impair the catalytic ability of the enzyme. Believing that Y105W also has little effect on the acylation of β -lactams, this mutation was introduced to PenPC based biosensor. The substrate binding is not significantly impaired by this single point mutation, but it causes a large difference in the fluorescence signal profile of labeled PenPC E166C.

H-MBP-PenPC Y105W/E166Cb showed an impaired response to penicillin G and cefuroxime as compared to H-MBP-PenPC E166Cb. The smaller bathochromic shift and fluorescence signal in Y105W/E166Cb that indicated the badan label experienced a lower change in solvent accessibility than in E166Cb. The environment of badan molecule should be similar in E166Cb and Y105W/E166Cb as the fluorescence properties of both free enzymes are very similar. In other words, the smaller change in fluorescence in Y105W/E166Cb is caused by the reduction of fluorescence intensity of bound-state of Y105W/E166Cb. Probably, the larger size tryptophan imposed a steric effect on the badan label which caused a smaller change in environment upon the binding of antibiotic.

Y105W/E166Cf showed a significant signal improvement over E166Cf, and it

could be resulting from a different molecular event. Based on our previously proposed signal generation mechanism, the change in fluorescence signal is caused by the increase in solvent accessibility of the FM label in the bound state. The molecular model constructed previously showed that the FM label is fully exposed to solvent in the substrate-bound state [86]. Thus, the larger change in fluorescence signal in Y105W/E166Cf is likely caused by a reduction of the fluorescence in the unbound state. This implies that the tryptophan at position 105 either provides a more hydrophobic environment to FM than tyrosine, or a more effective PET quenching effect has occurred. Tryptophan has a higher reduction potential than tyrosine and therefore should be a more effective quencher. It is believed that the latter mechanism is more likely because no bathochromic shift was observed in the emission spectra in the presence of antibiotics.

The mutant labeled with TMRM has the highest sensitivity among all the biosensors prepared. The tryptophan mutation improves the sensitivity of E166Cr from 1.6 folds to 4 folds. This mutant was therefore studied in details and the results are discussed as follows.

5.4.4 Properties of TMRM labeled H-MBP-PenPC Y105W/E166C

TMR, together with other rhodamine and fluorescein derivatives, are known as xanthene fluorophores. These fluorophores are commonly used in biological events because of the relatively high quantum yield and visible range excitation. Moreover, many of these dyes are sensitive to pH, solvent viscosity and polarity, making them useful environment sensitive fluorophores. Indeed, TMR have a higher quantum yield in a more viscous and lower polarity solvent which can be used for a probe for environmental polarity. This phenomenon can be explained by the non-radiative relaxation process of this fluorophore. It is believed that a twisted intramolecular charge transfer (TICT) process is the most dominant non-radiative relaxation for rhodamine derivatives with rotating dialkylamine moiety [126-128]. This process generates dual emission in some dialkylamino aromatic compounds, such as p-dimethylamino benzonitrile, but non-emissive biradicaloid charge transferred species in xanthene dyes [129]. High viscosity and lower polarity reduce this quenching process and thus raise the quantum yield of TMR.

This solvent response is opposite to FM which shows a higher quantum yield in a more polar environment. In addition, the similar molecular size and shape between

FM and TMRM should result in similar dynamic and conformation after labeled on the cysteine residue. If the change in solvent accessibility of the fluorophore is responsible for the signal generation mechanism, the effect of β -lactam binding on the fluorescence signal of FM and TMRM labeled E166C should be opposite. However, our experimental results showed that the fluorescence of both fluorophore labeled mutants were enhanced in the presence of β -lactams. One might argue that the dynamic and conformation of the FM and TMRM labels are different, as TMRM has the dimethyl substituents and a positively charged xanthene ring in contrast to the negatively charged ring in FM. This might affect the direction of movement of the fluorophore upon substrate binding. However, the addition of tryptophan, which has similar hydrophobicity as tyrosine, caused a huge increase in fluorescence signal. Moreover, the quantum yield of Y105W/E166Cr is significantly smaller than E166Cr, i.e. the Y105W mutation causes a significant fluorescence quenching. All these phenomena cannot be easily explained by the “solvent accessibility hypothesis” only. Most probably, the large change in fluorescence signal of Y105W/E166Cr is due to the suppression of the background fluorescence through a PET quenching process as proposed in the previous chapter. The interaction between tryptophan and TMR is stronger than fluorescein [130, 131], and as a result, the relative fluorescence change of Y105W/E166Cr caused by substrate binding is larger than Y105W/E166Cf.

Interestingly, the TMRM label on Y105W/E166C changed the decay pattern to biexponential, but did not greatly alter the average fluorescence lifetime. The appearance of a longer lifetime species could be due to the steric hindrance on the rotation of the dimethylamino group, thus inhibiting the TICT non-radiative decay. The faster decay species, which has a much shorter lifetime than that of free TMRM, could arise from environment factor as well as intermolecular quenching. Reduction of the electronic conjugation between the phenyl-carboxyl group and the xanthene ring on the TMRM label can cause a decrease in fluorescence lifetime. Thus the conformation of TMRM in this fast decay species may involve some interaction between the phenyl-carboxyl groups with an amino acid residue. Another possibility is dynamic fluorescence quenching of the TMRM by a nearby amino acid residue. Addition of penicillin G raises the lifetime of both species for about 0.5 ns, meaning that this relaxation factor is shared between the two species. However, the proportion of the fast decay process is increased, and as a result, the average fluorescence lifetime is slightly increased by 0.2 ns. The similarity in fluorescence lifetime means that the dynamic quantum yield of both substrates bound and unbound state are similar. By using equation 5 in section 4.4.2, the ratio of static quantum yield of the unbound over bound state was found to be 3.7. This showed that the addition of penicillin G mainly increased the static quantum, i.e. preventing TMRM from static

quenching. Indeed, it has been reported that the quenching mechanism of TMR by tryptophan can be either dynamic or static [130].

The fluorescence time profile of H-MBP-PenPC Y105W/E166Cr is quite similar to H-MBP-PenPC E166Cf, except that the decreasing phase is absent at high concentration of penicillin type antibiotics. This can be attributed to the Y105W mutation which lowers the hydrolytic activity of the enzyme. Since the effect is small, the deacylation still happened and the decreasing phase can be observed at lower concentrations. Although the penicillin antibiotics have very similar molecular structure, penicillin V and ampicillin gave lower fluorescence signal. This could be due to the specific interaction between antibiotics and TMRM. The fluorescence time profile in detecting of cephalosporins is also similar to H-MBP-PenPC E166Cf, the detection of cefuroxime and moxalactam by both biosensors showed a significant faster increasing phase than cefoxitin. Therefore, the Y105W mutation and the change of fluorophore from FM to TMRM did not affect the substrate specificity.

Unfortunately, the detection limit is still similar to H-MBP-PenPC E166Cf even though the fluorescence signal is largely improved. Most importantly, the concentration of biosensor used is at about 10^{-7} M, and it is almost impossible to

detect antibiotic at nanomolar concentration range. This is because the enzyme concentration is about 100 folds larger than the substrate concentration when antibiotic is at 10^{-9} M. Assuming all antibiotic molecule effectively bound to the biosensor and without dissociation, there are only 1 % biosensor responsible for the fluorescence signal. In the case of H-MBP-PenPC Y105W/E166Cr, the change in fluorescence is 4 folds, which means 1 % of the biosensor will give 4 % increase in fluorescence. To detect such small signal, a very sensitive spectrofluorometer is required.

5.5 Concluding remark

The gene of H-MBP-PenPC E166C has been successfully cloned into pRsetK and pHMal-c2xK. Three different tagged proteins, H-PenPC E166C, PenPC-H E166C and H-MBP-PenPC E166C, were expressed and purified with 95% purity. Labeling these mutants with FM showed that direct attachment of his-tag to a fluorophore labeled biosensor can affect the fluorescence signal. On the contrary, fusing a large tag with a flexible linker to a fluorescent biosensor will not significantly affect the sensitivity. This his-tagged MBP-PenPC fusion protein was selected for further optimization – different residues on Ω -loop were mutated to be cysteine for fluorophore labeling. Most of the labeled mutants showed small or even no fluorescence signal upon addition of β -lactams. Only two mutants E166C and N170C showed distinct changes. H-MBP-PenPC N170Cb showed a large quench in fluorescence, upon the binding of β -lactamase, which is in contrast to PenP N170Cb. The labeled PenPC E166C with the largest increase in fluorescence was subjected to further modification in order to improve the sensitivity. Based on the mechanism proposed in previous chapter, a more reducing residue, tryptophan, was selected to replace the tyrosine at position 105. This mutation increased the fluorescence quenching efficiency of free H-MBP-PenPC Y105W/E166Cr but had little effect on

the quantum yield of the β -lactam-bound H-MBP-PenPC Y105W/E166Cr.

Chapter 6

Conclusions

PenP and PenPC β -lactamase based fluorescent biosensors with E166C mutation and badan or FM labels have been reported previously. These biosensors have a maximum of about 2 folds increase in fluorescence upon binding to β -lactam antibiotics. To improve the performance of fluorescent β -lactamase based biosensors, three class A β -lactamaes, namely PenP, PenPC and TEM, were chosen for further modification and optimization in this study

Different positions for fluorophore labeling were selected in the three enzymes. The criterion for selecting the right amino acid residue for fluorophore labeling was to pick those with side chain pointing inward to the active site. Labeled E166C β -lactamase mutants generate fluorescence signal but the N170Cb of PenP and V216Cf of TEM-1 give the largest increase in fluorescence in these two enzymes. For PenPC, the E166C mutant always gives the largest fluorescence signal

Further improvement of fluorescence signal was conducted by modification of the active site, which was performed on TEM and PenPC based biosensors. The active site of the TEM β -lactamase was enlarged by inserting 3 mutations, E104K, M182T and G238S, to TEM-1 V216C to give the TEM-52 V216C mutant. The TEM-52 V216C mutant labeled with FM showed a 3.6 folds increase in fluorescence upon

addition of penicillin G and is significantly improved over TEM-1 and other previous β -lactamase based biosensors. Interestingly, this large change in fluorescence is not accompanied with any bathochromic shift. Lifetime study on this biosensor showed that the fluorescence of FM is quenched dynamically in the free form, whereas the average fluorescence lifetime of FM is raised by β -lactam binding. It is proposed that the fluorescence of FM is quenched by the Tyr-105 residue before substrate binding, and the binding of substrate releases the fluorophore from quenching. This process, in addition to change in solvent accessibility of the fluorophore, is responsible for the sensing mechanism of the biosensors.

The active site of PenPC was modified by a single point mutation Y105W. This mutation dramatically increased the sensitivity of the TMRM labeled mutant, with a 4 folds change in fluorescence. This improvement in fluorescence response can be attributed to the quenching of the fluorescence intensity of the free enzyme by the tryptophan 105 residue.

The results of this study provide important clues to further improve these fluorophore labeled β -lactamase biosensors. The background fluorescence of free biosensor can be suppressed by introducing selected amino acid residues which

quench the background fluorescence by PET. Actually, the open and highly accessible β -lactamase active site imposes maximum limit on the difference in solvent accessibility of the fluorophore between the substrate-bound and free states. However, fluorescence quenching of the free unbound state of the enzyme can be achieved by mild modification (e.g. with tryptophan mutation). This provides a new and promising direction to improve the fluorescence signals of β -lactamase based biosensors, or even other fluorophore conjugated protein biosensors.

In order to make these biosensors to be applicable, some improvements have to be achieved. For example, the detection limit should be at sub-nanomolar level, and the the time required for the detection should be as short as 15 min. In addition, the interference from the matrix in the sample, e.g. colloid which may scatter emission light from the biosensors should be taken into account.

In these improved biosensors, however, the detection of sub-nanomolar concentration β -lactams was not successful. This is caused by not just the sensitivity, but also the relatively slow and weak binding of β -lactams to the biosensors. Therefore, binding of substrate to the biosensors have to be further improved, e.g. by applying directed evolution to these β -lactamase to raise the binding affinity and rate

of association between β -lactams and biosensors.

Reference

1. Hutchinson, J. M., Patrick, D. M., Marra, F., Ng, H., Bowie, W. R., Heule, L., Muscat, M., and Monnet, D. L., Measurement of antibiotic consumption: A practical guide to the use of the Anatomical Therapeutic Chemical classification and Defined Daily Dose system methodology in Canada. *The Canadian Journal of Infectious Diseases*, 2004. **15**(1): 29-35.
2. Harte, H., Palmer, N. O. A., and Martin, M. V., An investigation of therapeutic antibiotic prescribing for children referred for dental general anaesthesia in three community national health service trusts. *British Dental Journal*, 2005. **198**(4): 227-31.
3. Campos, J., Ferech, M., Lazaro, E., de Abajo, F., Oteo, J., Stephens, P., and Goossens, H., Surveillance of outpatient antibiotic consumption in Spain according to sales data and reimbursement data. *Journal of Antimicrobial Chemotherapy*, 2007. **60**(3): 698-701.
4. Elander, R. P., Industrial production of beta-lactam antibiotics. *Applied Microbiology and Biotechnology*, 2003. **61**(5-6): 385-92.
5. Bryskier, A., *Antimicrobial Agents: Antibacterials and Antifungals*, Washington, D.C.: American Society for Microbiology, 2005, 1426.
6. O'Grady, F., Finch, R. G., Lambert, H. P., and Greenwood, D., *Antibiotic and Chemotherapy, Seventh Edition: Anti-Infective Agents and their Use in*

- Therapy*, Edinburgh: Churchill Livingstone, 1997, 987
7. Mascaretti, O. A., *Bacteria Versus Antibacterial Agents: An Integrated Approach*, Washington, D. C.: American Society for Microbiology, 2003, 420.
 8. Periti, P. and Nicoletti, P., Classification of beta -lactam antibiotics according to their pharmacodynamics. *Journal of Chemotherapy*, 1999. **11**(5): 323-330.
 9. Bryskier, A., Classification of beta-lactams. *Pathologie Biologie*, 1984. **32**(5): 658-67.
 10. Page, M. I., *The Chemistry of beta -Lactams*, Glasgow: Blackie, 1993, 351.
 11. Del Rosso, J. A., *Drug Actions, Reactions and Interactions*, Philadelphia: Elsevier Inc. 2007. 270
 12. Duguid, J. P., The sensitivity of bacteria to the action of penicillin. *Edinburgh Medical Journal*, 1946. **53**: 401-12.
 13. Tipper, D. J. and Strominger, J. L., Mechanism of action of penicillins: a proposal based on their structural similarity to acyl-D-alanyl-D-alanine. *Proceedings of the National Academy of Sciences of the United States of America*, 1965. **54**(4): 1133-41.
 14. Blumberg, P. M. and Strominger, J. L., Interaction of penicillin with the bacterial cell. Penicillin-binding proteins and penicillin-sensitive enzymes. *Bacteriological Reviews*, 1974. **38**(3): 291-335.

15. Schleifer, K. H. and Kandler, O., Peptidoglycan types of bacterial cell walls and their taxonomic implications. *Bacteriological Reviews*, 1972. **36**(4): 407-77.
16. White, D., *The Physiology and Biochemistry of Prokaryotes, 2nd Edition*, New York: Oxford University Press, 2000, 565
17. Sauvage, E., Kerff, F., Terrak, M., Ayala, J. A., and Charlier, P., The penicillin-binding proteins: structure and role in peptidoglycan biosynthesis. *FEMS Microbiology Reviews*, 2008. **32**(3): 556.
18. Popham, D. L., Gilmore, M. E., and Setlow, P., Roles of low-molecular-weight penicillin-binding proteins in *Bacillus subtilis* spore peptidoglycan synthesis and spore properties. *Journal of Bacteriology*, 1999. **181**(1): 126-132.
19. Goffin, C. and Ghuysen, J.-M., Multimodular penicillin-binding proteins: an enigmatic family of orthologs and paralogs. *Microbiology and Molecular Biology Reviews*, 1998. **62**(4): 1079-1093.
20. Di Guilmi, A. M., Mouz, N., Petillot, Y., Forest, E., Dideberg, O., and Vernet, T., Deacylation Kinetics Analysis of *Streptococcus pneumoniae* Penicillin-Binding Protein 2x Mutants Resistant to beta-Lactam Antibiotics Using Electrospray Ionization- Mass Spectrometry. *Analytical Biochemistry*, 2000. **284**(2): 240-246.

21. Macheboeuf, P., Lemaire, D., Dos Santos Martins, A., Dideberg, O., Jamin, M., and Dessen, A., Trapping of an Acyl-Enzyme Intermediate in a Penicillin-Binding Protein (PBP)-Catalyzed Reaction. *Journal of Molecular Biology*, 2008. **381**(1): 248.
22. Lu, W.-P., Sun, Y., Bauer, M. D., Paule, S., Koenigs, P. M., and Kraft, W. G., Penicillin-Binding Protein 2a from Methicillin-Resistant *Staphylococcus aureus*: Kinetic Characterization of Its Interactions with beta -Lactams Using Electrospray Mass Spectrometry. *Biochemistry*, 1999. **38**(20): 6537-6546.
23. Di Guilmi, A. M., Dessen, A., Dideberg, O., and Vernet, T., Functional characterization of penicillin-binding protein 1b from *Streptococcus pneumoniae*. *Journal of Bacteriology*, 2003. **185**(5): 1650-1658.
24. Roychoudhury, S., Dotzlaf, J. E., Ghag, S., and Yeh, W. K., Purification, properties, and kinetics of enzymic acylation with beta-lactams of soluble penicillin-binding protein 2a. A major factor in methicillin-resistant *Staphylococcus aureus*. *Journal of Biological Chemistry*, 1994. **269**(16): 12067-73.
25. Zapun, A., Contreras-Martel, C., and Vernet, T., Penicillin-binding proteins and beta -lactam resistance. *FEMS Microbiology Reviews*, 2008. **32**(2): 361-385.

26. Samraoui, B., Sutton, B. J., Todd, R. J., Artymiuk, P. J., Waley, S. G., and Phillips, D. C., Tertiary structural similarity between a class A beta-lactamase and a penicillin-sensitive D-alanyl carboxypeptidase-transpeptidase. *Nature*, 1986. **320**(6060): 378-80.
27. Challis, G. L. and Hopwood, D. A., Synergy and contingency as driving forces for the evolution of multiple secondary metabolite production by *Streptomyces* species. *Proceedings of the National Academy of Sciences of the United States of America*, 2003. **100**(Suppl. 2): 14555-14561.
28. Hall, B. G. and Barlow, M., Evolution of the serine beta -lactamases: past, present and future. *Drug Resistance Updates*, 2004. **7**(2): 111-123.
29. Selwyn, S., Lacey, R. W., and Bakhtiar, M., *The Beta-Lactam Antibiotics: Penicillins and Cephalosporins in Perspective*, London: Hodder and Stoughton, 1980, 364.
30. Fisher, J. F., Meroueh, S. O., and Mobashery, S., Bacterial resistance to beta -lactam antibiotics: Compelling opportunism, compelling opportunity. *Chemical Reviews*, 2005. **105**(2): 395-424.
31. Woodruff, H. B. and Foster, J. W., Microbiological aspects of penicillin. VII. Bacterial penicillinase. *Journal of Bacteriology*, 1945. **49**: 7-17.
32. Bush, K., Characterization of beta -lactamases. *Antimicrobial Agents and*

- Chemotherapy*, 1989. **33**(3): 259-63.
33. Bush, K., Jacoby, G. A., and Medeiros, A. A., A functional classification scheme for beta -lactamases and its correlation with molecular structure. *Antimicrobial Agents and Chemotherapy*, 1995. **39**(6): 1211-33.
34. Hall, B. G. and Barlow, M., Revised Ambler classification of beta -lactamases. *Journal of Antimicrobial Chemotherapy*, 2005. **55**(6): 1050-1051.
35. Fleming, P. C., Goldner, M., and Glass, D. G., Observations on the nature, distribution, and significance of cephalosporinase. *Lancet*, 1963. **1**(7296): 1399-401.
36. Richmond, M. H. and Sykes, R. B., The beta-lactamases of gram-negative bacteria and their possible physiological role. *Advances in Microbial Physiology*, 1973. **9**: 31-88.
37. Sawai, T., Mitsunashi, S., and Yamagishi, S., Drug resistance of enteric bacteria. XIV. Comparison of beta -lactamases in gram-negative rod bacteria resistant to alpha -aminobenzylpenicillin. *Japanese Journal of Microbiology*, 1968. **12**(4): 423-34.
38. Sykes, R. B. and Matthew, M., The beta-lactamases of Gram-negative bacteria and their role in resistance to beta -lactam antibiotics. *Journal of Antimicrobial Chemotherapy*, 1976. **2**(2): 115-57.

39. Ambler, R. P., The structure of beta-lactamases. *Philosophical Transactions of the Royal Society of London. Series B, Biological Sciences*, 1980. **289**(1036): 321-31.
40. Ambler, R. P., Coulson, A. F. W., Frere, J. M., Ghuysen, J. M., Joris, B., Forsman, M., Levesque, R. C., Tiraby, G., and Waley, S. G., A standard numbering scheme for the Class A beta-lactamases. *Biochemical Journal*, 1991. **276**(1): 269-70.
41. Galleni, M., Lamotte-Brasseur, J., Rossolini, G. M., Spencer, J., Dideberg, O., Frere, J.-M., Amicosante, G., Franceschini, N., Bush, K., Concha, N. O., Herzberg, O., Livermore, D. M., Nordmann, P., Rasmussen, B. A., Rodrigues, J., Saavedra, M. J., Sutton, B., Fabiane, S. M., and Toney, J. H., Standard numbering scheme for class B beta -lactamases. *Antimicrobial Agents and Chemotherapy*, 2001. **45**(3): 660-663.
42. Daiyasu, H., Osaka, K., Ishino, Y., and Toh, H., Expansion of the zinc metallo-hydrolase family of the beta -lactamase fold. *FEBS Letters*, 2001. **503**(1): 1-6.
43. Garau, G., Di Guilmi, A. M., and Hall, B. G., Structure-based phylogeny of the metallo-beta -lactamases. *Antimicrobial Agents and Chemotherapy*, 2005. **49**(7): 2778-2784.

44. Murphy, B. P. and Pratt, R. F., Evidence for an oxyanion hole in serine beta-lactamases and DD-peptidases. *Biochemical Journal*, 1988. **256**(2): 669-72.
45. Nahm, K., Theoretical study on tetrahedral intermediate formation by class A beta -lactamase: the effects of the oxyanion hole and substrate specificity. *Bulletin of the Korean Chemical Society*, 1998. **19**(10): 1029-1031.
46. Banerjee, S., Pieper, U., Kapadia, G., Pannell, L. K., and Herzberg, O., Role of the omega-loop in the activity, substrate specificity, and structure of class A beta-lactamase. *Biochemistry*, 1998. **37**(10): 3286-96.
47. Vijayakumar, S., Ravishanker, G., Pratt, R. F., and Beveridge, D. L., Molecular Dynamics Simulation of a Class A beta -Lactamase: Structural and Mechanistic Implications. *Journal of the American Chemical Society*, 1995. **117**(6): 1722-30.
48. Knap, A. K. and Pratt, R. F., Chemical modification of the RTEM-1 thiol beta-lactamase by thiol-selective reagents: evidence for activation of the primary nucleophile of the beta-lactamase active site by adjacent functional groups. *Proteins*, 1989. **6**(3): 316-23.
49. Gibson, R. M., Christensen, H., and Waley, S. G., Site-directed mutagenesis of beta-lactamase I. Single and double mutants of Glu-166 and Lys-73.

- Biochemical Journal*, 1990. **272**(3): 613-9.
50. Escobar, W. A., Tan, A. K., and Fink, A. L., Site-directed mutagenesis of beta-lactamase leading to accumulation of a catalytic intermediate. *Biochemistry*, 1991. **30**(44): 10783-7.
51. Leung, Y. C., Robinson, C. V., Aplin, R. T., and Waley, S. G., Site-directed mutagenesis of beta-lactamase I: role of Glu-166. *Biochemical Journal*, 1994. **299** (3): 671-8.
52. Guillaume, G., Vanhove, M., Lamotte-Brasseur, J., Ledent, P., Jamin, M., Joris, B., and Frere, J. M., Site-directed mutagenesis of glutamate 166 in two beta-lactamases. Kinetic and molecular modeling studies. *The Journal of Biological Chemistry*, 1997. **272**(9): 5438-44.
53. Hermann, J. C., Ridder, L., Mulholland, A. J., and Hoeltje, H.-D., Identification of Glu166 as the General Base in the Acylation Reaction of Class A beta -Lactamases through QM/MM Modeling. *Journal of the American Chemical Society*, 2003. **125**(32): 9590-9591.
54. Bradford, P. A., Extended-spectrum beta-lactamases in the 21st century: Characterization, epidemiology, and detection of this important resistance threat. *Clinical Microbiology Reviews*, 2001. **14**(4): 933-951.
55. Labia, R., Plasticity of class a beta -lactamases, an illustration with TEM and

- SHV enzymes. *Current Medicinal Chemistry: Anti-Infective Agents*, 2004. **3**(4): 251-266.
56. Osuna, J., Perez-Blancas, A., and Soberon, X., Improving a circularly permuted TEM-1 beta-lactamase by directed evolution. *Protein Engineering*, 2002. **15**(6): 463-470.
57. Ostermeier, M. A. and Guntas, G., *Development of Domain Insertion Fusion Proteins Capable of Acting as Molecular Switches Using Circular Permutation Libraries*. 2005, (Johns Hopkins University, USA). p. 146
58. Barany, F., Two-codon insertion mutagenesis of plasmid genes by using single-stranded hexameric oligonucleotides. *Proceedings of the National Academy of Sciences of the United States of America*, 1985. **82**(12): 4202-6.
59. Erster, O., Eisenstein, M., and Liscovitch, M., Ligand interaction scan: a general method for engineering ligand-sensitive protein alleles. *Nature Methods*, 2007. **4**(5): 393-395.
60. Mathonet, P., Deherve, J., Soumillion, P., and Fastrez, J., Active TEM-1 beta-lactamase mutants with random peptides inserted in three contiguous surface loops. *Protein Science*, 2006. **15**(10): 2323-2334.
61. Vandevenne, M., Filee, P., Scarafone, N., Cloes, B., Gaspard, G., Yilmaz, N., Dumoulin, M., Francois, J.-M., Frere, J.-M., and Galleni, M., The Bacillus

- licheniformis BlaP beta-lactamase as a model protein scaffold to study the insertion of protein fragments. *Protein Science*, 2007. **16**(10): 2260-71.
62. Santos, J., Risso, V. A., Sica, M. P., and Ermacora, M. R., Effects of serine-to-cysteine mutations on beta-lactamase folding. *Biophysical Journal*, 2007. **93**(5): 1707-1718.
63. Mitchell, J. M. G., M. W.; Mcewen, S. A.; McNab, W. B.; Yee, A. J., Antimicrobial drug residues in milk and meat: causes, concerns, prevalence, regulations, tests, and test performance. *Journal of Food Protection*, 1998. **61**(6): 742-756.
64. Torrence, M. E. I., Richard E, *Microbial Food Safety in Animal Agriculture: Current Topics*. 2003. 420
65. Dewdney, J. M. M., L.; Raynaud, J. P.; Blanc, F.; Scheid, J. P.; Jackson, T.; Lens, S.; Verschueren, C, Risk assessment of antibiotic residues of beta-lactams and macrolides in food products with regard to their immunoallergic potential. *Food and Chemical Toxicology*, 1991. **29**(7): 477-83.
66. Finegold, S. M., Mathisen, G. E., and George, W. L., Changes in human intestinal flora related to the administration of antimicrobial agents. *Human Intestinal Microflora in Health and Disease*, Academic Press, New York,

London, Paris, 1983, 568.

67. Pires de Abreu, L. R. O., Rodrigo Agustin Mas; Calafatti de Castro, Silvana; Pedrazzoli, Jose, Jr., HPLC determination of amoxicillin comparative bioavailability in healthy volunteers after a single dose administration. *Journal of Pharmacy & Pharmaceutical Sciences*, 2003. **6**(2): 223-230.
68. Serrano, J. M. S., M., Use of SDS micelles for improving sensitivity, resolution, and speed in the analysis of .beta.-lactam antibiotics in environmental waters by SPE and CE. *Electrophoresis*, 2007. **28**(18): 3242-3249.
69. Riediker, S. S., R. H, Simultaneous Determination of Five .beta.-Lactam Antibiotics in Bovine Milk Using Liquid Chromatography Coupled with Electrospray Ionization Tandem Mass Spectrometry. *Analytical Chemistry*, 2001. **73**(7): 1614-1621.
70. Ireland, F. S. A. i., *Rapid Test Kits for the Detection of Antibiotics and Sulphonamides in Milk*. 2002.
71. Andrew, S. M. F., R. A.; Paape, M. J.; Maturin, L. J, Evaluation of selected antibiotic residue screening tests for milk from individual cows and examination of factors that affect the probability of false-positive outcomes. *Journal of Dairy Science*, 1997. **80**(11): 3050-3057.

72. Gustavsson, E. S., A, Biosensor analysis of .beta.-lactams in milk: Comparison with microbiological, immunological, and receptor-based screening methods. *Journal of AOAC International*, 2004. **87**(3): 614-620.
73. Kai, M., Kinoshita, H., Ohta, K., Hara, S., Lee, M.K., Lu, J., Sensitive determination of a beta-lactam antibiotic, cefaclor by liquid chromatography with chemiluminescence detection. *Journal of Pharmaceutical and Biomedical Analysis*, 2003. **30**: 1765-1771.
74. Liang, P., Sanchez, R.I. and Martin, M.T., Electrochemiluminescence-based detection of beta-lactam antibiotics and beta-lactamase. *Analytical Chemistry*, 1996. **68**: 2426-2431.
75. Gustavvson, E., Degelaen, J., Bjurling, P., and Sternesjo, A. , Determination of beta-lactams in milk using a surface plasmon resonance-based biosensor. *Journal of Agricultural and Foond Chemistry*, 2004. **52**: 2791-2796.
76. Chan, P. H., So, P. K., Ma, D. L., Zhao, Y., Lai, T. S., Chung, W. H., Chan, K. C., Yiu, K. F., Chan, H. W., Siu, F. M., Tsang, C. W., Leung, Y. C., and Wong, K. Y., Fluorophore-Labeled beta-Lactamase as a Biosensor for beta -Lactam Antibiotics: A Study of the Biosensing Process. *Journal of the American Chemical Society*, 2008. **130**(20): 6351-6361.
77. Au, H. W., Properties of Fluorophore-Labeled Derivatives of Class A

- beta-Lactamases, *MPhil thesis*, 2006, The Hong Kong Polytechnic University.
78. Abraham, E. P., Chain, E., Fletcher, C. M., Gardner, A. D., Heatley, N. G., Jennings, M. A., and Florey, H. W., Further observations on penicillin. *Lancet*, 1941. **2**: 177-88.
 79. Pollock, M. R., Purification and properties of penicillinases from two strains of *Bacillus licheniformis*; a chemical, physicochemical, and physiological comparison. *Biochemical Journal*, 1965. **94**(1): 666-75.
 80. Dubnau, D. A. and Pollock, M. R., The genetics of *Bacillus licheniformis* penicillinase: a preliminary analysis from studies on mutation and inter-strain and intra-strain transformations. *Journal of General Microbiology*, 1965. **41**(1): 7-21.
 81. Gebhard, L. G., Risso, V. A., Santos, J., Ferreyra, R. G., Noguera, M. E., and Ermacora, M. R., Mapping the distribution of conformational information throughout a protein sequence. *Journal of Molecular Biology*, 2006. **358**(1): 280-288.
 82. Frate, M. C., Lietz, E. J., Santos, J., Rossi, J. P. F. C., Fink, A. L., and Ermacora, M. R., Export and folding of signal-sequenceless *Bacillus licheniformis* beta-lactamase in *Escherichia coli*. *European Journal of Biochemistry*, 2000. **267**(12): 3836-3847.

83. Moews, P. C., Knox, J. R., Dideberg, O., Charlier, P., and Frere, J. M., Beta-lactamase of *Bacillus licheniformis* 749/C at 2 Å resolution. *Proteins*, 1990. **7**(2): 156-71.
84. Knox, J. R., Moews, P. C., Escobar, W. A., and Fink, A. L., A catalytically-impaired class A beta-lactamase: 2 Å crystal structure and kinetics of the *Bacillus licheniformis* E166A mutant. *Protein Engineering*, 1993. **6**(1): 11-8.
85. Vanhove, M., Houba, S., Lamotte-Brasseur, J., and Frere, J. M., Probing the determinants of protein stability: comparison of class A beta-lactamases. *Biochemical Journal*, 1995. **308**(3): 859-64.
86. Chan, P. H., Liu HB, Chen YW, Chan KC, Tsang CW, Leung YC, Wong KY, Rational design of a novel fluorescent biosensor for beta-lactam antibiotics from a class A beta-lactamase. *Journal of the American Chemical Society*, 2004. **126**(13): 4074-5.
87. Kresken, M., Jansen, A., and Wiedemann, B., Prevalence of resistance of aerobic gram-negative bacilli to broad-spectrum antibacterial agents: results of a multicenter study. *Journal of Antimicrobial Chemotherapy*, 1990. **25**(6): 1022-4.
88. Livermore, D. M. and Seetulsingh, P., Susceptibility of *Escherichia coli*

- isolates with TEM-1 beta-lactamase to combinations of BRL42715, tazobactam or clavulanate with piperacillin or amoxicillin. *Journal of Antimicrobial Chemotherapy*, 1991. **27**(6): 761-7.
89. Roy, C., Segura, C., Tirado, M., Reig, R., Hermida, M., Teruel, D., and Foz, A., Frequency of plasmid-determined beta-lactamases in 680 consecutively isolated strains of Enterobacteriaceae. *European Journal of Clinical Microbiology*, 1985. **4**(2): 146-7.
90. Datta, N. and Kontomichalou, P., Penicillinase synthesis controlled by infectious R factors in Enterobacteriaceae. *Nature*, 1965. **208**(5007): 239-41.
91. Sturenburg, E. and Mack, D., Extended-spectrum beta-lactamases: implications for the clinical microbiology laboratory, therapy, and infection control. *The Journal of Infection*, 2003. **47**(4): 273-95.
92. Datta, N. and Richmond, M. H., The purification and properties of a penicillinase whose synthesis is mediated by an R-factor in Escherichia coli. *Biochemical Journal*, 1966. **98**(1): 204-9.
93. Ambler, R. P. and Scott, G. K., Partial amino acid sequence of penicillinase coded by Escherichia coli plasmid R6K. *Proceedings of the National Academy of Sciences of the United States of America*, 1978. **75**(8): 3732-6.
94. Matthew, M. and Hedges, R. W., Analytical isoelectric focusing of R

- factor-determined beta-lactamases: correlation with plasmid compatibility. *Journal of Bacteriology*, 1976. **125**(2): 713-18.
95. Sougakoff, W., Goussard, S., Gerbaud, G., and Courvalin, P., Plasmid-mediated resistance to third-generation cephalosporins caused by point mutations in TEM-type penicillinase genes. *Reviews of Infectious Diseases*, 1988. **10**(4): 879-84.
96. Sirot, D., Sirot, J., Labia, R., Morand, A., Courvalin, P., Darfeuille-Michaud, A., Perroux, R., and Cluzel, R., Transferable resistance to third-generation cephalosporins in clinical isolates of *Klebsiella pneumoniae*: identification of CTX-1, a novel beta-lactamase. *Journal of Antimicrobial Chemotherapy*, 1987. **20**(3): 323-34.
97. Goussard, S. and Courvalin, P., Updated sequence information for TEM beta-lactamase genes. *Antimicrobial Agents and Chemotherapy*, 1999. **43**(2): 367-370.
98. Bush, K. and Jacoby, G., Nomenclature of TEM beta-lactamases. *Journal of Antimicrobial Chemotherapy*, 1997. **39**(1): 1-3.
99. Leflon-Guibout, V., Heym, B., and Nicolas-Chanoine, M., Updated sequence information and proposed nomenclature for bla(TEM) genes and their promoters. *Antimicrobial Agents and Chemotherapy*, 2000. **44**(11): 3232-4.

100. Chaibi, E. B., Sirot, D., Paul, G., and Labia, R., Inhibitor-resistant TEM beta-lactamases: phenotypic, genetic and biochemical characteristics. *Journal of Antimicrobial Chemotherapy*, 1999. **43**(4): 447-458.
101. Paterson, D. L. and Bonomo, R. A., Extended-spectrum beta-lactamases: a clinical update. *Clinical Microbiology Reviews*, 2005. **18**(4): 657-686.
102. Orenca, M. C., Yoon, J. S., Ness, J. E., Stemmer, W. P. C., and Stevens, R. C., Predicting the emergence of antibiotic resistance by directed evolution and structural analysis. *Nature Structural Biology*, 2001. **8**(3): 238-242.
103. Watt, R. M. and Voss, E. W., Jr., Mechanism of quenching of fluorescein by anti-fluorescein IgG antibodies. *Immunochemistry*, 1977. **14**(7): 533-51.
104. Templeton, E. F. G. and Ware, W. R., Charge transfer between fluorescein and tryptophan as a possible interaction in the binding of fluorescein to anti-fluorescein antibody. *Molecular Immunology*, 1985. **22**(1): 45-55.
105. Marme, N., Knemeyer, J.-P., Sauer, M., and Wolfrum, J., Inter- and Intramolecular Fluorescence Quenching of Organic Dyes by Tryptophan. *Bioconjugate Chemistry*, 2003. **14**(6): 1133-1139.
106. Mezes, P. S. F., Wang, W., Yeh, E. C. H., and Lampen, J. O., Construction of penP.D1, *Bacillus licheniformis* 749/C beta-lactamase lacking site for lipoprotein modification. Expression in *Escherichia coli* and *Bacillus subtilis*.

- Journal of Biological Chemistry*, 1983. **258**(18): 11211-18.
107. Kogut, M., Pollock, M. R., and Tridgell, E. J., Purification of penicillin-induced penicillinase of *Bacillus cereus* NRRL 569: a comparison of its properties with those of a similarly purified penicillinase produced spontaneously by a constitutive mutant strain. *Biochemical Journal*, 1956. **62**: 391-401.
 108. Kuwabara, S., Purification and properties of two extracellular beta-lactamases from *Bacillus cereus* 569-H. *Biochemical Journal*, 1970. **118**(3): 457-65.
 109. Aschaffenburg, R., Phillips, D. C., Sutton, B. J., Baldwin, G., Kiener, P. A., and Waley, S. G., Preliminary crystallographic data for beta-lactamase I from *Bacillus cereus* 569. *Journal of Molecular Biology*, 1978. **120**(3): 447-9.
 110. Hussain, M., Pastor, F. I., and Lampen, J. O., Cloning and sequencing of the blaZ gene encoding beta-lactamase III, a lipoprotein of *Bacillus cereus* 569/H. *Journal of Bacteriology*, 1987. **169**(2): 579-86.
 111. Evans, J., Galindo, E., Olarte, J., and Falkow, S., beta-Lactamase of R factors. *Journal of Bacteriology*, 1968. **96**(4): 1441-2.
 112. Hou, J. P. and Poole, J. W., Measurement of beta-lactamase activity and rate of inactivation of penicillins by a pH-stat alkalimetric titration method. *Journal of Pharmaceutical Sciences*, 1972. **61**(10): 1594-8.

113. Pratt, R. F. and Loosemore, M. J., 6-beta-Bromopenicillanic acid, a potent beta-lactamase inhibitor. *Proceedings of the National Academy of Sciences of the United States of America*, 1978. **75**(9): 4145-9.
114. Kiener, P. A. and Waley, S. G., Reversible inhibitors of penicillinases. *Biochemical Journal*, 1978. **169**(1): 197-204.
115. Kiener, P. A. and Waley, S. G., Substrate-induced deactivation of penicillinases. Studies of beta-lactamase I by hydrogen exchange. *Biochemical Journal*, 1977. **165**(2): 279-85.
116. Durkin, J. P. and Viswanatha, T., Clavulanic acid inhibition of beta-lactamase I from *Bacillus cereus* 569/H. *The Journal of antibiotics*, 1978. **31**(11): 1162-9.
117. Mezes, P. S. F., Blacher, R. W., and Lampen, J. O., Processing of *Bacillus cereus* 569/H beta-lactamase I in *Escherichia coli* and *Bacillus subtilis*. *Journal of Biological Chemistry*, 1985. **260**(2): 1218-23.
118. Ozer, J. H., Lowery, D. L., and Saz, A. K., Derepression of beta-lactamase (penicillinase) in *Bacillus cereus* by peptidoglycans. *Journal of Bacteriology*, 1970. **102**(1): 52-63.
119. Waley, S. G., pH-dependence and group modification of beta -lactamase I. *Biochemical Journal*, 1975. **149**(3): 547-51.
120. Little, C., Emanuel, E. L., Gagnon, J., and Waley, S. G., Carboxy groups as

- essential residues in beta-lactamases. *Biochemical Journal*, 1986. **240**(1): 215-19.
121. Terpe, K., Overview of tag protein fusions: from molecular and biochemical fundamentals to commercial systems. *Applied Microbiology and Biotechnology*, 2003. **60**(5): 523-533.
122. Arnau, J., Lauritzen, C., Petersen Gitte, E., and Pedersen, J., Current strategies for the use of affinity tags and tag removal for the purification of recombinant proteins. *Protein Expression and Purification*, 2006. **48**(1): 1-13.
123. Fonze, E., Vanhove, M., Dive, G., Sauvage, E., Frere, J.-M., and Charlier, P., Crystal structures of the *Bacillus licheniformis* BS3 class A beta-lactamase and of the acyl-enzyme adduct formed with cefoxitin. *Biochemistry*, 2002. **41**(6): 1877-85.
124. Doucet, N., De Wals, P.-Y., and Pelletier, J. N., Site-saturation Mutagenesis of Tyr-105 Reveals Its Importance in Substrate Stabilization and Discrimination in TEM-1 beta-Lactamase. *Journal of Biological Chemistry*, 2004. **279**(44): 46295-46303.
125. Doucet, N. and Pelletier Joelle, N., Simulated annealing exploration of an active-site tyrosine in TEM-1 beta-lactamase suggests the existence of alternate conformations. *Proteins*, 2007. **69**(2): 340-8.

126. Ferreira, J. A. B., Costa, S. M. B., and Ferreira, L. F. V., Activated Radiationless Decay of Rhodamine 3B: Polarity and Friction Effects. *Journal of Physical Chemistry A*, 2000. **104**(51): 11909-11917.
127. Ferreira, J. A. B. and Costa, S. M. B., Activated radiationless decay of rhodamine-3B: Nonequilibrium polarization effects in viscous solvents. *Journal of Chemical Physics*, 2004. **120**(17): 8095-8106.
128. Magde, D., Rojas, G. E., and Seybold, P. G., Solvent dependence of the fluorescence lifetimes of xanthene dyes. *Photochemistry and Photobiology*, 1999. **70**(5): 737-744.
129. Vogel, M., Rettig, W., Sens, R., and Drexhage, K. H., Evidence for the formation of biradicaloid charge-transfer (BCT) states in xanthene and related dyes. *Chemical Physics Letters*, 1988. **147**(5): 461-5.
130. Marme, N., Knemeyer, J.-P., Sauer, M., and Wolfrum, J., Inter- and intramolecular fluorescence quenching of organic dyes by tryptophan. *Bioconjugate Chemistry*, 2003. **14**(6): 1133-9.
131. Doose, S., Neuweiler, H., and Sauer, M., A close look at fluorescence quenching of organic dyes by tryptophan. *Chemical Physics and Physical Chemistry*, 2005. **6**(11): 2277-85.

Appendix

Sequencing Alignment of TEM, PenP and PenPC β -lactamase

| | | |
|-----------|---|------------------|
| TEM |HPETLVKVKDAEDQ | 14 [↓] |
| PenP |KTEMKDDFAKLEEQ | 14 [↓] |
| PenPC |HKNQATHKEFSQLEKK | 16 [↓] |
| Consensus | e [↓] | |
| ↓ | | |
| TEM | LGARVGYIELDLNSGKILESFRPEERFPMMSTFKVLLCGA | 54 [↓] |
| PenP | FDAKLGIFALDTGTMRTVA.YRPDERFAFASTIKALTVGV | 53 [↓] |
| PenPC | FDARLGVYAIDTGTNQTIS.YRPNERFAFASTYKALAAGV | 55 [↓] |
| Consensus | a g d r p e r f s t k l g [↓] | |
| ↓ | | |
| TEM | VLSRVDAGQEQLGRRIHYSQNDLVEYSPVTEKHLTDGMTV | 94 [↓] |
| PenP | LLQ..QKSIDLNQRITYTRDDLVNYPITEKHVDTGMTL | 91 [↓] |
| PenPC | LLQ..QNSIDSLNEVITYTKEDLDVYSPVTEKHVDTGMKL | 93 [↓] |
| Consensus | l l i y d l v y p t e k h g m [↓] | |
| ↓ | | |
| TEM | RELCSAAITMSDNTAANLLLTIGGPKELTAF LHMGDHV | 134 [↓] |
| PenP | KELADASLRYSDNAAQNLIKQIGGPE SLKKELRKIGDEV | 131 [↓] |
| PenPC | GEIAEAAVRSSDNTAGNILFNKIGGPKGYEKALRHMGDRI | 133 [↓] |
| Consensus | e a s d n a n i g g p l g d [↓] | |
| ↓ | | |
| TEM | TRLDR WEPELNEAIPNDERD TTMPAAMATTLRKLTTGELL | 174 [↓] |
| PenP | TNPER FEPELNEVNPGETQ DTSTARALVTSLRAFALEDKL | 171 [↓] |
| PenPC | TMSNR FE TELNEAIPGDIR DTSTAKAIATNLKAF TVGNAL | 173 [↓] |
| Consensus | t r e e l n e p d t a t l l [↓] | |
| ↓ | | |
| TEM | TLASRQQLIDWMEADKVAGPLLR S ALPAGWFIADKSGAGE | 214 [↓] |
| PenP | PSEKRELLIDWMKRNTTGDALIRAGVPDGWEVADKTGAAS | 211 [↓] |
| PenPC | PAEKRKILTEWMKGNATGDKLIRAGIPTDWVVGDKSGAGS | 213 [↓] |
| Consensus | r l w m l r p w d k g a [↓] | |
| ↓ | | |
| TEM | RGSRGIIAALGPDGKPSRIVVIYTTGSQATMDERNRQIAE | 254 [↓] |
| PenP | YGTRNDIAIIWPPKGDVVLA VLSSRDKKDAKYDDKLI AE | 251 [↓] |
| PenPC | YGTRNDIAVVWPPNRAP IIIAILSSKDEKEAIYDNQLIAE | 253 [↓] |
| Consensus | g r i a p i a e [↓] | |
| ↓ | | |
| TEM | IGASLIKHW..... | 263 [↓] |
| PenP | ATKVVMKALNMNGK..... | 265 [↓] |
| PenPC | ATKVIVKALR..... | 263 [↓] |
| Consensus | k [↓] | |

Sequence Identity

PenP vs PenPC = 57.3%

PenP vs TEM = 35.5%

TEM vs PenPC = 36.5%